DISTRIBUTION, SOURCE AND CYCLING OF ORGANIC CARBON AND NITROGEN IN THE ICY SOILS OF UNIVERSITY VALLEY (MCMURDO DRY VALLEYS OF ANTARCTICA).

Benoit Faucher

A thesis submitted to the
Faculty of Graduate and Postdoctoral Studies
in partial fulfillment of the requirements
for the degree of
Master of Science in Geography

Department of Geography
University of Ottawa

Acknowledgements

J'aimerais premièrement remercier mon superviseur de maîtrise, Denis Lacelle, sans qui l'achèvement de cette thèse aurait été impossible. Denis, merci de m'avoir donné la chance de travailler sur ce passionnant projet et d'avoir été patient tout au long du processus; ce fut réellement une expérience inoubliable et j'en ressors surtout avec du positif.

J'aimerais aussi remercier mon comité d'évaluation, Bernard Lauriol ainsi que Ian D. Clark, pour leurs judicieux commentaires et propositions en lien avec cette thèse. Merci Mr. Lauriol de m'avoir mis en contact avec Denis lorsque j'ai terminé de rédiger mon mémoire de baccalauréat sous votre tutelle et de m'avoir transférer votre enthousiasme pour la recherche.

Merci aussi au personnel du laboratoire d'isotopes stable G.G. Hatch de l'Université d'Ottawa (Wendy Abdi, Patricia Wickham et Paul Middlestead) pour leur expertise en lien avec les multiples analyses élémentaires et isotopiques qui ont fourni les résultats de cette thèse. Merci aussi à Jean Bjornson (Université d'Ottawa) pour ses astucieux conseils en lien avec mes analyses en laboratoires.

Je voudrais aussi prendre l'opportunité de remercier Caroline Bujold pour sa patience et son support tout au long de ma maîtrise. Merci aussi à mes collègues de bureau (Hugo Crites, Marjolaine Verret et Lindsay Armstrong) pour votre support durant les deux dernières années. Finalement, merci à mes parents, Johanne et François, pour leurs encouragements et leur soutient tout au long de mon cheminement scolaire; un jour je ne serai plus un étudiant je vous le promets.

Abstract

Between 2009 and 2013, 16 ice-bearing permafrost cores were collected from 10 polygons along the floor of University Valley (McMurdo Dry Valleys of Antarctica) and were subsequently analysed in order to assess the geochemical properties of the valley's icy soils and ground ice. Elemental analysis showed that icy soils located in the seasonally non-cryotic zone (NCZ) of the valley contained (on average) twice as much organic carbon (1.19 mg C/g^{-1}) as the ice cemented permafrost soils sampled in its perennially cryotic zone (PCZ). It also showed that nitrogen accumulation in the icy soils was a result of atmospheric fallout and chemical weathering of mineral soils. Isotopic analysis showed that the organic matter contained in the valley's icy soils are mostly derived from the deposition and burial of cryptoendolithic communities living in the adjacent sandstone valley walls. Dissolved organic carbon (DOC) concentration measures indicated that soils containing the highest amounts of DOC were enriched in $^{13}C_{DOC}$ relatively to soils with low DOC concentrations. This indicated that microbial activity in soils was the highest during past super interglacial periods. A soil habitability index calculation from Stoker et *al*. (2010) was used to establish that soils located in the NCZ were more habitable than soils sampled in the PCZ and also presumably more habitable than soils at many Mars landing sites.

Résumé

Entre 2009 et 2013, 16 carottes de pergélisol ont été forées dans 10 sols polygonaux de *University Valley* (vallées sèches McMurdo d'Antarctique) et ont ensuite été analysées pour déterminer les caractéristiques géochimiques de ses sédiments cryotiques et de la glace contenue dans ces derniers. Une analyse élémentaire a indiqué que les sols gelés situées dans la section pérennement non-cryotique (PNC) de la vallée contenaient (en moyenne) deux fois plus de carbone organique (1.19 mg C/g^{-1}) que ceux situés dans la section pérennement cryotique (PC). Cette analyse a aussi montré que l'azote contenu dans le pergélisol de la vallée provenait de déposition atmosphérique et de météorisation du sol minéral. Une analyse isotopique a aussi permis de déterminer que la biomasse contenue dans le sol gelé provenait de la déposition et de l'enfouissement de cryptoendolithes vivants dans les parois latérales de la vallée. Des mesures de concentrations de carbone organique dissous (COD) ont indiqué que les sols qui contenaient le plus de COD étaient aussi enrichis en $^{13}C_{COD}$, relativement aux sols moins concentrés en COD. Ceci a indiqué que l'activité microbienne dans les sols de *University Valley* était probablement plus accentuée durant la période interglaciaire de l'Eémien. Un index d'habitabilité développé par Stoker et *al*. (2010) a été utilisé pour déterminer que les sols de la section PNC étaient plus habitables que ceux situés dans la zone PC et que ceux de plusieurs sites d'atterrissage sur Mars.

Table of contents

List of figures

List of tables

List of abbreviations

a.s.l.	Above sea level
C	Carbon
C_{org}	Organic carbon
C_{inorg}	Inorganic carbon
CTZ	Coastal thaw zone
DOC	Dissolved organic carbon
EDOM	Endolith-derived organic matter
HCO	Holocene climatic optimum
IMZ	Intermediate zone
LDOM	Lacustrine-derived organic matter
MDOM	Marine-derived organic matter
MDV	McMurdo Dry Valleys
N	Nitrogen
NCZ	Seasonally non-cryotic zone
OSL	Optically stimulated luminescence dating
P	Phosphorus
PCZ	Perennially cryotic zone
SIC	Soil inorganic carbon
SICC	Soil inorganic carbon concentration
SOC	Soil organic carbon
SOCC	Soil organic carbon concentration
SUZ	Stable upland zone
TV	Taylor Valley
UG	University Glacier
UV	University Valley
VPDB	Vienna Pee-Dee Belemnite
VV	Victoria Valley
WV	Wright Valley
$\delta^{13}C_{org}$	Delta ^{13}C of organic carbon
$\delta^{13}C_{DOC}$	Delta ^{13}C of dissolved organic carbon
$\delta\,^{14}C_{org}$	Delta ^{14}C of organic carbon

1. Introduction

The McMurdo Dry Valleys (MDV) of Antarctica are a hyper arid polar desert that can be divided into three zones: i) the coastal thaw (or subxerous) zone, where mean daily summer air temperatures exceed 0°C and liquid water can exist seasonally; ii) the inland mixed (or xerous) zone where summer air temperatures may rise above 0°C for short periods and liquid water may be present periodically; and iii) the stable upland (or ultraxerous) zone located in the Quartermain Mountains and other high elevation regions where maximum air temperatures rarely exceed 0°C and little to no melting of snow and/or ice occurs (Doran *et al.,* 2002; Marchant and Head, 2007). The MDV lack vascular plants and the terrestrial ecosystem in the subxerous zone is composed of sparse cryptogamic vegetation (mosses and lichens), low diversity of invertebrates and active communities of heterotrophic soil organisms and endolithic autotrophs in the interstitial space of sandstone outcrops (Horowitz et *al*., 1972; Freckman and Virginia, 1997; Bargagli et *al*., 1999; Moorhead et *al*., 2002; Barrett et *al*., 2008). By contrast, the ultraxeous zone lacks all types of vegetation and supports active endolithic autotrophs; heterotrophic microbial communities are present in soils but their activity has not been detected (Friedmann, 1982; Goordial et *al*., 2016).

Previous studies on the abundance and origin of soil organic carbon (SOC) and biogeochemical stoichiometry in the soils (C:N) of the MDV have mainly been undertaken in the warm-wet subxerous zone. Abundance of SOC was highly variable, but was closely related to distance to perennially ice-covered lakes, the major sites of primary organic carbon (C_{org}) production by mosses, lichens, algae and cyanobacteria (Elberling et *al*., 2006; Barrett et *al*., 2007). However, during past warmer interglacial periods, extensive lakes occupied the lower valleys and a significant proportion of the SOC has been produced and deposited in the sediments of these paleo-lakes (Higgins et *al*., 2000; Burkins et *al*., 2001; Barrett et *al*., 2004). Using $\delta^{13}C_{org}$ as a tracer of the source of C_{org}, it was shown that the SOC in proximity to lakes had $\delta^{13}C_{org}$ signatures approaching that of the ancient and modern lacustrine detritus. Soils distant from sources of liquid water or where lacustrine productivity was very low had $\delta^{13}C_{org}$ signatures characteristic of

endolithic sources, and some soils had mixed $\delta^{13}C_{org}$ values suggesting that mobilization and re-deposition of various sources of SOC by glaciers and/or wind occurred (Burkins et *al*., 2000; Barrett et *al*., 2006; Hopkins et *al*., 2009). Investigation of the C_{org}:N:P ratios showed a biological imbalance in some soils, suggesting that physical processes influenced the geochemical stoichiometry (Barrett et *al*., 2007). Despite the numerous studies from the subxerous zone, little is known about the abundance, origin and age of SOC and potential biogeochemical stoichiometry in the soils of the colder-drier ultraxerous zone. Given that this region is deemed among the coldest and driest on Earth, it offers the potential to investigate the limiting factors that regulate longevity and activeness of biomolecules (Cowan, 2014).

This thesis investigates the distribution, origin and age of organic carbon and nitrogen in the soils of University Valley, a small valley found in the Quartermain Mountains, and determines whether biological (conform to Redfield ratio) or geochemical processes dominate the ecosystem stoichiometry (cycling of nutrients). To accomplish this objective, 16 ice-bearing permafrost cores (up to 1m in depth) were collected from 10 sites along the valley floor and analyzed for dissolved ion concentrations, C_{org}-N concentration, $\delta^{13}C_{org}$, dissolved organic carbon (DOC), $\delta^{13}C_{DOC}$ and $^{14}C_{org}$. To assess the potential of unfrozen liquid water in the cryotic soils that would support active heterotrophic microbial communities and transport nutrients, the concentration of total soluble ions was determined to estimate the freezing point depression and a laboratory experiment was conducted to determine the amount of unfrozen water by measuring the dielectric constant of natural soils over the temperature range of 0 to –20°C. The results from this thesis allow a better understanding of the effect of temperature and liquid water as limiting factors in cryo-environments on abundance, distribution and cycling of organic carbon and nitrogen.

1.1. Research questions

A) What are the concentrations of soil organic carbon, nitrogen and dissolved organic carbon in University valley's icy soils? Are there differences within polygons (center vs. shoulder) and along the valley floor?

B) What is the source of organic carbon in this valley's icy soils? Was it produced *in situ* by microbes and bacteria that were able to survive due to a potential transient source of water, does it originate from nearby cryptoendoliths, or do we observe distant lacustrine detritus source transported by winds? Are there differences between the PCZ and the NCZ?

C) Are the ice-cemented permafrost soils of polygons located in the valley's NCZ more habitable than the ones located in the PCZ? How do they compare to Mars landing sites?

D) What is the concentration of soluble ions in University valley's icy permafrost? Are there differences within polygons (center vs. shoulder) and along the valley floor?

2. Study area

2.1 The McMurdo Dry Valleys

The McMurdo Dry valleys (MDV) of Antarctica (Fig. 1) occupy the continent's largest glacier-free area (4800 km^2) and are considered as some of the world's coldest and driest environments (Doran et *al*., 2002; Bockheim et *al.*, 2007). Located in southern Victoria Land, the MDV are a series of generally east-west trending glacial valleys, comprised between the Ross Sea and McMurdo Sound and the Polar plateau near the East Antarctic Ice Sheet (Marchant and Head, 2007). Elevation in the MDV ranges from sea level (near the Ross Sea) to 2000 m a.s.l., near the Polar Plateau (Doran et *al*., 2002). The MDV are ice-free because the Transantarctic Mountains blocks the flow of glacial ice originating from the East Antarctic Ice Sheet (McKay et *al.,* 1998).

In the MDV, the mean annual air temperature ranges from -25° C to -17° C and total annual precipitation is <100 mm, classifying its climate as a hyper-arid polar desert. However, a strong gradient in temperature exists between the coast and the high elevation valleys, with summer air temperatures largely set by the dry adiabatic lapse rate of 10°C km^{-1} (Doran et *al*., 2002; Marchant and Head, 2007). Based on summer climate conditions, Marchant and Head (2007) classified the climate in the MDV into three separate zones: i) the coastal thaw zone (CTZ); ii) the mixed inland zone (MIZ); and iii) the stable upland zone (SUZ). The lower elevation valleys are situated in the coastal thaw zone where the summer air temperature and relative humidity average –5°C and 64%, respectively. In these valleys, the thaw degree-days range between 20 and 100 (Doran et *al*., 2002), which can result in surface snow to melt and infiltrate the near-surface soils. The high elevation MDV (> 1000 m) are located in the stable highland zone where the summer air temperature and relative humidity are much lower, averaging –10°C and 41%, respectively, and the number of thaw degree-days is less than 5 annually (Lacelle et *al.*, 2016).

Permafrost is pervasive in the MDV and has likely been present for at least the last 8 Ma years (Bockheim and Hall, 2002; McKay et *al.,* 1998). The cold and dry climate ensures that the near-surface soils are dry (<3% water by weight) with icy soils

encountered at some depth; the interface between the dry and icy soils being termed the ice table (Mellon et *al*., 2008). Active layer thickness in the MDV generally decreases from ca. 1 m in the coastal thaw zone to a few centimeters in the stable upland zone and its thickness is locally dependent on microclimatic factors (Adlam et *al*., 2010).

The MDV's hyper-arid polar desert conditions are such that only sparse moss, lichens, algae and microbial communities compose the terrestrial ecosystems (Horowitz et *al*., 1972; Freckman and Virginia, 1997; Bargagli et *al*., 1999; Moorhead et *al*., 2002; Barrett et *al*., 2007). However, in the upper valleys, cryptogamic vegetation is completely absent and only active autotrophic endoliths are found in sandstone outcrops, with heterotrophic microbial communities in the soils (Friedmann et *al*,. 1982; Hopkins et *al.,* 2009; Barrett et *al.,* 2006). The MDV also contain more than 20 permanent lakes and ponds (probable remnants of large glacial lakes that occupied the valleys during warmer-wetter periods), which are perennially ice-covered (except for the hypersaline Don Juan pond). These lakes and ponds contain vast arrays of planktonic and benthic communities (e.g., cyanobacteria, eukaryotic algae, heterotrophic bacteria) which support the primary production of organic carbon (Wharton et *al.*, 1989; Doran et *al*, 1994).

The soils in the MDV are largely derived from weathering of sandstones, dolerites, granites and metasedimentary rocks and have a tendency to be alkaline, coarse textured (medium to coarse sand). They contain an abundance of sodium, potassium, magnesium chloride, nitrates and sulfates salts derived from long-term accumulation of atmospheric fallout (Clarigde and Campbell, 1977; Bockheim, 1997; Ugolini and Bockheim, 2008). The concentration of salts in the soils demonstrates patterns related to soil ages (Bockheim and Hall, 2002) and elevations (Witherow *et al*., 2006). In general, young soils (< 200 ka years) and upland valleys typically contain the lowest concentration of salts; whereas older (> 1 Ma years) soils, located at mid-elevation in Taylor, Wright and Victoria valleys and in lower Beacon Valley, and coastal valleys contain the highest concentrations. The soils in the MDV are generally enriched, in phosphorus and nitrogen relative to organic carbon (Table 1) (Barrett et *al.,* 2007; Cowan, 2014).

Matsumoto et *al.* (1990) suggested that the SOC in the MDV soils could originate from three different sources: i) Erosion of the Beacon supergroup (Devonian to Triassic aged sandstones, siltstones and conglomerates); ii) Past biological activity during warmer periods; and iii) Wind-transported cyanobacterial mats. Burkins et *al.* (2000) compiled the isotopic composition ($\delta^{13}C$ and $\delta^{15}N$) of various potential sources of organic matter to facilitate the identification of its source in soils of the MDV. It has been established that the lake-derived organic matter (LDOM) have $\delta^{13}C$ values ranging from -7.5‰ to -27.7‰ and with $\delta^{15}N$ values that vary between -1.9‰ to -11.4‰; marine-derived organic matter (MDOM) and endolith-derived organic matter (EDOM) have $\delta^{13}C$ values ranging from -15.5‰ to -26.9‰ and from -26.5‰ to -26.7‰, respectively, with $\delta^{15}N$ values ranging from 0.5‰ to 3.4‰ and from -9.8‰ to -18.8‰, respectively. Based on the study, Burkins et *al.* (2000) proposed an alternate "legacy" source to explain the origin of an important proportion of this organic matter: it would have been laid down in ancient lakebed sediments during past interglacial periods.

Carbon cycling in the permafrost soils of the MDV (and especially in its high elevation valleys) is, to this day, still poorly characterized. Generally carbon turnover rates are quite high, ranging from ~20 to 120 years (Barret et *al.,* 2006; Burkins et *al.,* 2001; Barrett et *al.,* 2005; Elberling et *al.,* 2006; Hopkins et *al.*, 2009). However, further research is necessary to fully assess the local parameters (i.e. soil moisture, distance from the sea, climatic conditions) that control the origin and cycling of SOC in this polar desert environment.

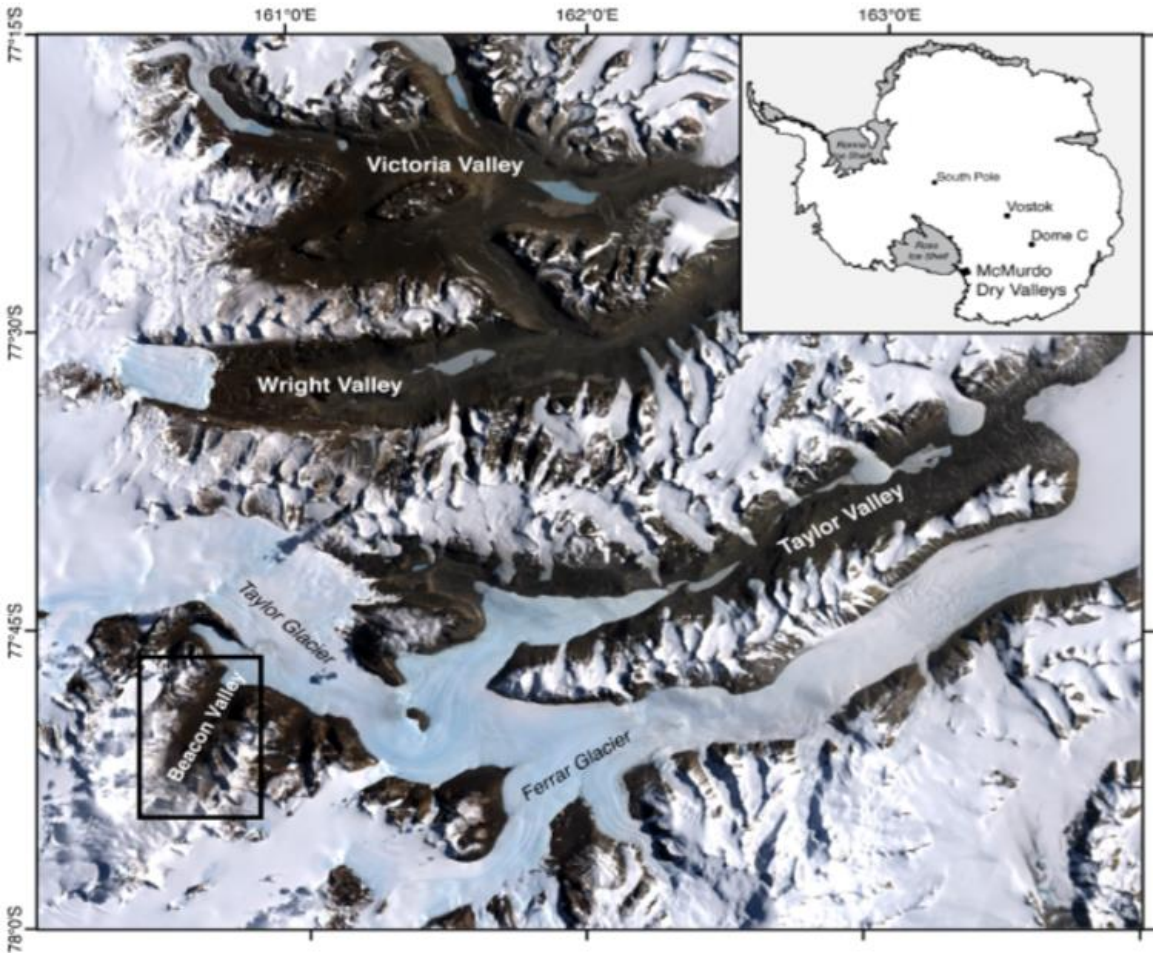

Figure 1: Relative location of the MDV, with regards to the Antarctic continent.

Table 1: Average organic carbon and nitrogen concentrations in various soils of the MDV (from Barrett et *al*., 2007; Hopkins et *al.*, 2009).

Soil sampling sites	Organic Carbon (mg C/g^{-1} soil)	SD	Total N (mg N/g^{-1} soil)	SD	C:N
Garwood Valley hillslope	0.51	0.13	0.13	0.6	3.9
Garwood Valley floor (polygons)	0.62	0.16	0.14	0.6	4.4
Garwood lake margins	0.96	0.34	0.15	0.8	6.2
Garwood stream margin	0.64	0.15	0.16	0.2	4.1
Wright valley floor	0.11	0.05	0.04	0.001	3.1
Wright Valley Dais (highland)	0.07	0.05	0.02	0.001	3.5
Victoria Valley	0.21	0.04	0.08	0.01	2.7
Taylor Valley	0.13	0.04	0.05	0.006	2.5
Lake Fryxell, Taylor Valley	0.43	0.04	0.02	0.001	25.1
Lake Hoare, Taylor Valley	0.24	0.04	0.04	0.004	7.0
Lake Bonney, Taylor Valley	0.18	0.03	0.03	0.018	6.4
Pearse Valley	0.15	0.02	0.17	0.008	1.1
Beacon Valley	0.15	0.03	0.37	0.203	0.5
Arena Valley	0.18	0.02	0.5	0.179	0.4

2.2 University Valley, Quartermain Mountains

University Valley (UV) is a northwest facing U-shaped valley (1600-1800 m a.s.l., 1.5 km long and 500 m wide) located in the SUZ and is situated approximately 450 m above the floor of Beacon Valley (Fig. 2). Polygonal patterned ground and sand wedges are ubiquitous along its floor and are sometimes present on some of its talus cones (Mellon et *al*., 2014; Lapalme et *al.,* 2016). A down-valley gradient exists in the diameter of UV polygons, ranging from ca. 10 m in the upper section of the valley to ca. 20 m in the lower section (Mellon et *al.,* 2014). Snow patches are also found on UV's floor but mainly in polygonal troughs. A small glacier (given the unofficial name of University Glacier) is situated in the upper portion of the valley and has a maximum thickness of ca. 150 m (Lapalme, 2015).

The local geology consists of sills of Ferrar Dolerite (Jurassic age intrusives) and sedimentary rock of the Beacon Supergroup (Devonian to Triassic age sandstones and conglomerates) (Barrett, 1981; Cox *et al.,* 2012). The surface sediments consist of undifferentiated till and alpine drift on the valley floor and of colluvium on talus cones at the base of the valley walls (Cox *et al.,* 2012). The alpine drift is restricted to the upper

and central parts of the valley. Optically stimulated luminescence (OSL) ages obtained from a core in upper University Valley yielded ages of 17.9 ± 1.6 kyr for sediments at 2-5 cm depths whereas those at 90-95 cm depths were dated to 170 ± 36 kyr (Lacelle *et al.,* 2013). These ages fit reasonably well with those estimated from Cl concentration in near-surface soils (top 56 cm) where apparent minimum soil accumulation time ranges from 10-30 kyr near the glacier to 70-200 kyr in the central part of the valley (Jackson *et al.,* 2016). The undifferentiated till, which is confined to the lower part of the valley and contains granite erratics, is likely associated with the Taylor 4b Drift (>2.7 Ma) or an older glaciation (Cox et *al.,* 2012).

Climatic records obtained from an automated weather station in UV, for the 2009-2012 period, indicated a mean annual air temperature of –23.4 ± 0.9°C, and a mean annual relative humidity of 45.5 ± 14% (Lacelle et *al.,* 2016). No annual precipitation data records are available for the valley, but estimations based on forecast modeling by Powers et *al.* (2003) have shown that it could perhaps receive up 10 mm swe yr^{-1}. In University Valley, the mean annual soil surface temperature was near −26°C along the valley floor; however, soils in the upper section of the valley experienced colder mean summer ground surface temperatures (–13.0°C) than those in the central and lower parts (–11.2°C) (Lacelle et *al*., 2016). Based on ground surface temperatures and insolation received at the surface, Lacelle et *al.* (2016) identified three zones on the valley floor with distinct ground surface temperatures: i) a perennially cryotic zone (PCZ), where the ground surface temperature was always stay below 0°C, because of topographic shadowing; ii) a seasonally non-cryotic zone (NCZ), where ground surface air temperature reached values above 0 °C for a few hours, on sunny summer days; and iii) an intermediate mixed zone, a transitional area between the PCZ and NCZ that may exhibit characteristics of either zones.

In contrast to the permafrost and ground ice conditions map of the MDV, which suggest that dry permafrost should be encountered throughout University Valley (Bockheim et *al*., 2007), measurements of ice table depths in University Valley, generally increased with distance from University Glacier from <1 cm in proximity to the glacier to

>50 cm at the mouth of the valley, indicating the presence of widespread ice-bearing soils overlain by dry soils (McKay, 2009, Marinova *et al.,* 2013). Below the ice table, the ice-bearing permafrost contains variable amounts of ground ice, with excess ice and volumetric ice contents reaching 93% (Lacelle et *al*., 2013; Lapalme et *al*., 2016). In addition, two massive ice bodies are also present in the valley: one of them is located near University glacier and the other one is near the mouth of the valley (Lacelle et *al*., 2011; Pollard et *al.,* 2012),

The soils in the valley consist of a homogenous medium sand texture with <5% fines (Lapalme et *al*., 2016). Jackson et *al.* (2016) demonstrated that the Cl^- and NO_3^- salts concentration in the dry soils fluctuates between 10-1000 mg/kg^{-1} dry soil and that ClO_4^- and ClO_3^- were present in trace concentrations ($\mu g/kg^{-1}$ soils range). Additionally, Jackson et *al*. (2016) showed that these ions have a predominantly stratospheric fallout origin.

In University Valley, active autotrophic endoliths are found in north and east-facing sandstone outcrops (dominated by *Chaetothyriales*) (Friedmann et *al*., 1982). In the soils, microbial biomass was found to be extremely low ($1.4–5.7\times10^3$ $cells/g^{-1}$ soil) and more abundant near the soil surface than at the ice table (Tamparri et *al*., 2012; Goordial et *al*., 2016). DNA analysis from 2 soil profiles in the valley (5 and 12cm ice table depth) yielded 6 heterotroph isolates with bacterial community mainly comprising Gammaproteobacteria (25%) and Betaproteobacteria (9%). Firmicutes, Actinobacteria and Bacteroidetes were also variably present in samples. Seven assays for heterotrophic microbial activity yielded no level of radiorespiration activity, which suggests that unlike the endoliths in the sandstones, the heterotrophic microbial communities in the soils are not active (Goordial et *al.,* 2016).

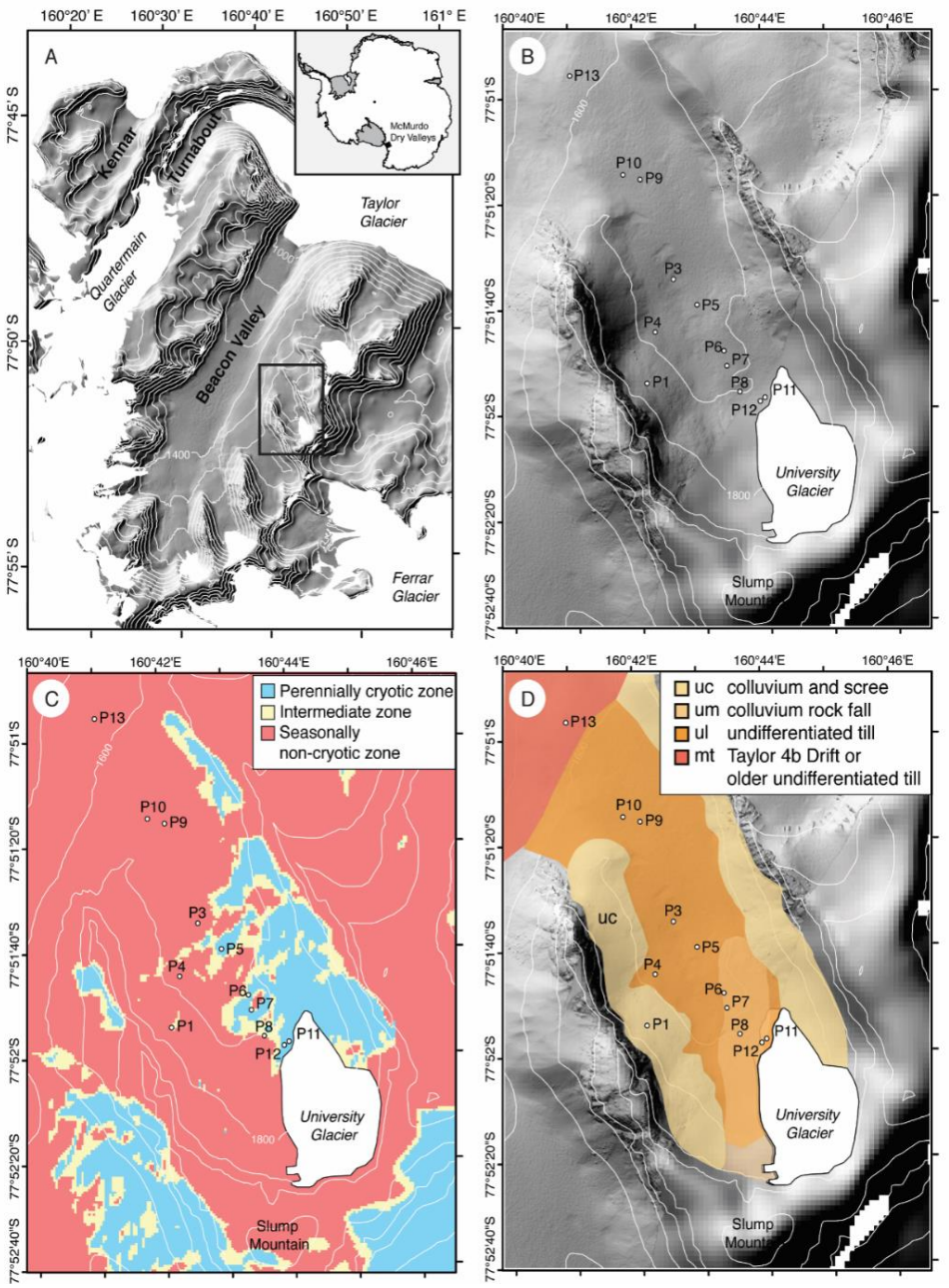

Figure 2: A) Hillshade image showing location of University Valley in the Quartermain Mountains of the McMurdo Dry Valleys of Antarctica. Contour lines (100 m interval) are indicated with thin white lines. B) Hillshade image of University Valley showing location of sampled polygons. Contour lines (100 m interval) are indicated with thin white lines; C) Map showing ground surface tempeature zones map of University Valley and location of sampled polygons (from Lacelle et *al*., 2016); D) Surface geology map of University Valley and location of sampled polygons. Surface geology is derived from Cox et *al*. (2012). For A) and B) the hillshade image was derived from a LiDAR digital elevation model (http://usarc.usgs.gov/lida_dload.shtml) embedded into a 15 m ASTER digital elevation model of the upper McMurdo Dry Valley's region (http://asterweb.jpl.nasa.gov/data/asp) (from Lapalme et *al*., 2016).

3. Methodology

3.1 Field sampling

Between 2009 and 2013, 16 ice-bearing permafrost cores were collected from 10 polygons along the floor of University Valley by D. Lacelle and A. Davila (Table 2). Three polygons (P8, P6, and P1) were cored in the center and shoulders and seven polygons (P4, P5, P7, P9, P10, P11, and P12) were cored only in the center or the shoulder of the polygon depending on the depth of the ice table (Fig. 2). Polygons 5, 8, 11 and 12 were located in the PCZ; polygons 1, 4, 7, 9, 10, MI-1 and MI-2 were situated in the NCZ; and polygon 6 was located in the intermediate mixed zone.

The permafrost cores were collected using an 11.5 cm diameter gas powered SIPRE core barrel. Prior to coring, the dry loose soil layer above the ice-bearing permafrost was removed (and not sampled). Each core was retrieved in 10 to 50 cm long segments, wrapped in plastic cores sleeves and were subsequently shipped, in thermally insulated box, to the Cryolab for Arctic, Antarctic and Planetary Studies located at the University of Ottawa. In the laboratory, the ice-bearing permafrost cores were cut into ca. 2 cm thick slices using a RIGID circular saw with a 0.8 mm thick diamond blade and allowed to thaw in sealed plastic bags and then transferred into graduated 50 ml polypropylene tubes

The permafrost cores were first analysed by Lapalme (2015) and Lapalme et *al*. (2016), who quantified the ground ice content, described their cryostructures via CT-scanning and inferred the origin of the ground ice. These studies demonstrated that ground ice was ubiquitous in the upper 2 m of permafrost soils, with excess ice and volumetric ice contents reaching 93%, but also showed that ground ice conditions were not homogeneous. Ground ice content was variable within polygons and along the valley floor, decreasing in the centers of polygons and increasing in the shoulders of polygons towards the mouth of the valley. Ground ice also had different origins: vapor-deposition in the PCZ, freezing of partially evaporated snow meltwater in the NCZ and buried glacier ice. This thesis expands the previous work done in University Valley by investigating the distribution and source of organic carbon and nitrogen in the soils.

Table 2: Information on University Valley's ice cemented permafrost cores (adapted from Lapalme, 2015).

Polygon	Core ID	Sampling location	Easting	Northing	Core length (cm)	Ice table depth (cm)	Distance from University glacier (m)
P1	P1-C1	Center	160.70158	77.86508	107	30	860
P1	P1-C2	Right shoulder	160.70158	77.86508	102	19	860
P1	P1-C3	Left shoulder	160.70158	77.86508	60	28	860
P2	P2-C2	Deflation surface	160.70936	77.85950	22	20	1076
P4	P4-C1	Center	160.70402	77.86233	15	2	943
P5	P5-C1	Center	160.71527	77.86091	23	19	866
P6	P6-C3	Center	160.72222	77.86341	100	25	545
P6	P6-C5	Left shoulder	160.72222	77.86341	70	20	545
P7	P7-C1	Center	160.72297	77.86422	27	22	466
P8	P8-C3	Center	160.72627	77.86563	68	2	304
P8	P8-C5	Right shoulder	160.72627	77.86563	73	2	304
P8	P8-C6	Left shoulder	160.72627	77.86563	39	2	304
P9	P9-C1	Right shoulder	160.70086	77.85408	20	30	1692
P9	P9-C2	Left shoulder	160.70086	77.85408	10	30	1692
P10	P10-C1	Right shoulder	160.69633	77.85383	167	16	1076

3.2 Bulk organic carbon, inorganic carbon and nitrogen

The concentration of organic C, inorganic carbon and nitrogen in the icy soils at ca. 5 cm depth interval was determined using an *Elementar VarioEL III* instrument (G.G. Hatch laboratory, UOttawa). All samples were analysed twice: once un-acidified to determine total carbon content and then acidified with 10% HCl to remove the inorganic carbonates. The difference between total carbonate and organic carbon contents provided the inorganic carbon content.

Elemental analysis was undertaken by weighing ca. 10 mg of dried soils (<2mm fraction) and a series of standards, in tin capsules to which 30 mg of tungstic oxide (WO_3), a combustion catalyst, was added. Samples were then flash combusted with the addition of oxygen at 1800°C. The resulting gases were carried by helium through columns of reducing and oxidizing chemicals to get N_2 and CO_2 These gases were then separated using the ”purge and trap” method of specific absorption columns and were measured separately by a thermal conductivity detector (TDC). Approximately 3% of the samples

were analysed as duplicates during the process. Analytical precision of the analysis was +/- 0.1%.

3.3 ^{13}C organic carbon

The δ^{13}Corg composition of ice-cemented permafrost soils was determined after the concentration of C_{org} was determined. The δ^{13}Corg composition was determined to assess the source(s) of organic carbon in the vapor-derived ice-cemented permafrost cores and in the liquid-water derived ice-cemented permafrost cores of UV.

The weight of each sample that was used in this analysis depended on their nitrogen concentration; approximately 100 μg of nitrogen per sample was required for analysis. The appropriate quantities of each sample, for this analysis, were then mixed with 100 mg of WO_3, and flash combusted. Resulting CO_2 and N_2 gases were separated using the ”purge and trap” method and were subsequently analysed by a *DeltaPlus Advantage* isotope ratio mass spectrometer (IRMS) coupled with the *ConFlo III* interface. Approximately one duplicate for each of the core's icy soils, was analysed for $\delta^{13}C_{org}$ (total of 10). The $^{13}C/^{12}C$ ratios are expressed in δ-notation, where δ represents the parts per thousand difference of $^{13}C/^{12}C$ in a sample with respect to the Vienna Pee-Dee Belemnite (VPDB) standard. Analytical precision was ±0.20‰.

3.4 Radiocarbon measurements

$^{14}C_{org}$ ages of the organic matter contained in the three ice cemented permafrost soil samples coming from the P11 core of UV's were determined by accelerating mass spectrometry (AMS), in November of 2011, at the BETA analytic inc. radiocarbon dating laboratory (Florida, U.S.A.). Organic sediments were acid washed prior to analysis and were also analyzed for $\delta^{13}C_{org}$.

3.5 Dissolved organic carbon (DOC) and $^{13}C_{DOC}$

The DOC concentration and δ^{13}C composition of the ice-cemented permafrost cores were determined on 40 ml of filtered supernatant water obtained following thawing

of the icy permafrost core samples. Since 40 ml of water was necessary for this analysis, samples were sometimes combined to obtain this quantity of water. DOC concentrations were determined with the use of an OI Analytical "TIC-TOC" Analyser Model 1030 coupled to a Finnigan Mat Delta+ isotope mass spectrometer (G.G. Hatch Laboratory, UOttawa) following the wet oxidation technique described by St-Jean (2003). The DOC concentrations were normalized using internal standards and the analytical precision was ±0.002 ppm. The $^{13}C/^{12}C$ ratios of the DOC are expressed in δ-notation, where δ represents the parts per thousand difference of $^{13}C/^{12}C$ in a sample with respect to the Vienna Pee-Dee Belemnite (VPDB) standard.

3.6 Concentration of soluble ions

Total soluble ions was extracted sequentially three times by C. Trinh-Le (MSc candidate at University of Victoria, New Zealand) using a soil-water ratio of 1:10 (which proved to be the most efficient soluble salts extraction method). The soil-water mixtures were shaken for 1 hour and were subsequently centrifuged and decanted. Water-soluble anion concentrations (SO_4^{2-}, Cl^- and NO_3^-) were determined by ion chromatography and water-soluble cation (Ca^{2+}, Mg^{2+}, Na^+ and K^+) concentrations were determined by Inductively Coupled Plasma Atomic Emission Spectrometry (ICP-AES). Analytical precision was ±5%.

The geochemical composition of icy soils was used to determine the unfrozen water content and freezing points using FREZCHEM hydro-geochemical software. FREZCHEM is an equilibrium chemical thermodynamic model parameterized for concentrated electrolyte solutions (to ionic strengths >20 molality) for the temperature range between –73 and 25°C (Marion and Kargel, 2008). Using FREZCHEM, the unfrozen water content in cryotic soils (with an initial mass of water of 1kg) under decreasing temperatures was calculated in step-wise fashion (1°C between from 0 to –60°C) using the equilibrium crystallization mode until the eutectic point of the aqueous solution was reached. FREZCHEM determines the presence of unfrozen water if the activity of water calculated from the Pitzer equations is less than the equilibrium constant for water-ice (Marion and Kargel, 2008).

3.7 Experimental determination of unfrozen water content

Many different methods have been employed to determine the unfrozen water content in frozen soils (i.e., Anderson and Morgenstern, 1973; Patterson and Smith, 1981). Time-domain reflectometry, a method that relies on the dielectric constant in soils, has been used to determine unfrozen water content in cryotic soils containing salts (Topp *et al*., 1980; Patterson and Smith, 1981). Following a similar approach to the time-domain reflectometry method, the unfrozen moisture content of the three bulk soil samples from University Valley (core 1, P11-C1 and P12-C1) was determined using Decagon 5TE 3-in-1 soil temperature, moisture and conductivity sensors. The soil moisture sensor measures the dielectric constant of soil at 70 MHz frequency and achieves similar performance results to that of time-domain reflectometry (Czarnomski et *al*., 2005).

Soils in University Valley consist of medium to coarse sand, with dominant mode fraction at 0 to 2 θ, and contain <1g L^{-1} of soluble salts of NO_3-SO_4-Ca geochemical facies (Lacelle *et al*., 2013; Lapalme et *al*., 2016). The soils were initially dried at 105°C, and approximately 500cc of bulk soils from each site were placed in 1L beakers. The soils were saturated with distilled water (18Ω) and the Decagon 5TE sensor placed in the wet soils. The beakers were then placed in a Burnsco environmental test chamber (Arnprior, ON, Canada) and the ambient temperature in the chamber was programmed to decrease from +2°C to –20°C, at steps of 1°C every 1.5 hours. After reaching –20°C, the ambient temperature was increased to +2°C at a rate of 1°C every 1 hour. This allowed determining the unfrozen water content during the cooling and warming of the soils as a slight hysteresis has been shown to occur (i.e., Williams and Smith, 1989). The Decagon 5TE sensors recorded temperature and apparent dielectric constant (Ka) at one-minute interval. To ensure the best accuracy in unfrozen water content, the measured apparent dielectric constant was first calibrated with the soils used in the experiments following the method described by Starr and Paltineanu (2002). The unfrozen water content (%wt; gH_2O/g soils) was reported using the calibration curve and the accuracy is ±0.5%. The sensor accuracy for soil temperature was ±1°C. From the temperature and unfrozen water content dataset, an unfrozen water content curve was produced for each soil sample.

3.8 Habitability index calculation

The habitability of UV's icy soils were assessed by using the habitability index defined by Stoker et *al*. (2010). Four key probabilistic factors were used by Stoker et *al.* (2010) to assess the habitability of the Phoenix landing site and other locations on Mars: i) the presence of liquid water (*Plw*); ii) the presence of available energy sources (*Pe*); iii) the presence of elements essential to life in a biologically available form (C, H, N, O, P, S; *Pch*); and iv) the presence of a physically and chemically favorable environment (*Pb*), which considers soil temperature, pH, water activity and toxicity of the environment. The following equation determines this habitability index (*HI*):

$$[\text{Eq. 1}] \quad HI = Plw \cdot \frac{Pe1 + Pe2}{2} \cdot \frac{Pch1 + Pch2 + Pch3 + Pch4 + Pch5 + Pch6}{6} \cdot \frac{Pb1 + Pb2 + Pb3 + Pb4}{4}$$

In Eq. 1, each factor is divided into sub-categories where they are assigned a value ranging from 0 to 1 (0: factor not observed; 0.5: factor observed, but measurement uncertain; 1: factor observed). Stoker et *al.'s* (2010) equation were used, in the context of this thesis, to determine the habitability in different thermal and moisture zones in UV. These habitability indexes were calculated for UV's icy soils and were compared with those previously calculated by Stoker et *al.* (2010), for various sites on Mars.

3.9 Statistical Analysis

The Shapiro-Wilk normality test was first performed on the dissolved ionic concentrations, $\%C_{org}$, $\%C_{inorg}$, %N and DOC (concentration and $^{13}C_{DOC}$) data of the ice-cemented permafrost cores. Since some of the data showed non-normal distribution, the Mann-Whitney U test was used to compare median values of $\%C_{org}$, $\%C_{inorg}$, %N, $\delta^{13}C_{org}$, $^{13}C_{DOC}$ and DOC, between and within polygons (for the top 20 cm, 50 cm and 100 cm sections of cores). This test calculated the sum of ranks between two different core sample groups, in order to evaluate their representability; a significant test ($P \leq 0.05$) indicated that it was very likely that these groups came from populations with different median values. All statistical analyses were performed using the R Studio statistical analysis software.

4. Results

4.1 Soluble ions distribution and concentration in the icy soils of UV

4.1.1 Soil depth profiles

In the 16 icy permafrost cores, the abundance of cations (Ca^{2+}, Na^{+} and Mg^{2+}) ranged from 1.5 to 603.4 mg/kg^{-1} of dry soil mass (Fig. 3). The highest concentrations were found in the upper section of the valley (i.e., P7-C1, P8-C3, P11-C1 and P11-C1), whereas the lowest concentrations were found in middle portion of the valley (i.e., P1-C1, P4-C1, P5-C1, P6-C3) (Fig. 8). In all vertical profiles, the concentration of cations showed no clear pattern. Na^{+} was the dominant cation, followed by Ca^{2+} and Mg^{2+}.

The concentration of Na^{+} in top 20 cm of the 16 permafrost cores fluctuated from 21.9 to 603.4 mg/kg^{-1}, and from 14.3 to 603.4 mg/kg^{-1} in the top 50 cm (Table 2). Moreover, the cumulative concentration of Na^{+} per unit area varied from 4.6 to 43.5 mg/m^{-2} in the top 20 cm of the permafrost cores, and from 4.6 to 116.8 mg/m^{-2}, in the top 50 cm.

The Ca^{2+} concentrations varied between 1.5 to 275.9 mg/kg^{-1} in the top 20 cm of the 16 cores and from 48.9 to 304.7 mg/kg^{-1} in the top 50 cm (Table 1). The maximum cumulative concentration of Ca^{2+} per unit area in the upper 20 cm of the icy soils fluctuated between 0.5 to 14.2 mg/m^{-2}, and varied from 3.5 to 48.8 mg/m^{-2} in the top 50 cm (Fig. 5).

The Mg^{2+} concentrations ranged from 3.0 to 162.6 mg/kg^{-1} in the top 20 cm and from 1.6 to 175.8 mg/kg^{-1} in the top 50 cm (Table 3). The cumulative concentration of Mg per unit area in the top 20 cm and 50 cm varied from 0.8 to 10.2 mg/m^{-2}, and from 1.7 to 29.3 mg/m^{-2}, respectively.

The abundance of anions (Cl^{-}, SO_4^{2-} and NO_3^{-}) in the 16 icy permafrost cores ranged from 0.5 to 1441 mg/kg of dry soil mass (Fig. 4). Similar to cations, the highest concentrations were found in the upper section of the valley (especially in the P11-C1 and P12-C1 cores, which have concentrations 1 or 2 orders of magnitude higher than the ones for other sampled icy soils), and lower concentrations were found in the middle portion

of the valley (Fig. 9). In all vertical profiles, the concentration of anions showed no clear pattern. SO_4^{2-} was the dominant ions, followed by NO_3^- and Cl^-.

The SO_4^{2-} concentrations varied between 1.1 and 1441.5 mg/kg^{-1} in the top 20 cm and fluctuated between 3.6 and 1441.5 mg/kg^{-1} in the top 50 cm. The cumulative concentration SO_4^{2-} per unit area ranged from 0.7 to 74.6 mg/m^{-2} and from 3.1 to 248.9 mg/m^{-2} in the top 20 and 50 cm, respectively.

The NO_3^- concentrations ranged from 1.1 to 999.7 mg/kg^{-1} in the top 20 cm of the 16 cores and from 1.0 to 999.7 mg/kg^{-1} in the top 50 cm (Table 6). The cumulative concentration per unit area varied from 0.3 to 72.9 mg/m^{-2} in the top 20 cm of the permafrost cores and from 0.7 to 171.5 mg/m^{-2} in the top 50 cm.

Cl^- was the least abundant soluble anion in the icy permafrost cores. The concentrations of Cl^- in the top 20 cm varied between 0.5 and 269.4 mg/kg^{-1} and ranged from 0.4 to 269.4 mg/kg^{-1} in the top 50 cm (Table 4). Cumulative Cl^- concentration values per unit area in the upper 20 cm and 50 cm varied from 0.1 to 20.3 mg/m^{-2}, and from 0.24 to 47.36 mg/m^{-2} respectively (Fig. 6).

Overall, a SO_4-NO_3-Na-Ca geochemical facies dominated the water-soluble ions with total soluble ion concentration within a sample ranging from 28.63 to 3297.49 mg/kg^{-1}.

4.1.2 Ionic ratios of water-soluble salts

Claridge and Campbell (1977), and McLeod et *al*. (2008) analyzed soils from the MDV and provided average ionic ratios of water-soluble salts relative to potassium (K), which removed the effect of salt content within a parent material. Using the same method, the values for soil Ionic ratios in University Valley was calculated (Fig. 7). The Ca/K ratios in the upper section of the valley ranged from 0.5 to 20.6, whereas they showed a narrower range in the middle (0.1 – 13.1) and lower section of the valley (2.2 - 7.0). Mg/K ratios followed the same trend as Ca/K ratios: they were highest in UV's upper valley icy soils (1.0 – 16.5) and were similar in the middle (0.9 – 4.8) and lower section of the valley (1.2 – 2.5). Na/K ratios were generally highest in the upper section of the valley

(5.9 - 69.2) and were lowest in the middle (3.3 and 66.1) lower section of the valley (7.7 – 15.3). SO_4/K ratios in the upper section of the valley (0.3 – 59.8) were much higher (sometimes 1 order of magnitude higher) than in the middle (0.1 – 7.4) and lower (0.1 – 0.5) sections of the valley. Similarly, the highest Cl/K ratios were found in the upper section of the valley (0.1 – 24.1); these ratios were once again sometime 1 order of magnitude higher than the ones in the middle (0.1 – 1.5) and lower (0.1 – 0.4) sections of the valley.

Finally, to assess the contribution of sea-salts, the Na/Cl ratio was also determined. The Na/Cl ratios were similar between ice cemented permafrost cores, but are the highest in UV's mid valley (26.1 - 252.5) and the lowest in upper UV's icy soils (2.4 - 153.1) (Fig. 7). Additionally, the Na/Cl ratios for the P10-C1 core (located in the lowest portion of UV) ranged between 27.15 and 114.83.

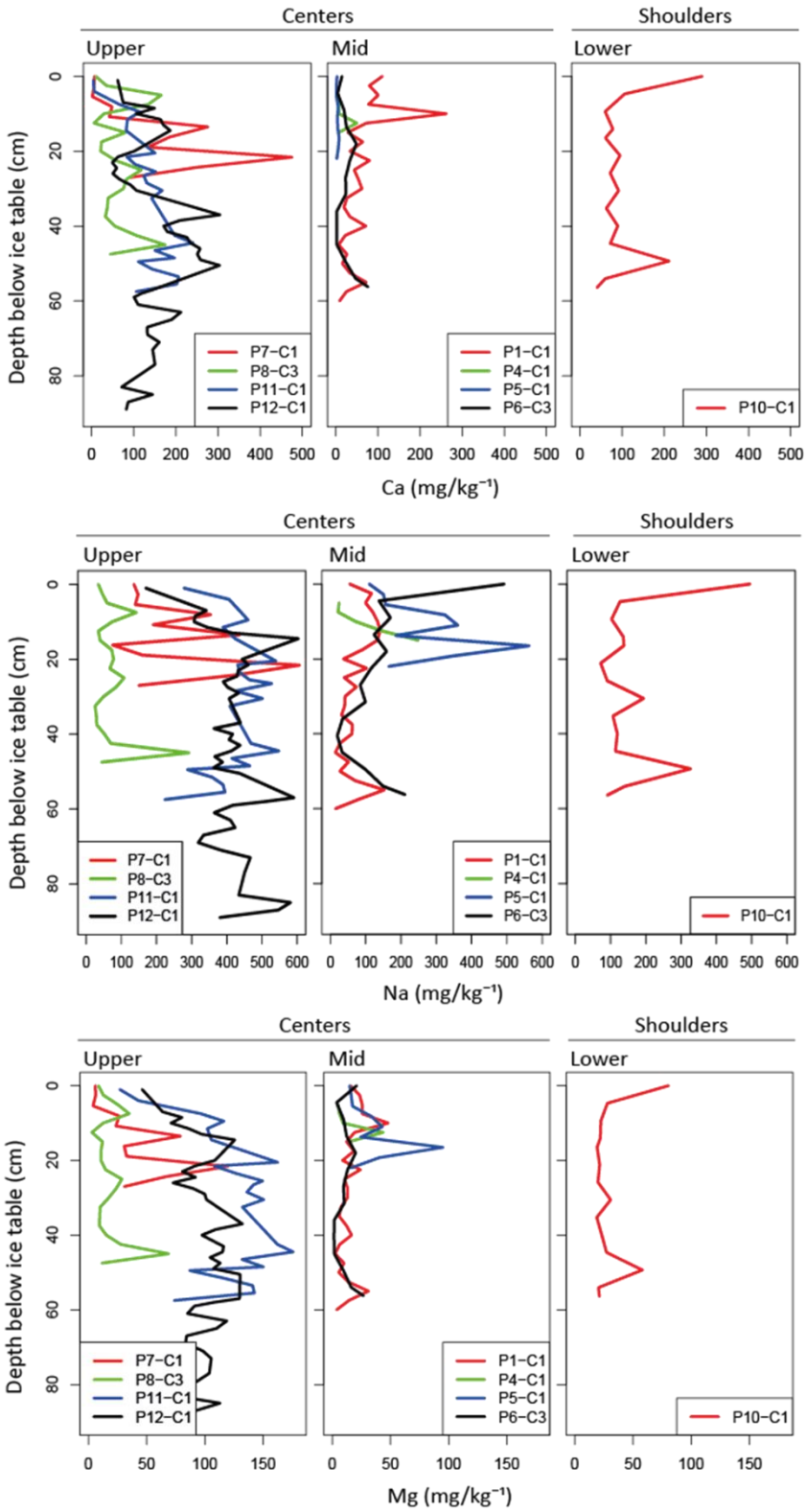

Figure 3 : Concentrations (mg/kg^{-1}) of cations (Ca^{2+}, Na^{+} and Mg^{+}) in the icy soils of UV's middle and upper valley polygon centers and lower valley shoulders.

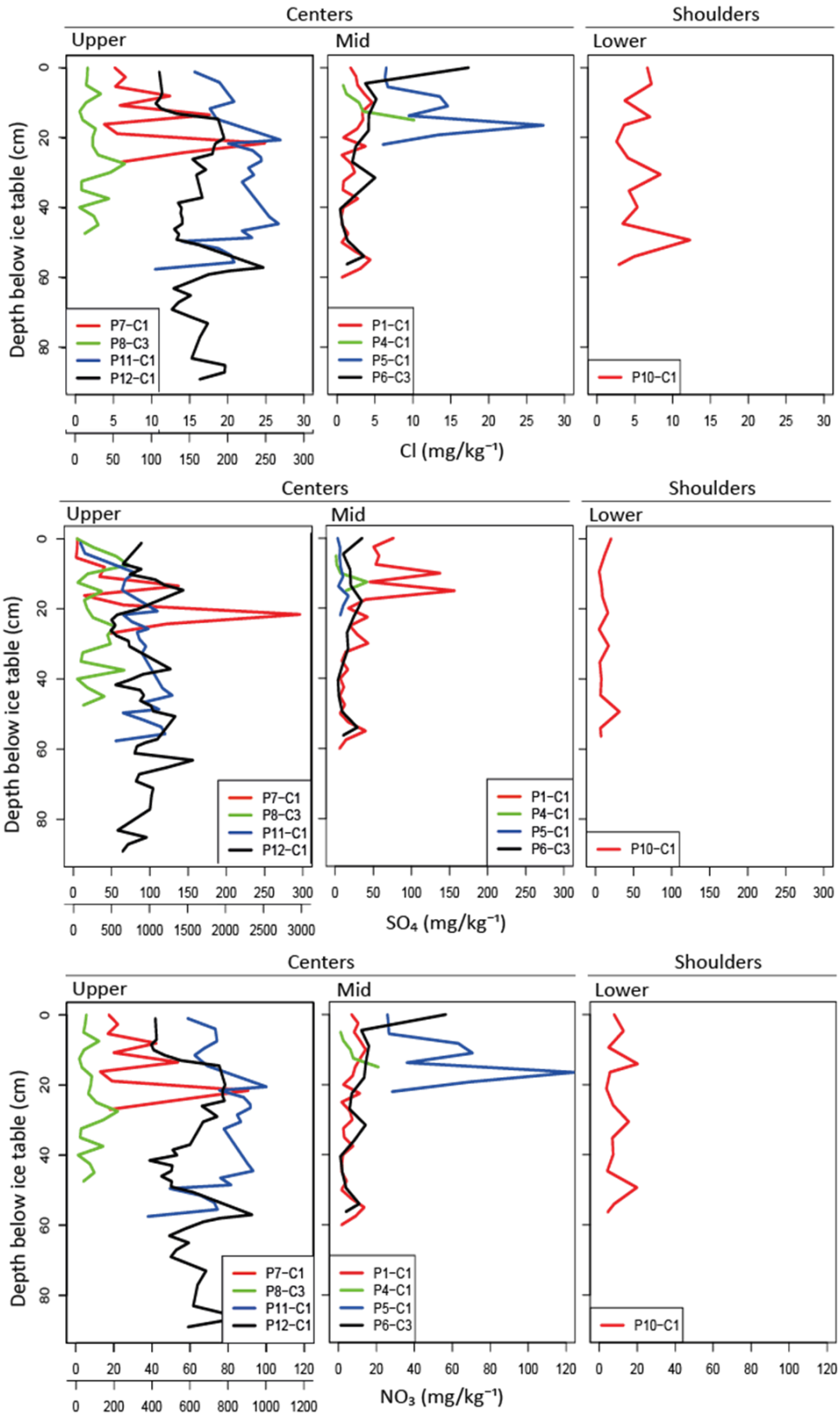

Figure 4 : Concentrations (mg/kg^{-1}) of anions (Cl^-, SO_4^{2-} and NO_3^-) in the icy soils of UV's middle and upper valley polygon centers and lower valley shoulders.

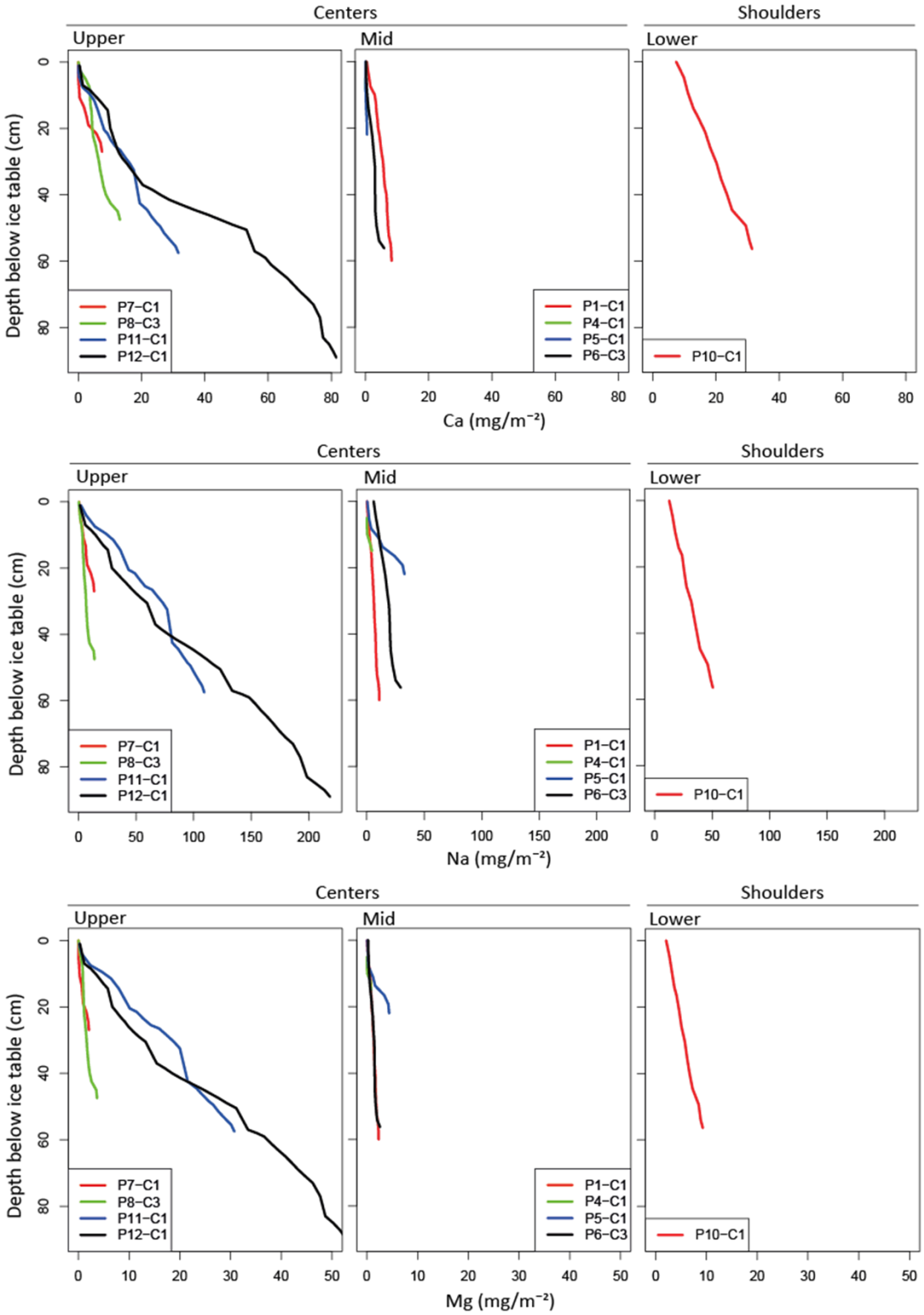

Figure 5 : Cumulative concentration (mg/m^{-2}) of cations (Ca^{2+}, Na^{+} and Mg^{+}) in the icy soils of UV's middle and upper valley polygon centers and lower valley shoulders.

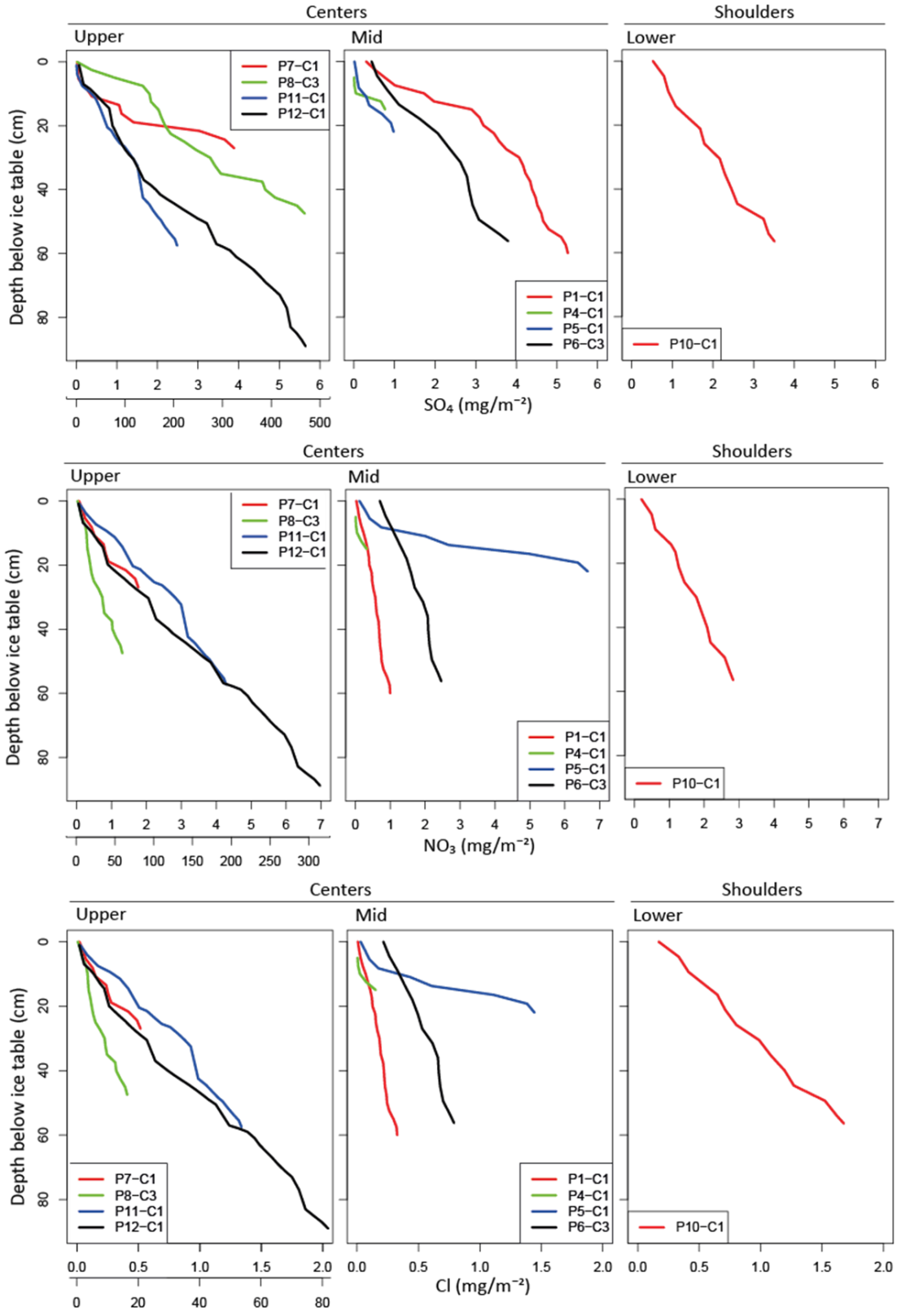

Figure 6 : Cumulative concentration (mg/m^{-2}) of anions (SO_4^{2-}, NO_3^- and Cl^-) in the icy soils of UV's middle and upper valley polygon centers and lower valley shoulders.

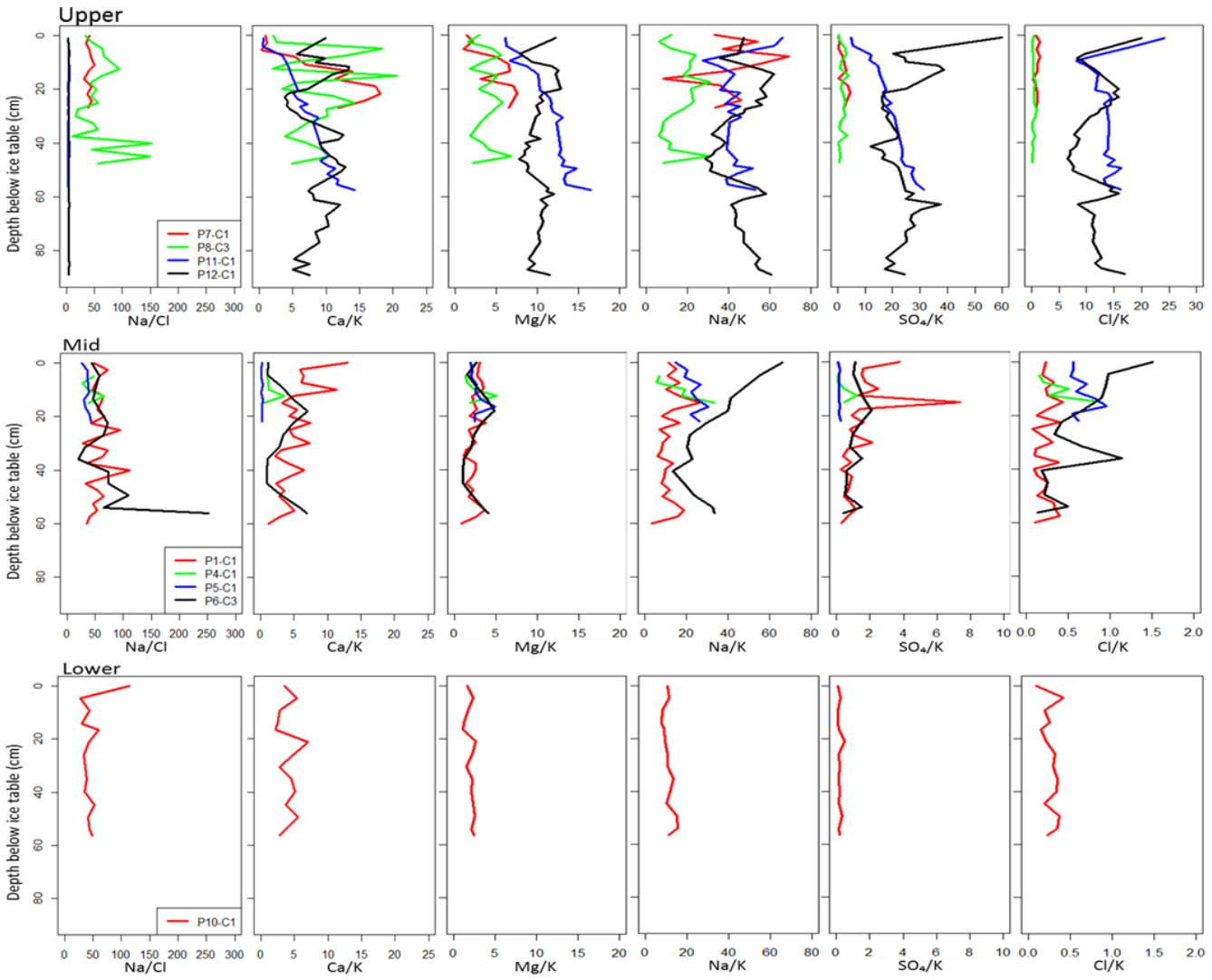

Figure 7 : Ionic ratios between UV's icy soil samples.

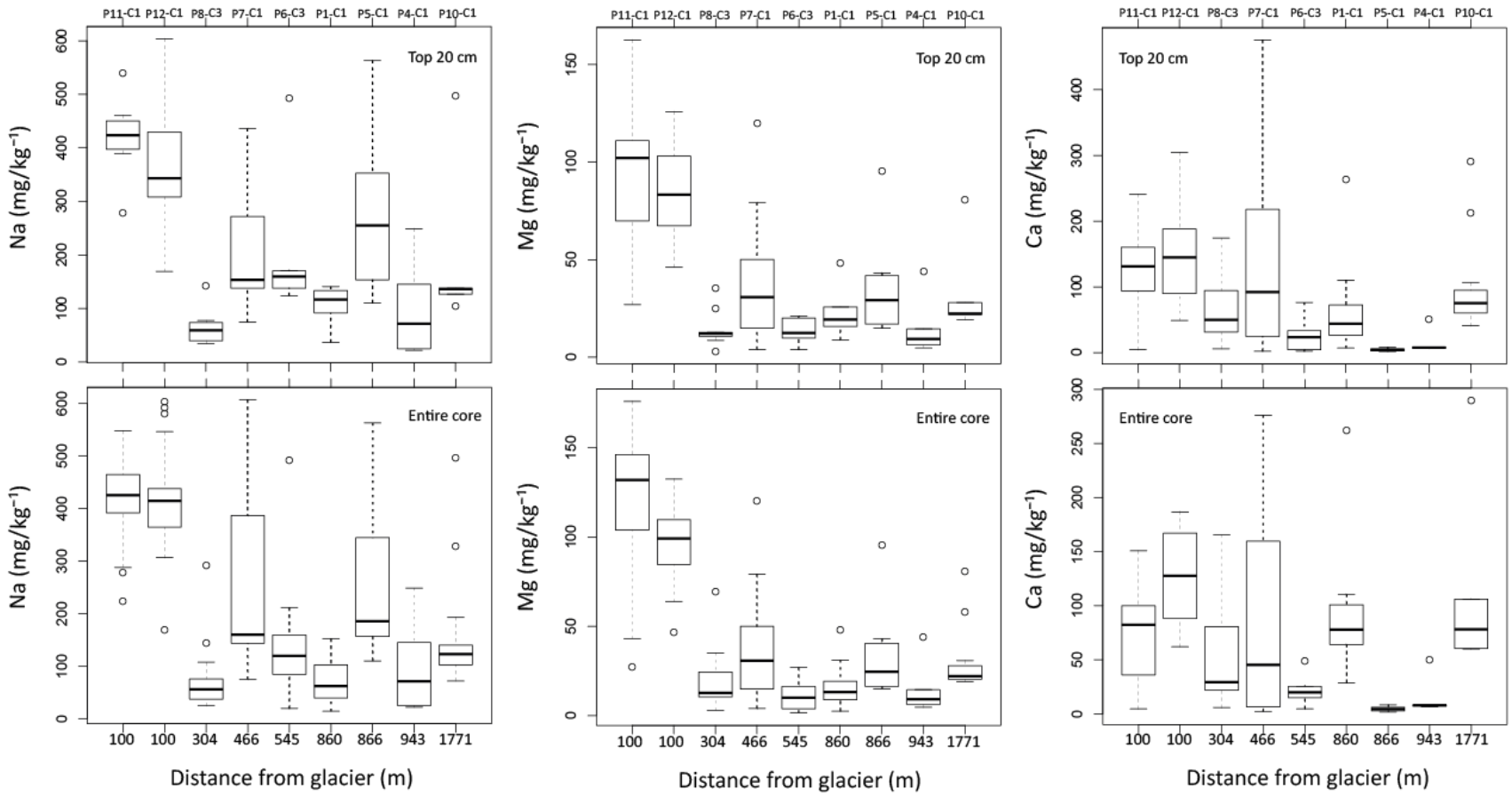

Figure 8 : Cation concentration (Na^+, Mg^+ and Ca^{2+}; mg/kg^{-1}) boxplots for UV's icy soils, with regards to their distance from UG.

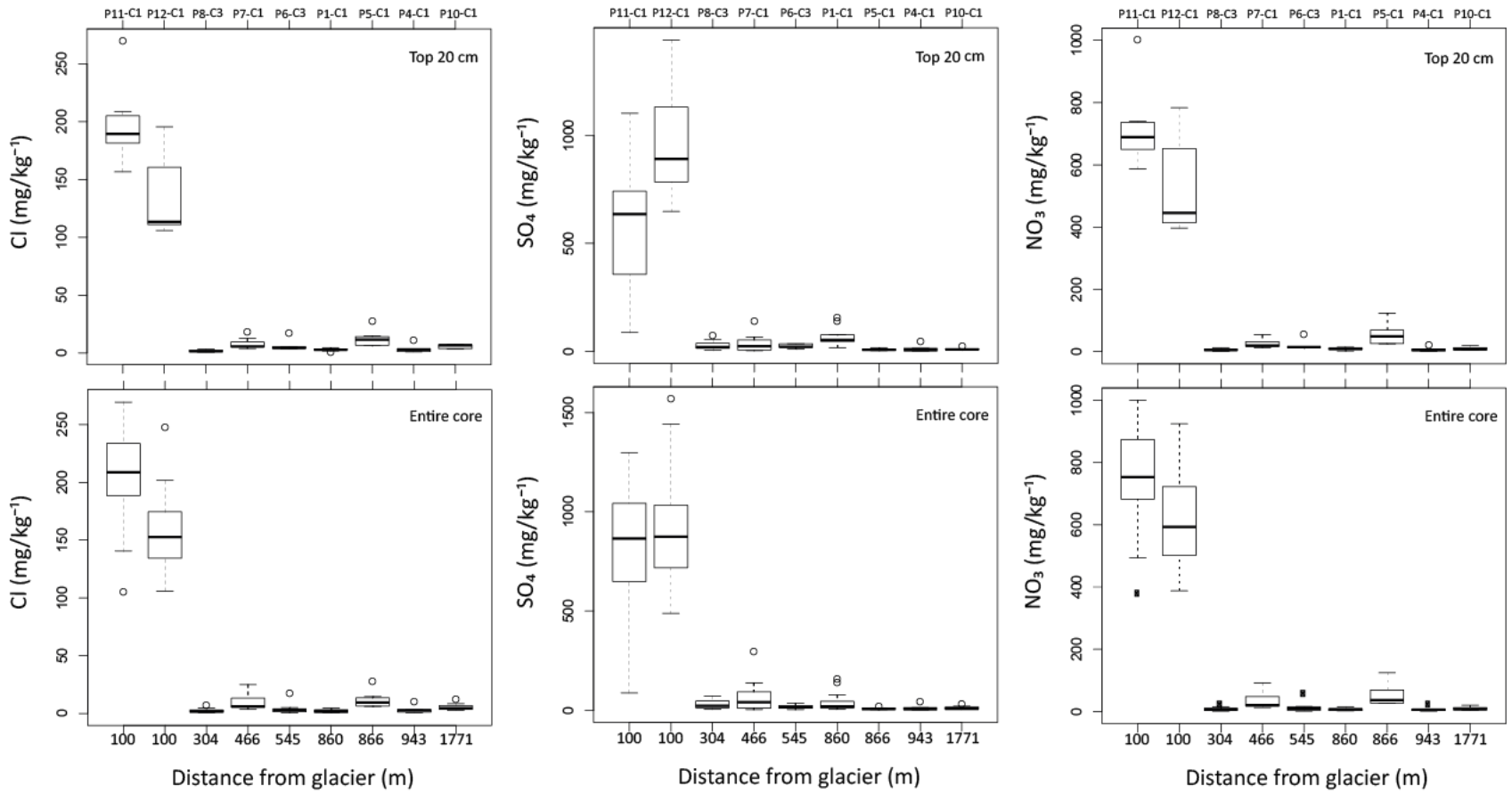

Figure 9 : Anion concentration (Cl^-, SO_4^{2-} and NO_3^-; mg/kg^{-1}) boxplots for UV's icy soils, with regards to their distance from UG.

Table 3: Summary statistics for Ca^{2+} concentrations (mg/kg^{-1}) in the first 20 and 50 cm of UV's icy soils.

		Top 20 cm					Top 50 cm				
Core ID	location	Mean	Median	Max	Min	SD	Mean	Median	Max	Min	SD
P1-C1	Center	92.21	77.73	262.22	28.68	69.19063	61.511	53.64	262.223	6.962	54.41651
P4-C1	Center	15.809	7.756	50.012	6.335	19.13104	--	--	--	--	--
P5-C1	Center	4.423	4.296	8.184	1.543	2.255086	--	--	--	--	--
P6-C3	Center	22.62	19.67	48.94	4.46	16.58749	18.727	21.388	48.944	2.321	14.2449
P7-C1	Center	87.514	45.32	275.986	1.95	100.955	--	--	--	--	--
P8-C3	Center	56.211	29.269	165.31	5.777	57.75142	66.495	49.929	174.49	5.777	49.87677
P10-C1	Right shoulder	118.81	78.19	289.69	59.78	97.35098	107.32	83.96	289.69	59.78	70.45565
P11-C1	Center	72.718	82.166	150.711	4.502	53.67349	121.519	123.9	241.072	4.502	60.53646
P12-C1	Center	126.72	127.59	186.69	61.93	46.91308	149.71	156.71	304.73	48.95	78.83334

Table 4: Summary statistics for Na^{+} concentrations (mg/kg^{-1}) in the first 20 and 50 cm of UV's icy soils.

		Top 20 cm					Top 50 cm				
Core ID	location	Mean	Median	Max	Min	SD	Mean	Median	Max	Min	SD
P1-C1	Center	103.19	116.54	140.99	37.13	36.40806	71.54	61.44	140.99	14.26	40.54817
P4-C1	Center	102.48	71.37	248.78	21.92	95.82694	--	--	--	--	--
P5-C1	Center	274.4	255	562.8	110.1	152.2845	--	--	--	--	--
P6-C3	Center	216.8	159.6	492.3	123.8	155.0969	130.91	107.51	492.35	19.66	123.7905
P7-C1	Center	204.73	153.73	435.81	75.08	123.5994	--	--	--	--	--
P8-C3	Center	64.62	59.55	142.82	34.49	33.99112	71.63	55.79	292.29	25.22	59.49804
P10-C1	Right shoulder	199.8	136	495.5	102.8	165.9188	168.43	122.83	495.53	71.75	122.6252
P11-C1	Center	419.5	423.5	539.6	278.1	79.22563	437.6	436.6	547.6	278.1	70.98774
P12-C1	Center	366.8	343.1	603.4	169.2	126.1173	395	406.3	603.4	169.2	76.33823

Table 5: Summary statistics for Mg^{+} concentrations (mg/kg^{-1}) in the first 20 and 50 cm of UV's icy soils.

		Top 20 cm					Top 50 cm				
Core ID	location	Mean	Median	Max	Min	SD	Mean	Median	Max	Min	SD
P1-C1	Center	22.026	19.281	48.037	8.952	11.33698	15.572	13.054	48.037	2.535	10.13998
P4-C1	Center	15.745	9.329	43.801	4.787	16.11936	--	--	--	--	--
P5-C1	Center	35.77	29.22	95.16	15.03	26.37634	--	--	--	--	--
P6-C3	Center	13.446	12.386	21.041	3.885	7.215512	9.613	9.732	21.041	1.589	6.614077
P7-C1	Center	26.141	25.064	79.175	4.047	24.43491	--	--	--	--	--
P8-C3	Center	14.57	12.167	35.116	3.017	9.612375	18.474	12.746	68.953	3.017	14.40906
P10-C1	Right shoulder	34.42	22.46	80.46	19.22	25.93511	30.98	22.82	80.46	18.92	18.87315
P11-C1	Center	93.36	102.14	162.56	27.05	45.61776	121.42	131.99	175.85	27.05	39.01067
P12-C1	Center	84.93	83.32	125.73	46.18	25.50105	96.25	98.75	132.35	46.18	20.13536

Table 6 : Summary statistics for Cl^{-} concentrations (mg/kg^{-1}) in the first 20 and 50 cm of UV's icy soils.

		Top 20 cm					Top 50 cm				
Core ID	location	Mean	Median	Max	Min	SD	Mean	Median	Max	Min	SD
P1-C1	Center	2.8331	2.7107	4.6401	0.8468	1.099008	15.572	13.054	48.037	2.535	1.254567
P4-C1	Center	3.7082	2.9073	10.1669	0.8088	3.774273	--	--	--	--	--
P5-C1	Center	12.213	11.397	27.227	6.341	6.96316	--	--	--	--	--
P6-C3	Center	6.921	4.199	17.353	3.722	5.855617	4.1089	3.2043	17.3526	0.4111	4.46388
P7-C1	Center	7.771	5.665	17.641	3.787	4.758595	--	--	--	--	--
P8-C3	Center	1.749	1.5453	3.3288	0.5615	0.8582621	2.2619	1.9339	6.4823	0.5241	1.547031
P10-C1	Right shoulder	5.62	6.654	7.196	3.584	1.831731	5.7	4.79	12.278	2.587	2.758919
P11-C1	Center	198.3	189.3	269.4	156.6	35.60747	216	219	269.4	140.6	35.30406
P12-C1	Center	133.9	113.4	195.5	105.8	36.55333	146.9	140.1	195.5	105.8	26.98715

Table 7 : Summary statistics for SO_4^{2-} concentrations (mg/kg^{-1}) in the first 20 and 50 cm of UV's icy soils.

		Top 20 cm					Top 50 cm				
Core ID	location	Mean	Median	Max	Min	SD	Mean	Median	Max	Min	SD
P1-C1	Center	70.5	53.31	156.54	17.34	46.39328	40.477	28.955	156.537	6.052	40.83234
P4-C1	Center	13.141	7.094	41.773	1.128	16.79831	--	--	--	--	--
P5-C1	Center	8.076	6.811	17.32	3.136	4.536158	--	--	--	--	--
P6-C3	Center	24.08	20.37	35.32	10.44	10.72457	17.023	16.217	35.316	3.629	10.47695
P7-C1	Center	38.35	24.228	137.69	3.642	45.68571	--	--	--	--	--
P8-C3	Center	28.096	18.954	71.895	4.461	22.94059	29.575	22.285	71.895	4.461	21.2959
P10-C1	Right shoulder	10.88	8.997	20.4	4.821	5.888105	11.962	8.64	31.265	4.65	7.994959
P11-C1	Center	574.36	635.67	1102.71	86.88	357.6082	795.83	833.85	1296.19	86.88	311.0848
P12-C1	Center	963.1	891.6	1441.5	647.8	259.3291	835	852.6	1441.5	488.2	251.9367

Table 8 : Summary statistics for NO_3^- concentrations (mg/kg^{-1}) in the first 20 and 50 cm of UV's icy soils.

		Top 20 cm					Top 50 cm				
Core ID	location	Mean	Median	Max	Min	SD	Mean	Median	Max	Min	SD
P1-C1	Center	9.076	8.789	14.346	2.619	3.367833	6.336	6.861	14.346	1.615	3.970221
P4-C1	Center	7.772	6.264	21.06	1.082	7.906711	--	--	--	--	--
P5-C1	Center	55.24	49.6	124.22	25.81	34.10125	--	--	--	--	--
P6-C3	Center	22.55	14.5	56.62	12.07	19.09822	12.934	10.138	56.62	1.028	14.68047
P7-C1	Center	25.44	19.42	53.74	12.73	14.50262	--	--	--	--	--
P8-C3	Center	5.719	4.865	12.07	1.744	3.163653	7.301	5.963	21.99	1.103	5.290326
P10-C1	Right shoulder	10.304	7.851	20.225	4.962	6.333694	9.712	7.342	20.225	3.811	5.889884
P11-C1	Center	721.2	689.3	999.7	587.4	134.5153	784.3	777.1	999.7	494	131.7852
P12-C1	Center	525.6	445.8	783.7	397.2	157.6548	574.7	520.1	783.7	387.7	139.9142

4.2 Distribution of inorganic carbon in the icy soils

The abundance of soil inorganic carbon (SIC) in the 16 ice-cemented permafrost cores ranged from 0 to 2.5 mg/g^{-1} dry soil (Fig. 10). With the exception of P10, little variation in abundance was observed with depth in the icy soils. Samples collected from both the center and shoulders of three polygons: P8 (304 m from the glacier), P6 (545 m from the glacier) and P1 (860 m from the glacier), were used to assess changes in inorganic carbon content within polygons. Based on the Mann-Whitney U test (Appendix 2M; Appendix 2N; Appendix 2O), the median inorganic carbon content in P8 was statistically similar between the center (P8-C3) and shoulders (P8-C5; P8-C6) of the polygon in the top 20 and 50 cm. In P6, the shoulders (P6-C5) of the polygon contained significantly higher abundance of inorganic carbon relative to its center (P6-C3) in both the upper 20 and 50 cm. Finally, no significant differences between the median inorganic carbon concentrations were observed in P1 for the upper 20 cm portion; however, there is significantly more inorganic carbon in the center of the polygon (P1-C1) relative to the shoulders (P1-C2) in the top 50 cm.

Along the valley floor (Fig. 11), the concentrations of SIC were similar for icy soils sampled between 304 and 1076 m distance of UG (Fig. 12); albeit a small non-significant increase was observed for the P6-C5 site (shoulder of polygon) situated at 545 m distance. The icy soils in lower section of the valley, P9 and P10 (1692 and 1771 m distance, respectively), contained the highest SIC concentrations (up to 2.5 mg/g^{-1} dry soil).

The SIC stock per unit area (SICC; g/m^{-2}) in the icy soils was relatively similar throughout the valley, (Fig. 12). It fluctuated from 147.2 to 2043.6 g/m^{-2} in the 0-20 cm depth of icy soils situated in the NCZ and from 272.3 to 1186.4 g/m^{-2} in the same depth horizon sites in the PCZ. In the top 50 cm, the SIC stock for sites in the PCZ varied from 555.6 to 4410.1 g/m^{-2}, which was slightly higher than the icy soils sampled in the NCZ (which ranged from 264.0 to 3679.3 g/m^{-2}).

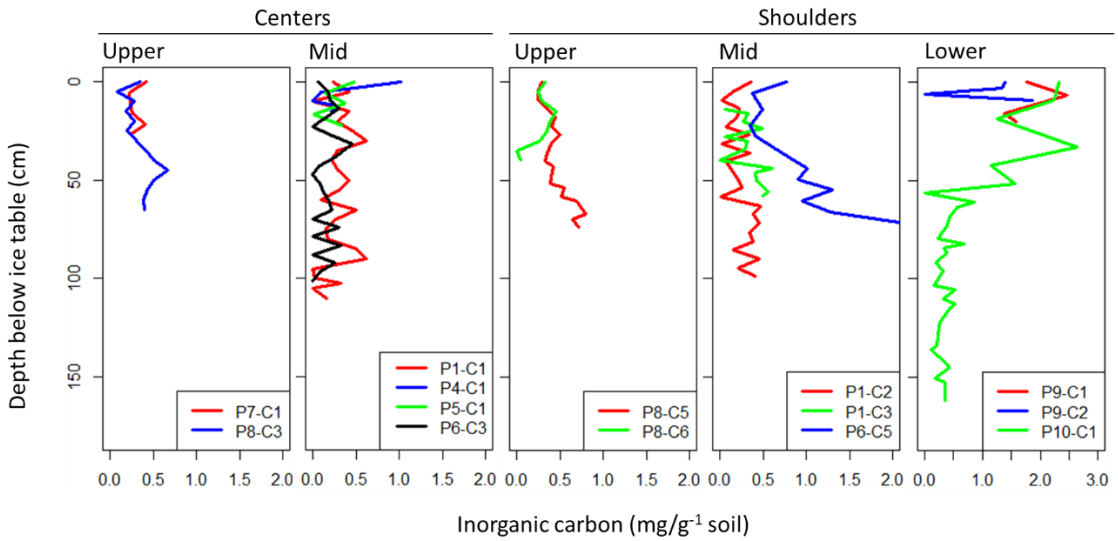

Figure 10: Inorganic carbon concentration (mg/g^{-1} soil), with depth, of UV's ice cemented permafrost cores.

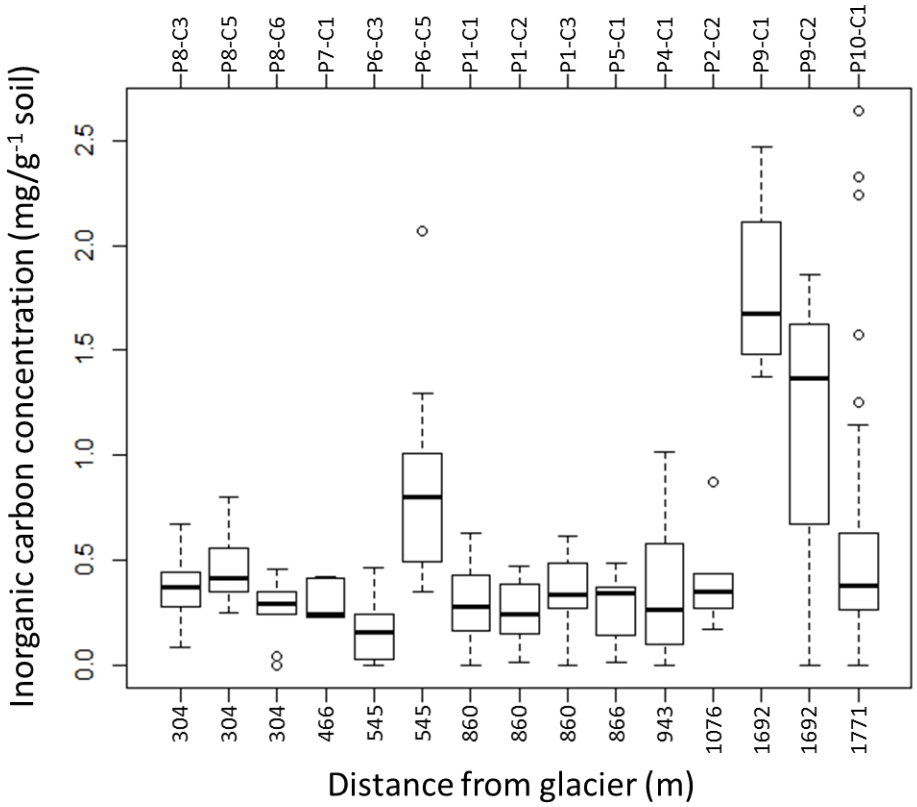

Figure 11: Relationship between the inorganic carbon concentration (mg/g^{-1} soil) of UV's icy soils and their distance from UG.

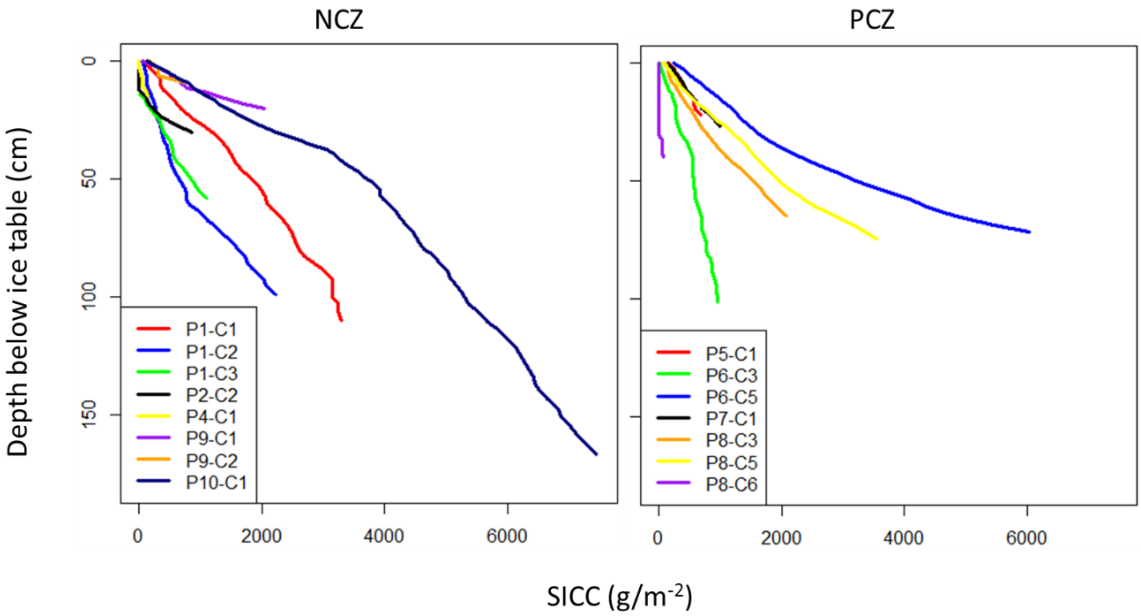

Figure 12 : Cumulative soil inorganic carbon concentration (SICC; g/m^{-2}) of UV's icy soils sampled in the NCZ and PCZ.

Table 9 : Summary statistics for UV's icy soils inorganic carbon concentrations (mg/g^{-1} soil).

		Top 20 cm					Top 50 cm					Top 1 m				
Core ID	Location	Mean	Median	Max	Min	SD	Mean	Median	Max	Min	SD	Mean	Median	Max	Min	SD
P1-C1	Center	0.272	0.283	0.427	0.001	0.174	0.332	0.290	0.627	0.001	0.163	0.300	0.283	0.627	0.000	0.188
P1-C2	Right Shoulder	0.196	0.195	0.367	0.023	0.124	0.185	0.195	0.367	0.023	0.128	0.254	0.241	0.474	0.016	0.152
P1-C3	Right Shoulder	0.221	0.268	0.333	0.061	0.142	0.298	0.312	0.614	0.000	0.194	N/A	N/A	N/A	N/A	N/A
P2-C2	Deflation surface	0.299	0.294	0.439	0.170	0.112	N/A	N/A	N/A	N/A	N/A	N/A	N/A	N/A	N/A	N/A
P4-C1	Center	N/A	N/A	N/A	N/A	N/A	N/A	N/A	N/A	N/A	N/A	N/A	N/A	N/A	N/A	N/A
P5-C1	Center	0.252	0.254	0.483	0.015	0.213	N/A	N/A	N/A	N/A	N/A	N/A	N/A	N/A	N/A	N/A
P6-C3	Center	0.178	0.171	0.308	0.057	0.090	0.171	0.171	0.463	0.000	0.140	0.158	0.164	0.463	0.000	0.129
P6-C5	Left Shoulder	0.546	0.492	0.774	0.373	0.481	0.634	0.607	1.007	0.349	0.244	N/A	N/A	N/A	N/A	N/A
P7-C1	Center	0.282	0.242	0.419	0.227	0.092	N/A	N/A	N/A	N/A	N/A	N/A	N/A	N/A	N/A	N/A
P8-C3	Center	0.237	0.277	0.351	0.088	0.101	0.344	0.303	0.671	0.088	0.169	N/A	N/A	N/A	N/A	N/A
P8-C5	Right Shoulder	0.317	0.291	0.446	0.249	0.083	0.363	0.348	0.506	0.249	0.081	N/A	N/A	N/A	N/A	N/A
P8-C6	Left Shoulder	0.341	0.328	0.458	0.241	0.084	0.263	0.291	0.458	0.000	0.152	N/A	N/A	N/A	N/A	N/A
P9-C1	Right Shoulder	1.797	1.672	2.471	1.372	0.476	N/A	N/A	N/A	N/A	N/A	N/A	N/A	N/A	N/A	N/A
P9-C2	Left Shoulder	N/A	N/A	N/A	N/A	N/A	N/A	N/A	N/A	N/A	N/A	N/A	N/A	N/A	N/A	N/A
P10-C1	Right Shoulder	1.940	2.243	2.327	1.250	0.599	1.921	2.243	2.642	1.145	0.678	0.916	0.567	2.642	0.000	0.823

4.3 Distribution, $\delta^{13}C$ and age of organic carbon in the icy soils

4.3.1 Soil depth profiles

4.3.1.1 C_{org}

The abundance of organic carbon in the 16 icy permafrost cores ranged from 0.1 to 9.3 mg/g^{-1} dry soil (Fig. 13). With the exception of P10, little variation in abundance of organic carbon was observed with depth at each site. Based on the Mann-Whitney U test (Appendix 2P; Appendix 2Q; Appendix 2R), the median organic carbon content in P8 (304 m from UG) was significantly higher in the top 20 cm of the left shoulder (P8-C6) of the polygon relative to the right shoulder (P8-C5) and center (P8-C3). However, there was no difference in organic carbon content between the center and shoulders in the top 50 cm. At P6 (545 m from UG), the organic carbon content was statistically similar in the top 20 cm between the center (P6-C3) and shoulder (P6-C5) of the polygon; however in the top 50 cm, the organic carbon content was significantly higher in the center of the polygon. At P1 (860 m from UG), the organic carbon content was significantly higher in the shoulders (P1-C3) relative to the center (P1-C1) of the polygon, this for both the top 20 and 50 cm.

Along the valley floor, the concentrations of organic carbon were similar for icy soils sampled between 304 and 1076 m distance of UG, ranging between 0.1 and 2 mg/g^{-1} dry soil (Fig. 14). However, the icy soils in lower section of the valley, P9 and P10 (1692 and 1771 m distance, respectively), contained the highest organic carbon concentrations (up to 9.3 mg/g^{-1} dry soil).

Soil organic carbon stock per unit area (SOCC; g/m^{-2}) were very similar for the sites in the PCZ, but those situated in the NCZ showed some variations (Fig. 15). The SOCC in the top 20 cm for sites in the PCZ varied from 723.2 to 1058.9 g/m^{-2}, whereas those from the NCZ ranged from 905.0 to 3621.6 g/m^{-2}. In the top 50 cm, the SOCC of the soils located in the PCZ and NCZ ranged from 1058.9 to 2968.5 g/m^{-2} and 2318.2 to 7842.6 g/m^{-2}, respectively.

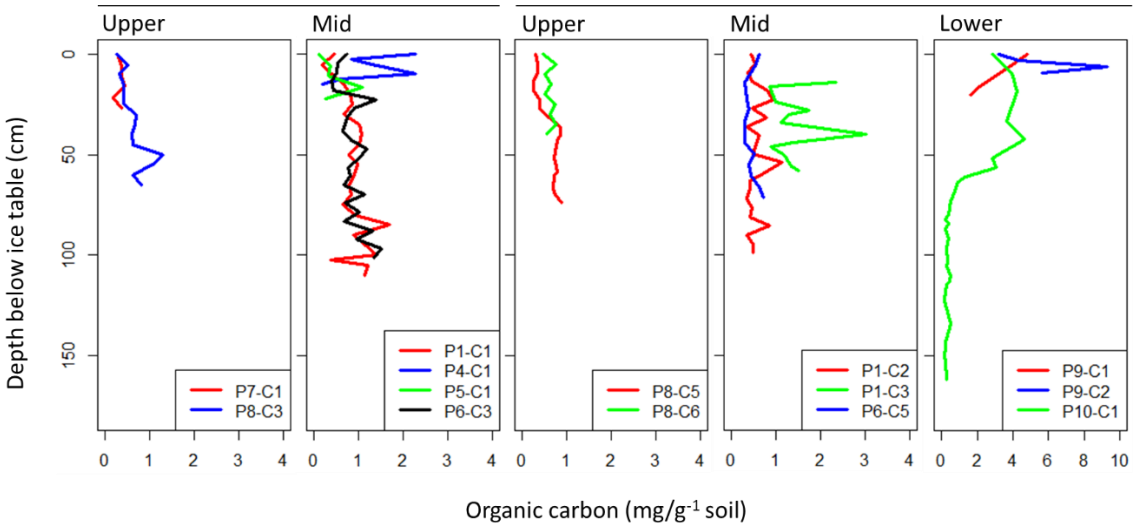

Figure 13 : Organic carbon concentration (mg/g^{-1} soil), with depth, of UV's icy soils.

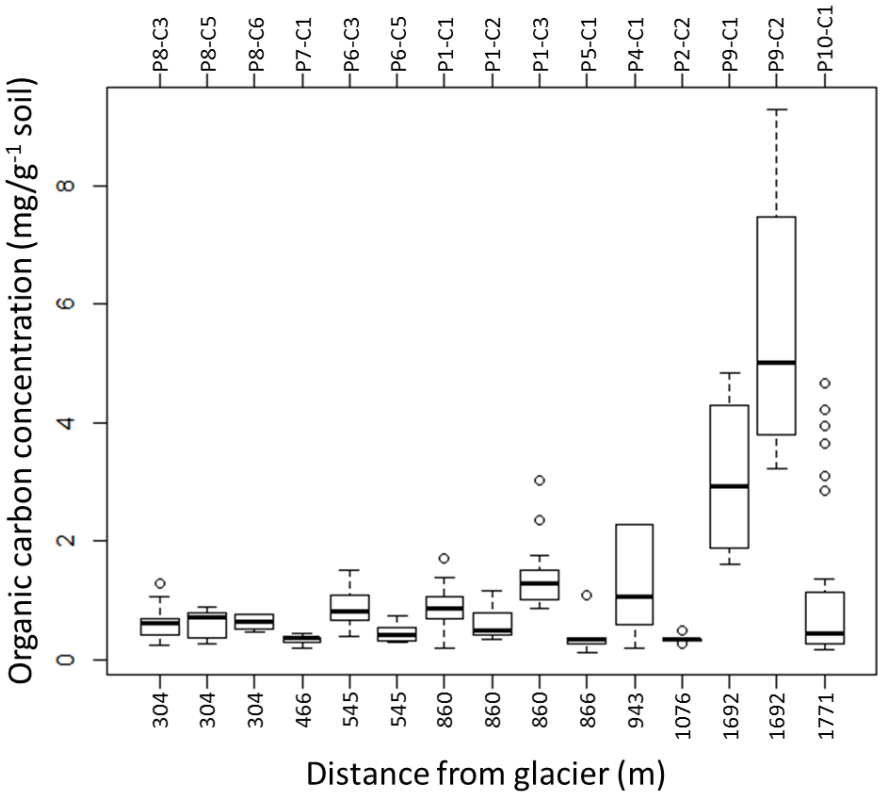

Figure 14: Relationship between the organic carbon concentration (mg/g^{-1} soil) of UV's icy soils and their distance from UG.

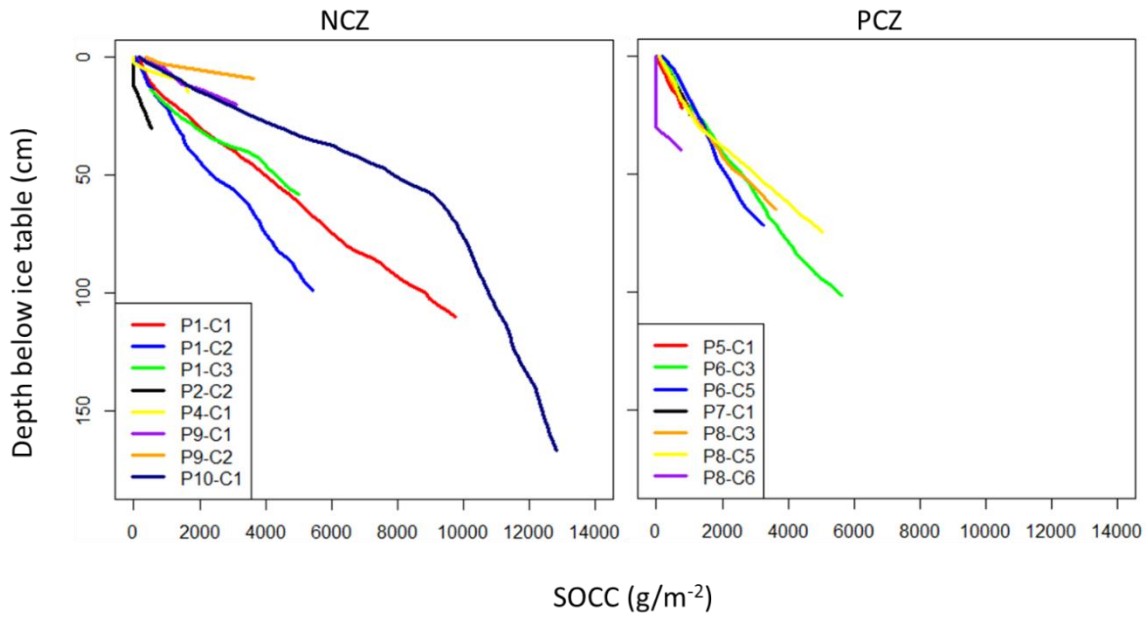

Figure 15 : Cumulative soil organic carbon concentration (SOCC; g/m^{-2}) of UV's icy soils sampled in the NCZ and PCZ.

4.3.2 $\delta^{13}C$ composition of organic carbon

In UV, the $\delta^{13}C_{org}$ of the ice cemented permafrost soils ranged from -31.7 to -24.1‰ and showed very little variation with depth (Table 10). Based on the Mann-Whitney U-test (Appendix 2V), the $\delta^{13}C_{org}$ values in the top 20 and 50 cm of P8 were similar in the center (P8-C3) and shoulders (P8-C5; P8-C6). A similar observation was made at P6 where the center and shoulder of the polygon had similar $\delta^{13}C_{org}$ values: the median $\delta^{13}C_{org}$ value for P6-C3 (center) and P6-C5 (shoulder) were respectively -26.0‰ and -25.6‰. At P1, the $\delta^{13}C_{org}$ values were significantly different between all soils of the three cores (entire length). Their median $\delta^{13}C_{org}$ values were -27.9‰ at the shoulder (P1-C3) and -25.9‰ at the center (P1-C1) (Table 9).

Along the valley floor, the range in $\delta^{13}C_{org}$ values at each site showed a non-significant trend towards lower values (Fig. 16). Median $\delta^{13}C_{org}$ values were generally highest in soils that were sampled in the PCZ: they varied between -26.8‰ and -25.6‰. Icy soils sampled in the NCZ were generally slightly more depleted in $\delta^{13}C_{org}$ (median values ranging from -29.9 to -25.7‰) relative to soils from the PCZ (Table 10).

Table 10: Summary statistics for the $\delta^{13}C_{org}$ signal of UV's ice cemented permafrost soils.

Core ID	Location	Mean	Median	Max	Min	SD
P1-C1	Center	-25.91	-25.66	-24.08	-28.35	1.122
P1-C2	Right Shoulder	-27.91	-27.97	-26.52	-29.8	0.719
P1-C3	Right Shoulder	-27.03	-26.95	-26.47	-28.15	0.509
P2-C2	Deflation surface	-27.5	-27.49	-26.62	-28.06	0.573
P4-C1	Center	-29.78	-29.95	-27.52	-31.68	1.410
P5-C1	Center	-27.8	-27.59	-27.45	-28.49	0.419
P6-C3	Center	-26.26	-26	-24.82	-30.26	1.153
P6-C5	Left Shoulder	-25.21	-25.64	-21.28	-27.06	1.663
P7-C1	Center	-26.26	-26.22	-25.89	-26.69	0.286
P8-C3	Center	-25.44	-26.12	-22.54	-27.28	1.709
P8-C5	Right Shoulder	-26.03	-25.73	-24.83	-28.04	1.151
P8-C6	Left Shoulder	-26.38	-26.79	-23.88	-27.48	1.123

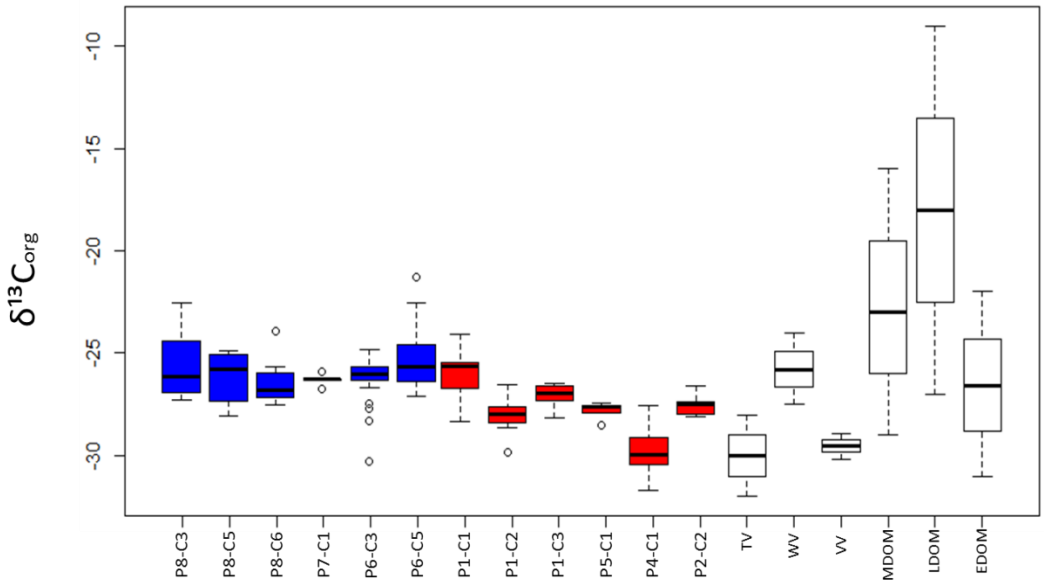

Figure 16 : $\delta^{13}C_{org}$ signal from UV's ice cemented permafrost soils (polygons are in order of distance from UG) compared to other soils in the MDV. Blue boxplots indicate cores taken from the PCZ and red boxplots indicate cores sampled in the NCZ. Abbreviations TV, WV, VV, MDOM, LDOM and EDOM stand for Taylor Valley, Wright Valley, Victoria Valley, marine-derived organic matter, lake-derived organic matter and endolith-derived organic matter (values taken from Hopkins et *al.*, 2009)

4.3.3 Age of organic carbon

Radiocarbon measurements of organic matter in the icy soils were performed only on the P11-C1 core. The three $^{14}C_{org}$ ages ranged from 11,700 to 9,950 yr BP (Table 11). P11-C1's youngest organic material was found 1 cm below the ice table (9,950 +/- 40 yr. BP.). The oldest organic material was located at 4 cm below ice table depth (11,700 +/- 50 yr. BP.). The age of the core's organic matter located 15 cm below the ice table fell between the two other samples (10,920 +/- 50 yr. BP).

Table 11 : $^{14}C_{org}$ ages of P11-C1's icy soils.

Depth below ice table (cm)	(14C yr. B.P.)	Calibrated age (2 σ ranges)	δ^{13}Corg
1	9,950 +/- 40	9,650 BC to 9,580 BC	-25.7‰
4	11,700 +/- 50	11,730 BC to 11,470 BC	-24.1‰
15	10,920 +/- 50	10,950 BC to 10,720 BC	-24.7‰

Table 12: Summary statistics for UV's icy soils organic carbon concentrations (mg/g^{-1} soil).

		Top 20 cm					Top 50 cm					Top 1 m				
Core ID	Location	Mean	Median	Max	Min	SD	Mean	Median	Max	Min	SD	Mean	Median	Max	Min	SD
P1-C1	Center	0.508	0.468	0.818	0.183	0.246	0.722	0.776	1.072	0.183	0.281	0.864	0.848	1.696	0.183	0.326
P1-C2	Right Shoulder	0.524	0.472	0.805	0.377	0.167	0.570	0.492	0.927	0.354	0.190	0.564	0.480	1.147	0.337	0.220
P1-C3	Right Shoulder	1.379	0.932	2.339	0.867	0.832	1.431	1.173	3.013	0.867	0.683	N/A	N/A	N/A	N/A	N/A
P2-C2	Deflation surface	0.351	0.330	0.481	0.261	0.093	N/A	N/A	N/A	N/A	N/A	N/A	N/A	N/A	N/A	N/A
P4-C1	Center	N/A	N/A	N/A	N/A	N/A	N/A	N/A	N/A	N/A	N/A	N/A	N/A	N/A	N/A	N/A
P5-C1	Center	0.473	0.346	1.085	0.117	0.422	N/A	N/A	N/A	N/A	N/A	N/A	N/A	N/A	N/A	N/A
P6-C3	Center	0.522	0.505	0.743	0.392	0.135	0.755	0.737	1.397	0.392	0.312	0.858	0.789	1.516	0.392	0.308
P6-C5	Left Shoulder	0.487	0.527	0.626	0.308	0.145	0.399	0.351	0.626	0.293	0.123	N/A	N/A	N/A	N/A	N/A
P7-C1	Center	0.368	0.372	0.446	0.281	0.067	N/A	N/A	N/A	N/A	N/A	N/A	N/A	N/A	N/A	N/A
P8-C3	Center	0.383	0.409	0.512	0.249	0.101	0.565	0.512	1.293	0.249	0.282	N/A	N/A	N/A	N/A	N/A
P8-C5	Right Shoulder	0.303	0.309	0.351	0.253	0.049	0.492	0.394	0.867	0.253	0.239	N/A	N/A	N/A	N/A	N/A
P8-C6	Left Shoulder	0.579	0.514	0.759	0.472	0.120	0.622	0.633	0.761	0.472	0.115	N/A	N/A	N/A	N/A	N/A
P9-C1	Right Shoulder	3.078	2.929	4.841	1.615	1.480	N/A	N/A	N/A	N/A	N/A	N/A	N/A	N/A	N/A	N/A
P9-C2	Left Shoulder	N/A	N/A	N/A	N/A	N/A	N/A	N/A	N/A	N/A	N/A	N/A	N/A	N/A	N/A	N/A
P10-C1	Right Shoulder	3.668	3.942	4.207	2.854	0.717	3.863	3.942	4.661	2.854	0.675	1.804	0.933	4.661	0.213	1.637

4.4 Distribution of nitrogen in icy soils

Nitrogen concentrations in soils that were sampled in UV's upper-valley polygons center and shoulders are quite similar (Fig. 17). The minimum and maximum nitrogen concentration values in the 0-20 cm depth horizon of soils sampled in UV's upper-valley polygon centers were 0.300 and 0.701 mg/g^{-1}, and were 0.300 and 0.778 mg/g^{-1} for soils from shoulders of the upper-valley polygons (these latter values are the same for the 0-50 cm depth interval) (Table 13).

Ice cemented permafrost soils from cores sampled in the middle portion of the valley contained similar quantities of nitrogen. However, the mid-valley cores contained slightly more nitrogen when they came from the polygons shoulders. As such, the nitrogen concentration values for the upper 20 cm section of cores taken at the polygons shoulders (for this section of the valley) fluctuated from 0.266 to 1.300 mg/g^{-1}, and varied from 0.300 to 0.972 mg/g^{-1} in cores taken at the center of these polygons. In the 0-50 cm depth interval, the nitrogen concentration values for soils sampled at the edge of UV's mid-valley polygon ranged from 0.252 to 1.300 mg/g^{-1}, and varied from 0.195 to 0.567 mg/g^{-1} in cores drilled at the center of these polygons. The highest measured nitrogen concentration value was also found in the P6-C5 core (1.500 mg/g^{-1}), at a depth of 71.5 cm below the ice table.

The nitrogen concentration values of icy soil samples taken from the lowest portion of the valley were not statistically different than the ones for soils sampled in the upper and mid portion of UV. The maximum and minimum values of nitrogen concentration, in the first 20 cm of these cores, were found in the P9-C1 core: 0.464 and 0.803 mg/g^{-1}.

Nitrogen concentrations were similar between all three upper 20 cm sections of P1 polygons cores (Appendix 2S). Nonetheless, in the 0-50 cm depth interval, the nitrogen concentration became significantly different between the two cores sampled at the right edge of this polygon (where P1-C2 had a higher median value than P1-C3), but remained similar to P1-C1's nitrogen concentration (polygon's center) (Appendix 2T). There was

also no noticeable differences between the amount of nitrogen contained in P1's center and right shoulder soils, in the cores 0-100 cm depth interval (Appendix 2U).

The soils sampled in the left shoulder of the P6 polygon (P6-C5) had the highest measured nitrogen concentrations for soils in UV and therefore contained significantly higher nitrogen concentrations, in their upper 20 cm and 50 cm sections, than the ones coming from the polygon's center core (P6-C3).

There were also no significant differences between the amounts of nitrogen contained in the 0-20 cm and 0-50 cm depth interval of soils which were sampled in the left (P8-C6) and right (P8-C5) edges and in the center (P8-C3) of the P8 polygon. Their median nitrogen concentration value was the same: 0.400 mg/g^{-1}.

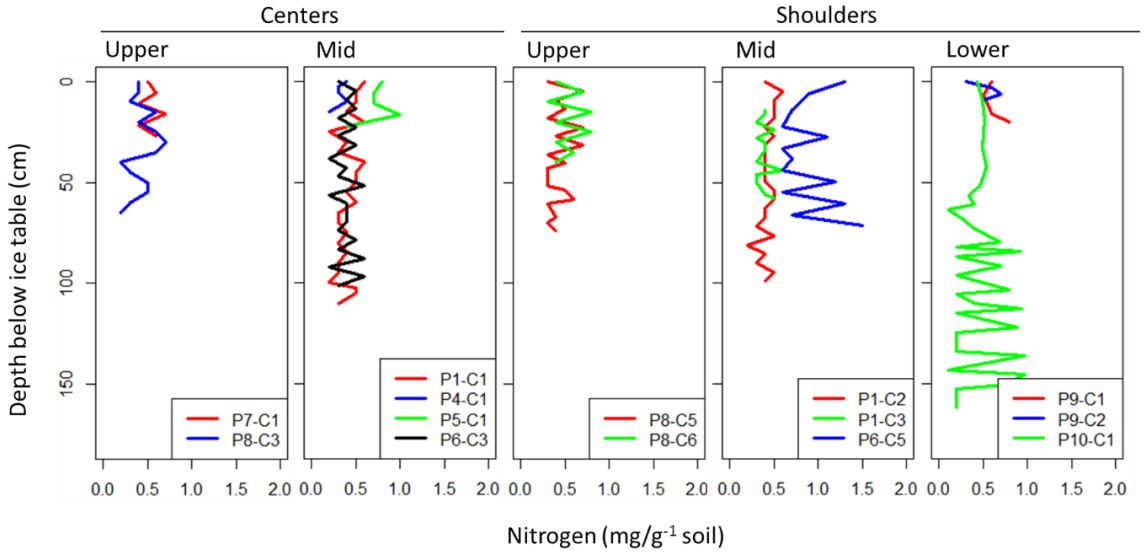

Figure 17 : Nitrogen concentration (mg/g^{-1} soil), with depth, in UV's icy soils.

Table 13 : Summary statistics for UV's icy soils Nitrogen concentrations (mg/g^{-1} soil).

		Top 20 cm					Top 50 cm					Top 1 m				
Core ID	Location	Mean	Median	Max	Min	SD	Mean	Median	Max	Min	SD	Mean	Median	Max	Min	SD
P1-C1	Center	0.512	0.551	0.567	0.400	0.069	0.454	0.500	0.567	0.195	0.125	0.404	0.400	0.567	0.190	0.119
P1-C2	Right Shoulder	0.514	0.512	0.627	0.400	0.081	0.467	0.449	0.627	0.392	0.071	0.438	0.439	0.627	0.200	0.093
P1-C3	Right Shoulder	0.366	0.400	0.431	0.266	0.088	0.379	0.399	0.560	0.252	0.097	N/A	N/A	N/A	N/A	N/A
P2-C2	Deflation surface	1.137	1.147	1.315	1.000	0.133	N/A	N/A	N/A	N/A	N/A	N/A	N/A	N/A	N/A	N/A
P4-C1	Center	N/A	N/A	N/A	N/A	N/A	N/A	N/A	N/A	N/A	N/A	N/A	N/A	N/A	N/A	N/A
P5-C1	Center	0.788	0.750	0.972	0.681	0.133	N/A	N/A	N/A	N/A	N/A	N/A	N/A	N/A	N/A	N/A
P6-C3	Center	0.397	0.400	0.516	0.300	0.098	0.375	0.400	0.516	0.200	0.100	0.390	0.400	0.598	0.200	0.122
P6-C5	Left Shoulder	0.857	0.768	1.300	0.651	0.270	0.827	0.664	1.300	0.600	0.270	N/A	N/A	N/A	N/A	N/A
P7-C1	Center	0.557	0.564	0.701	0.400	0.134	N/A	N/A	N/A	N/A	N/A	N/A	N/A	N/A	N/A	N/A
P8-C3	Center	0.407	0.400	0.553	0.300	0.092	0.455	0.400	0.746	0.200	0.164	N/A	N/A	N/A	N/A	N/A
P8-C5	Right Shoulder	0.444	0.400	0.677	0.300	0.164	0.459	0.400	0.702	0.300	0.162	N/A	N/A	N/A	N/A	N/A
P8-C6	Left Shoulder	0.525	0.400	0.778	0.300	0.220	0.539	0.400	0.788	0.300	0.195	N/A	N/A	N/A	N/A	N/A
P9-C1	Right Shoulder	0.615	0.597	0.803	0.464	0.140	N/A	N/A	N/A	N/A	N/A	N/A	N/A	N/A	N/A	N/A
P9-C2	Left Shoulder	N/A	N/A	N/A	N/A	N/A	N/A	N/A	N/A	N/A	N/A	N/A	N/A	N/A	N/A	N/A
P10-C1	Right Shoulder	0.483	0.496	0.516	0.436	0.042	0.496	0.496	0.538	0.436	0.038	0.434	0.436	0.923	0.100	0.212

4.5 Distribution of dissolved organic carbon (DOC) and $\delta^{13}C_{DOC}$ in icy soils

4.5.1 Dissolved organic carbon (DOC) concentrations

The DOC in UV's icy soils was measured for four cores only. In the top 50 cm of the sampled cores, DOC varied from 1.20 ppm C (P6-C3) to 4.62 ppm C (P10-C1), while DOC values for snow were at 3 ppm C (Fig. 18; Table 14). Below 50 cm depth, DOC values for the P12-C1 core increased substantially, and reached a maximum value of 11.56 ppm C, whereas DOC concentrations (ppm C) for the other cores (P10-C1, P9-C1 and P6-C3) remained similar to UV's snow. The ground ice at P12-C1 had two origins: P12-C1's upper vapor-derived ground ice portion (0-57 cm) had a median DOC value of 3.82 ppm C, but DOC increased to 7.87 ppm C in the lower water-derived ground ice section (57-92 cm). Ultimately, considering the entire length of the cores, P6-C3 has the least DOC and P12-C1 has significantly more DOC than P10-C1 (Appendix 2W).

The DOC concentration of these icy soils followed three major trends: i) the $\mu g/g^{-1}$ soil DOC concentration decreased with depth for the P10-C1 and P9-C1 cores; ii) it increased with depth for the P12-C1 core; and iii) remained stable with depth for the P6-C3 core. The highest concentrations were found in P12-C1 (11.31 $\mu g/g^{-1}$ soil; 59 cm) whereas the lowest was found in the P10-C1 core (0.42 $\mu g/g^{-1}$ soil; 142 cm).

P12-C1 had the highest concentration of DOC (ppm C) and was the nearest, out of the four analyzed cores, to UG (Fig. 22). By excluding P12-C1, a rising trend was observed in the median DOC (ppm C) concentrations of UV's analyzed icy sediments, with increasing distance from UG. These values for P6-C3, P9-C1, P10-C1 and P12-C1 were respectively 1.920 ppm C, 2.430 ppm C and 3.245 ppm C (Table 11).

Cumulative DOC concentrations varied from 0.27 to 1.31 $\mu g/m^{-2}$, in the cores first 20 cm, and fluctuated from 0.93 to 2.30 $\mu g/m^{-2}$, in their upper 50 cm section; P10-C1 and P12-C1 were respectively the most and least concentrated cores in both of these sections. The cumulative DOC concentration of the P12-C1 core increased considerably between 50 and 85 cm, until it became the most cumulatively concentrated, out of the 4 cores, at the latest depth (2.93 $\mu g/m^{-2}$).

Table 14: Summary statistics of DOC concentrations (ppm C) for the entire length of UV's icy soil cores.

Core ID	Mean	Median	Max	Min	SD
P6-C3	2.054	1.92	4.26	1.2	0.799297
P9-C1	2.8	2.43	3.73	2.24	0.8109871
P10-C1	3.096	3.245	4.62	1.38	0.7971171
P12-C1	5.169	3.695	11.56	2.42	2.808242

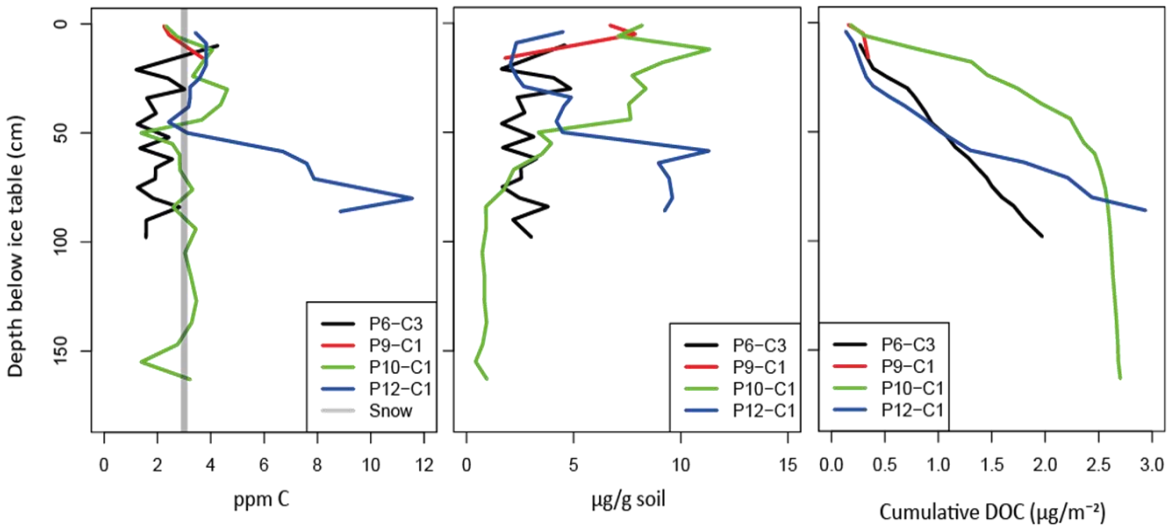

Figure 18 : DOC concentrations (ppm C, µg/g^{-1} soil and µg/m^{-2}) of UV's icy soils.

4.5.2 $\delta^{13}C$ of dissolved organic carbon

The $\delta^{13}C_{DOC}$ values of UV's Ice cemented permafrost cores indicated that the icy soils were generally enriched relatively to the snow (which has a $\delta^{13}C_{DOC}$ of -27 ‰) (Fig. 19; Fig. 20). P6-C3's ice cemented permafrost $\delta^{13}C_{DOC}$ values fluctuated from -27.23‰ to -15.14‰. The $\delta^{13}C_{DOC}$ values of P9-C1's icy sediments varied from -27.18‰ to -20.61‰ (the latter $\delta^{13}C_{DOC}$ values being found in the lowest portion of the core (16 cm)). P10-C1's ice cemented permafrost $\delta^{13}C_{DOC}$ values fluctuated from -27.86‰ to -21.44‰. Icy sediments from the P12-C1 core had $\delta^{13}C_{DOC}$ values that varied from -22.86‰ to -19.64‰. Altogether, the most depleted $\delta^{13}C_{DOC}$ values of analyzed icy soils (for their entire length) came from the P10-C1 core (-27.86 ‰), and the highest value was from the P6-C3 core (-15.14 ‰).

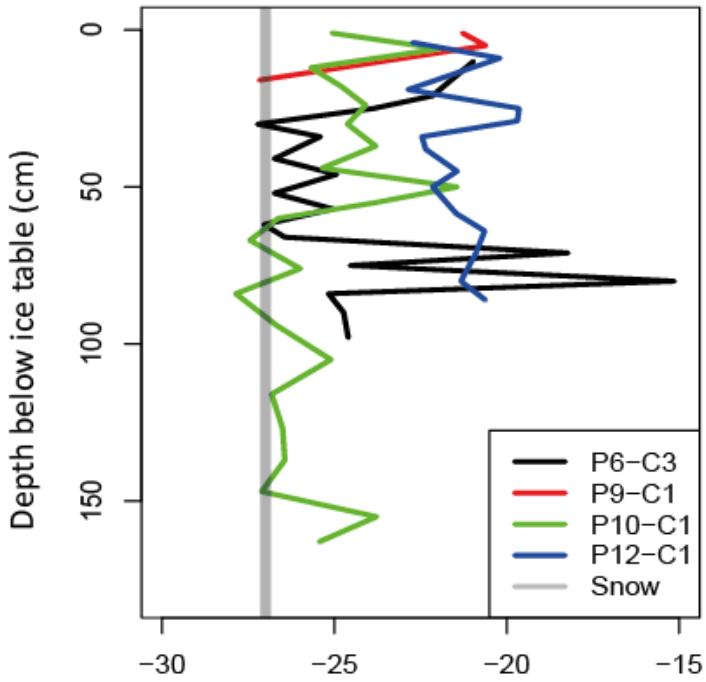

Figure 19 : $\delta^{13}C_{DOC}$ signal from UV's icy soils and snow.

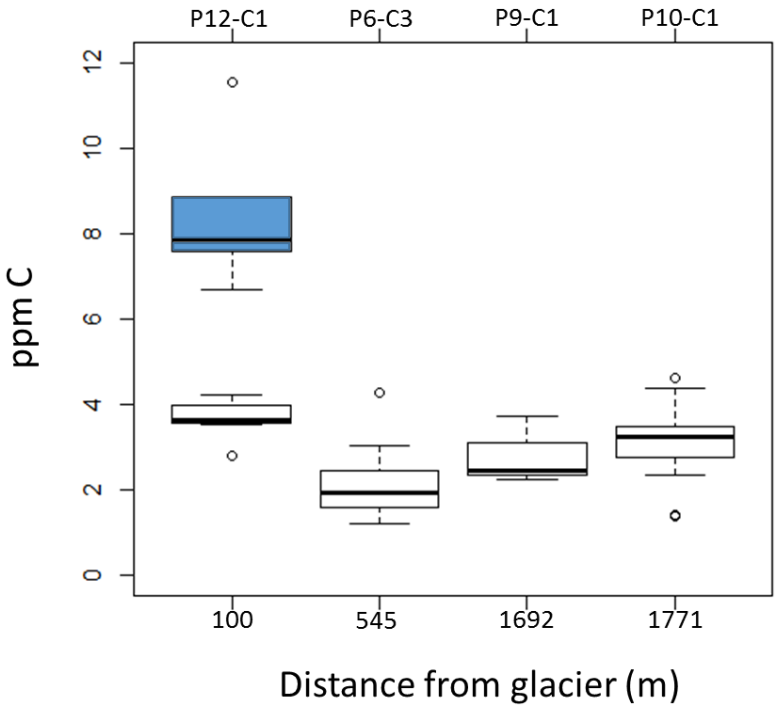

Figure 20 : DOC concentration (ppm C) of UV's icy soils, as a function of distance from UV (blue boxplot represents P12-C1's liquid water derived ground ice formed during the MIS 5e; P12-C1's white box presents the vapor-derived ground ice portion of the core).

4.6 Unfrozen water content in UV's soils

The unfrozen water content as a function of soil temperature, as determined in the experimental test chamber, is shown in Figure 21 for the three bulk soil samples from University Valley (Core 1; Core 5 and Core 7). Unfrozen water content curves describe a rapid transition from bulk to interfacial water, and a progressive decrease of the latter as hydrogen-bonds are slowly overcoming van Der Walls bonds at the mineral surfaces under cooling permafrost temperature. In all three soils, a considerable amount of unfrozen bulk water is found to exist in the soils at temperature above -1°C. The amount of unfrozen water decreases nearly 4-fold between the freezing point suppression and –4°C. At –15°C, the amount of unfrozen water reaches <2%wt in P11 and <1%wt in P12 soil samples. Considering similar freezing points suppression, the differing shape of the unfrozen water content curve may be attributed to slight variations in particle size distribution (i.e., Williams and Smith, 1989). Based on the experimental data, the relation between unfrozen water content and temperature below the freezing point suppression fit power equations. Based on the equations for P11 and P12, the amount of unfrozen water content at –50°C reaches <1.2%wt and <0.6%wt respectively.

To assess if the experimentally determined amount of unfrozen water content may be available for physical, chemical and biological processes, the amount of water that would be strongly bound to soil particles was computed using the Langmuir's absorption model (Langmuir, 1916), shown in equation 2:

[Eq. 2] $\theta = EK1/(K1 + K2)$

In equation 2, K1 and K2 are T (in kelvin) and P dependent constants; K1 = 2269.0189 [3.4738x10^{-4} (P-0.26)+0.002324] Exp(-2109.5/T); K2 = [7.0292x10^{-3} (P-0.26) + 0.2931] 8386.56 Exp(-2466.413/T); and $E = SSAm/a$; where *SSA* is the specific surface area of mineral particles ($m^2\ g^{-1}$) (SSA ranges from 1 to 16 $m^2\ g^{-1}$ for soils in adjacent Beacon Valley (Sizemore and Mellon, 2008)); *m* is the mass of a single water molecule (18/avagadro's number); *a* is the footprint area of a single water molecule on the mineral surface (2.6x10^{-16} cm^2).

Using a SSA of 1 to 20m^2 g^{-1}, the estimated values of a single layer water film that is absorbed on soil particles range from 0.005 to 0.1%wt at 0°C, respectively, and decrease from 0.01 to 0.06%wt at –40°C. Assuming that five layers of water starts to be available for water transport and other processes, the amount of unfrozen water would need to be >0.5%wt for SSA = 20 and >0.03%wt for SSA=1. The experimentally determined unfrozen interfacial water was always higher than the threshold for soils with SSA of 1; however, for soils with SSA of 20, as measured in Beacon Valley (Sizemore and Mellon, 2008), the amount of unfrozen interfacial water at soil temperature lower than –10°C started to be within the range of strongly bound water.

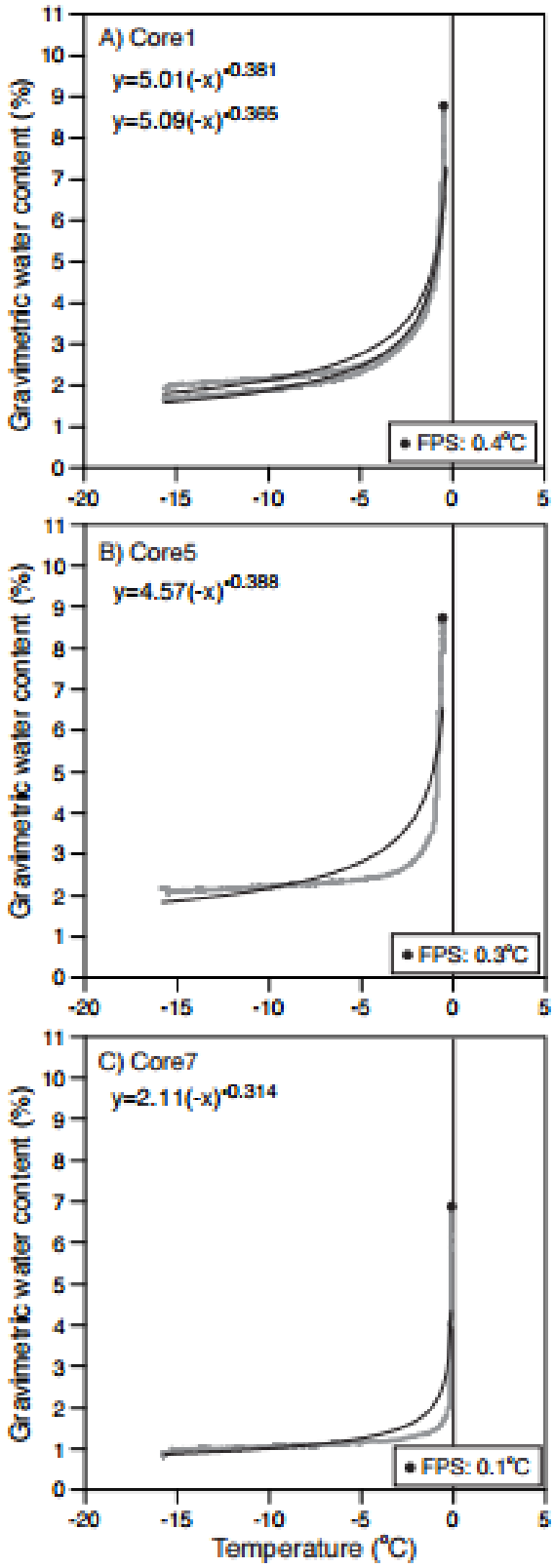

Figure 21 : Unfrozen water content (Gravimetric water content; GWC) in icy soils of UV (Core 1; Core 5 and Core 7), as a function of soil temperature.

4.7 Habitability indexes for soils of UV and various sites on Mars

Based on the results from UV (availability of liquid water, soluble ions, nutrient availability), the habitability of UV soils in the PCZ and NCZ was calculated using Stoker et *al*. (2010) habitability index. Table 15 presents the probabilities and factors used for this calculation. It was determined that PCZ soils had low probability of containing liquid water, hence it was attributed a 0.25 score for its probability of containing liquid water (*Plw).* However, we attributed a higher score for soils of UV's NCZ (0.75) since it was determined that it can contain liquid water during sunny summer days, and the ground ice in this zone was attributed a freezing of evaporated snow meltwater origin (Lapalme et *al*., 2016). The highest possible scores (1) for the probability of soils having a biologically available energy source (P_e) and for the probability of containing elements essential for life (P_{ch}) were assigned for both the PCZ and NCZ soils. The soil temperature able to support microorganism growth factor (F_T), water activity allowing growth factor (F_{AW}), and soil pH factor (F_{pH}) were taken into account in the calculation of the probability of having a chemically and physically benign environment (P_b) and were given the highest scores for both NCZ and PCZ soils, but the presence of organics factors (F_{org}) were different. Indeed, the score for the NCZ's soils F_{org} was estimated at 0.75; it was not given the maximum score of 1 since it still contained very low quantities or organics. Meanwhile UV's PCZ soils scored a 0.25 for the same factor, since they contained even lower concentrations of organic carbon than the NCZ's soils.

Ultimately, habitability index calculations, for soils of UV, indicated that the soils sampled in the NCZ had the highest computed index (0.70) out of all presented sites. Furthermore, the habitability index of icy soils from UV's PCZ (0.22) was found to be more than three times lower than it had been estimated for the NCZ soils.

Table 15: Factors and probabilities used for habitability index calculation of various sites on Mars and of soils located in the PCZ and NCZ of UV (data for Mars landing sites taken from Stoker et *al.* (2010)). Factors used to calculate the probability of having a present biologically available energy source (P_e) were the availability of photosynthetically active radiation (F_e1) and the presence of redox pairs available for metabolism (F_e2). Factors used to calculate the presence of elements essential to life (CHNOPS compounds) represented their respective availability. Factors used to calculate the presence of a chemically and physically benign environment (P_b) were: soil temperature able to support microorganism growth (F_T), water activity allowing growth (F_{AW}), soil pH (F_{pH}) and the presence of organics (F_{org}). *HI* indicates the computed habitability indexes, for each of the presented sites.

Sampling sites	(P_{lw})	(P_e)	(P_{ch})	(P_b)	*HI*
Phoenix	0.58	F_e1 =1 F_e2=1	F_C=1 F_H=1 F_N=0.5 F_O=1 F_P=1 F_S=1	F_T=1 F_{Aw}=1 F_{pH}=1 F_{org}=0.25	0.43
Meridiani	1	F_e1 =0.5 F_e2=0.5	F_C=1 F_H=1 F_N=0.5 F_O=1 F_P=1 F_S=1	F_T=1 F_{Aw}=0.25 F_{pH}=0.25 F_{org}=N/A	0.23
Gusev	0.78	F_e1 =0.5 F_e2=0.5	F_C=1 F_H=1 F_N=0.5 F_O=1 F_P=1 F_S=1	F_T=0.75 F_{Aw}=0.5 F_{pH}=N/A F_{org}=N/A	0.22
Pathfinder	0.21	F_e1 =0.5 F_e2=0.5	F_C=1 F_H=1 F_N=0.5 F_O=1 F_P=1 F_S=1	F_T=0.5 F_{Aw}=0.5 F_{pH}=N/A F_{org}=N/A	0.05
Viking 1	0.04	F_e1 =0.5 F_e2=0.5	F_C=1 F_H=1 F_N=0.5 F_O=1 F_P=1 F_S=1	F_T=0.5 F_{Aw}=0.75 F_{pH}=0.5 F_{org}=0	0.01
Viking 2	0.17	F_e1 =0.5 F_e2=1	F_C=1 F_H=1 F_N=0.5 F_O=1 F_P=1 F_S=1	F_T=1 F_{Aw}=0.75 F_{pH}=1 F_{org}=0	0.07
NCZ	0.75	F_e1 =1 F_e2=1	F_C=1 F_H=1 F_N=1 F_O=1 F_P=1 F_S=1	F_T=1 F_{Aw}=1 F_{pH}=1 F_{org}=0.75	0.70
PCZ	0.25	F_e1 =1 F_e2=1	F_C=1 F_H=1 F_N=1 F_O=1 F_P=1 F_S=1	F_T=1 F_{Aw}=1 F_{pH}=1 F_{org}=0.50	0.22

5. Discussion

5.1 Soluble ions concentrations and distribution in the soils of UV

Jackson et *al*. (2016) analyzed the concentration of Cl^-, NO_3^-, ClO_4^- and ClO_3^- in dry and icy soils of UV. They found that soluble salts concentrations were 1-2 orders of magnitude higher in the dry soils and that most salts were derived from atmospheric source with limited post-depositional transformation. Salt concentration also increased along the valley floor due to increased accumulation time in the dry soils.

In this study, the concentrations of soluble ions were determined for the icy soils only. The results showed that the abundance of cations and anions are relatively low and no pattern could be established with depth. However, soluble ion concentrations in UV's ice cemented permafrost soils were slightly higher in the upper sections of the valley (PCZ) relative to the NCZ, which differs from what had been observed by Jackson et *al*. (2016). This difference is likely due to the fact that only the icy soils were analyzed in this study and that the concentration of soluble salts in the dry soil layers is 1-2 order of magnitude higher than in the icy soils. The soils in the NCZ can experience liquid water; in fact the ground ice in this zone was attributed a freezing of snow meltwater origin. Therefore, the presence of liquid water in soils of UV's NCZ would facilitate the downward movements of ions in the soils of this section of the valley, In that sense, flushing events could produce salt enriched soil horizons in the icy soils of the NCZ (at the maximum infiltration depth of water during summer months), which would not have been reached during the sampling of the ice cemented permafrost soil cores (as it has been proposed by Jackson et *al.* (2016)).

The calculation of ionic ratios for the icy soils of UV suggest that some ions originate from the chemical weathering of parent material (Fig. 22). In UV, the bedrock consist of sandstone and dolerite which contains weatherable minerals. Therefore, the soluble salts contained in UV's icy soils would originate not only from atmospheric fallout but also from weathering of especially its granite erratics and the valley walls material (sandstone and dolerite).

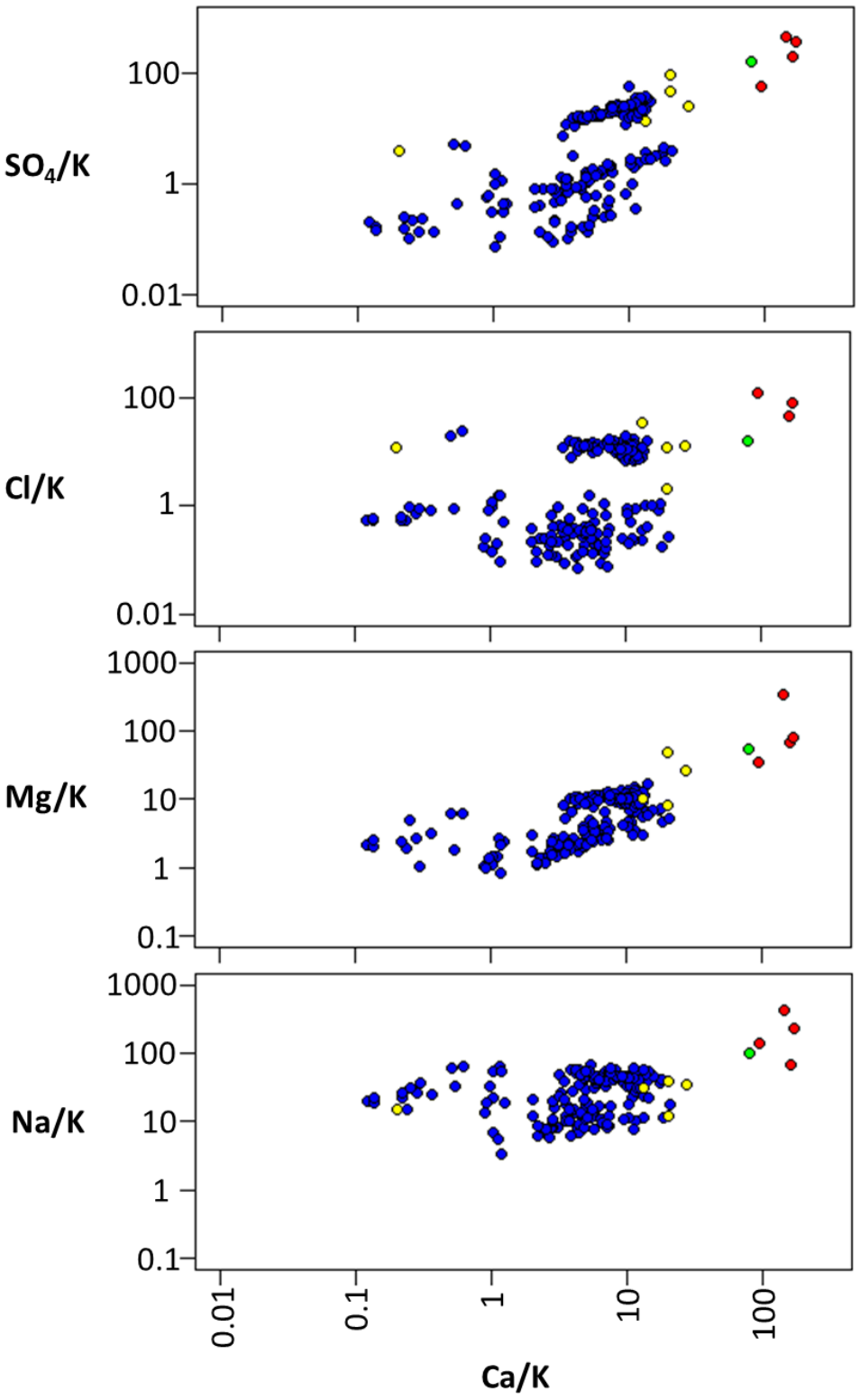

Figure 22: Ionic ratios for soils of University Valley (blue), compared to ionic ratios of other mineral soils in the MDV, from Claridge and Campbell (1977). Granite derived soils shown in yellow; dolerite derived soils shown in red; sandstone derived soils derived in green.

5.2 C_{org} and nitrogen abundance, distribution and origin: comparison with other soils in the MDV.

5.2.1 Organic carbon

SOC concentrations in soils of UV are similar to those measured in the MDV. The average SOC concentration in the icy soils of UV is 0.90 mg C/g^{-1} soil, which is amongst the highest concentrations of C_{org} measured in MDV soils, where this number fluctuates between 0.07 and 0.96 mg C/g^{-1} (Table 1). This is not consistent with what had previously been reported by Barret et *al.* (2007), which concluded that organic carbon concentrations in soils of the MDV should decrease with elevation. In fact, this high elevation valley is expected to contain limited traces of C_{org} (Goordial et *al.,* 2016). However, the SOCC of UV's soils averages 7.61 kg/m^{-2} for their upper 0-100 cm section: a mean value exceedingly lower than the ones for most gelisols located in northern circumpolar permafrost region (ranging from 22.6 to 66.6 kg/m^{-2}) (Tarnocai et *al.*, 2009).

The SOC concentrations of the ice cemented permafrost soils are the lowest in the valley's PCZ section, where it averages 0.62 mg C/g^{-1} and are on average almost twice as high in the NCZ portion of UV (1.19 mg C/g^{-1}). The highest concentrations of organic carbon are found in the soils sampled at the furthest distance of UG (P9 and P10); the soils in this section of the valley have the highest mean summer ground surface temperature. As such, one could suggest that the difference in SOC concentrations of soils located in the PCZ and NCZ sections of UV points to distinct abundance of carbon following availability of liquid water (or lack thereof). In fact, there is a positive correlation between the gravimetric water content (GWC) and the organic carbon concentration of ice cemented permafrost soils of UV (Fig. 23). The fit is actually better between GWC and C_{org} concentrations of UV'S NCZ soils. It is therefore possible that snow meltwater percolation in the dry soils would transport organic matter downward and subsequently freeze in the icy soils. This mechanism would allow SOC to be brought at lower depths than its original depositional depth and accumulate as the ice builds-up.

The source of SOC in UV's icy soils can be determined from its $\delta^{13}C_{org}$ composition (Fig. 16). The $\delta^{13}C_{org}$ values of organic matter contained in UV's ice cemented permafrost soil approaches those of MDV's endolith-derived organic matter (EDOM; median $\delta^{13}C_{org}$ value of -26.6‰) but are different from organic carbon of modern or ancient lakes or marine origin. This finding suggest that SOC in UV originate from the weathering of the the Beacon sandstone supergroup that hosts cryptoendolithic communities and that remobilization of organic carbon from other environments is minimal. This contrasts to most other lower elevation sites in the MDV where a "legacy" carbon source is inferred, either in situ or remobilized from ancient lakes and/or marine incursions.

Friedmann et al. (1993) suggested that the accumulation rate of cryptoendolithic communities in the soils of the McMurdo Dry Valleys was 30 mg C m^{-2} yr^{-1}. Based on a series of OSL dating of soils from the P1, P2 and P8 cores, the first 50 cm of UV's soils was accumulated over a 200,000 years period. The SOCC in the first 50 cm of these ice cemented permafrost soils (P1, P2 and P8) varies from 2,538.77 g m^{-2} (P8-C3) to 4,320.91 g m^{-2} (P1-C3) and based on $^{13}C_{org}$ values of the SOC, the source of organic C is derived from cryptoendoliths. Using the predicted accumulation rate of cryptoendolithic communities in MDV soils (30 mg C m^{-2} yr^{-1}) and the age of UV soils yield a SOCC derived from endolithic communities of ~6000 g C m in their first 50 cm. The SOCC in the first 50 cm of UV's soils is similar (slightly lower) to the predicted value of Friedmann et *al.* (1993) and indicates that cryptoendolith communities have been active in the surrounding sandstone outcrops, for at least 200,000 years.

The ^{14}C ages from EDOM-derived C_{org} indicated that the SOC found in soils of the upper 15 cm section of the P12-C1 core was of early Holocene age (11,700 to 9950 BP; Table 11). OSL dating of sediments from that same depth interval yielded ages ranging from 55 to 17 kyr (Lacelle et *al.,* 2013). This indicates that the organic carbon contained in UV's ice cemented permafrost soils was deposited after the initial deposition of the mineral soils. According to Goordial et *al*. (2016), the micro-organisms in the soils of the PCZ are not active; as such the $^{14}C_{org}$ ages from EDOM-derived SOC likely represents the

timing of SOC being deposited in the soils. However, it remains a possibility that the EDOM in soils maintained a level of activity during past climate conditions and as such the ^{14}C ages would represent the timing of inactivity in the soils. However, additional ^{14}C ages are required to support this possibility.

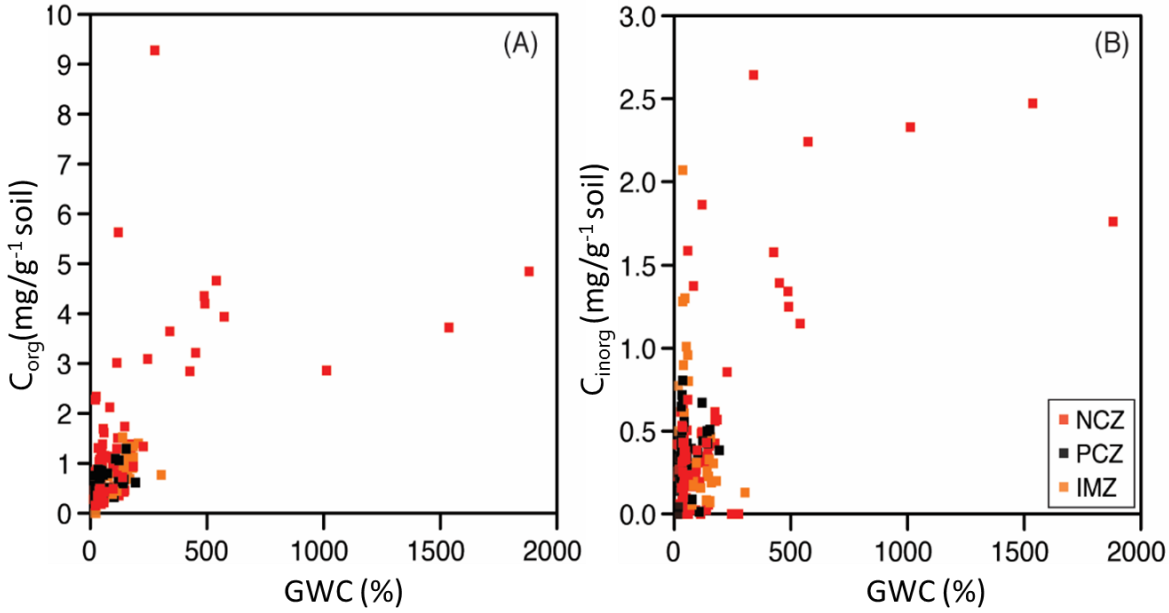

Figure 23: Relationship between gravimetric water content (GWC) of UV's soils and A) C_{org}; B)C_{inorg} concentrations (mg/g^{-1}).

5.2.2 Nitrogen

Nitrogen concentrations of UV's soils average 0.50 mg N/g^{-1}: this concentration is one of the highest measured in the MDV and is equal to the N concentration of Arena valleys soils (Table 1). The nitrogen concentrations of the icy soils are also quite similar to NO_3-N concentrations that were measured by Jackson et *al*. (2016).

Moreover, the concentrations of carbon and nitrogen in soils of UV are poorly positively correlated. In fact, there is an excess of nitrogen (points plotting below the Redfield ratio) in comparison to organic carbon, in most of the ice cemented permafrost soils of UV; this indicates biogeochemical imbalance and that geochemical processes are generally dominating in the soils (Fig. 24). According to Jackson, nitrogen in the soils has

been deposited by atmospheric fallout. However, some sites in the NCZ soils have C:N ratios which plot close to the Redfield ratio (P4,P9 and P10 soils). The latter soils from the NCZ are located in the warmest portion of the valley (P9 and P10 polygons) and in proximity to a frozen pond where sand flows were observed (P4). As such, conditions in those regions might be favorable to support active biological cycling by micro-organisms.

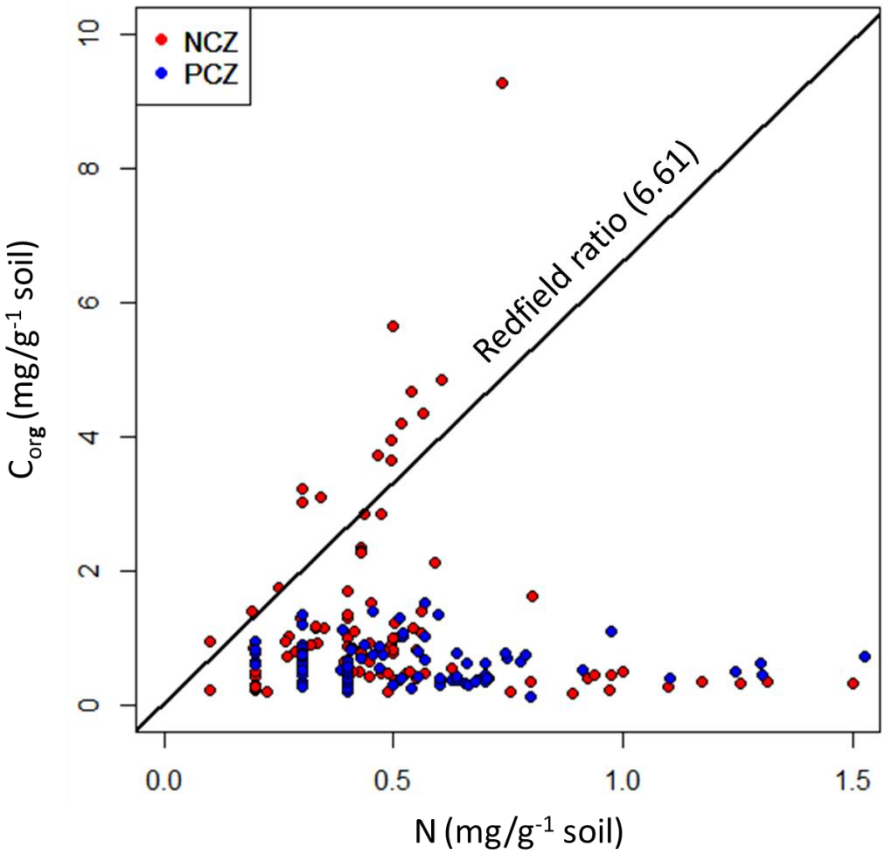

Figure 24 : Comparison of C_{org} and N concentrations (mg/g^{-1} soil) for UV's icy soils sampled in the NCZ and in the PCZ.

5.3 DOC and $\delta^{13}C_{DOC}$ of the icy soils

The DOC concentration at most sites is low and similar to that measured in snow. This suggests that DOC in the valley likely originates from atmospheric fallout. However, the P12-C1 core contains much higher DOC concentration below 57 cm depth than its upper section (Fig. 25). The ground ice in the lower portion of the P12-C1 core was attributed a liquid water origin (Lacelle et *al*., 2013), and based on OSL ages, the soils at

this depth have accumulated during the Eemian interglacial (MIS 5e; ca. 130 kyr ago) when liquid water was probably more abundant in soils of UV. In contrary, the upper soils have been accumulating since the Eemian until present-day and the ground ice portion ground ice was attributed a vapor deposition origin in colder and dryer climatic conditions since the MIS5e (Lacelle et *al*., 2013). In that sense, it is possible that microbial activity was higher in the lower portion of the P12-C1 core, when liquid water was infiltrating and freezing in these soils; this would explain why there is more DOC in the liquid-derived ground ice portion of P12-C1.

The previous hypothesis is supported by comparing the $\delta^{13}C_{DOC}$ and DOC (ppm C) (Fig. 26). There seems to be a positive correlation between the DOC concentration of UV's soils, and their $\delta^{13}C_{DOC}$ signal: soils that contain high concentrations of DOC are also enriched in $^{13}C_{org}$, relatively to soils containing low DOC concentrations. It has been proposed by many authors (e.g., Blair et *al*., 1985; Mary et *al*., 1992; Andresen et *al*., 2011) that fractionation of ^{13}C and ^{12}C might occur following respiration and decomposition of microbes. Furthermore, Yang et *al*. (2014) discovered that the fractionation of carbon increases as the complexity of microbial communities increases. If the organic carbon compounds found in soils of UV essentially originate from the deposition of cryptoendoliths, and that they can only remain dormant, then the $\delta^{13}C_{DOC}$ signal of the icy soils should stay at ~ -26‰. However, the soils containing the highest concentrations of DOC (Lower P12-C1) are also some of the most enriched in $\delta^{13}C$. As such, enrichment in $^{13}C_{DOC}$ in soils of UV could potentially indicate biologically derived ^{13}C fractionation and also the presence of complex microbial communities. The positive correlation between DOC concentrations and $^{13}C_{DOC}$ in icy soils of the valley points to increased microbial activity in soils during past super interglacial periods (i.e. MIS 5e).

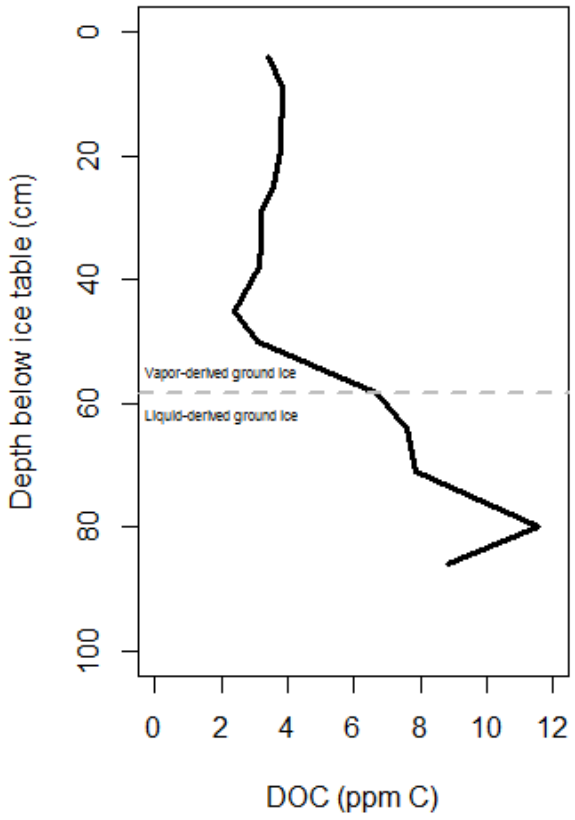

Figure 25: Variations of DOC concentration with depth, in the vapor and liquid-derived ground ice sections of UV's P12-C1 core.

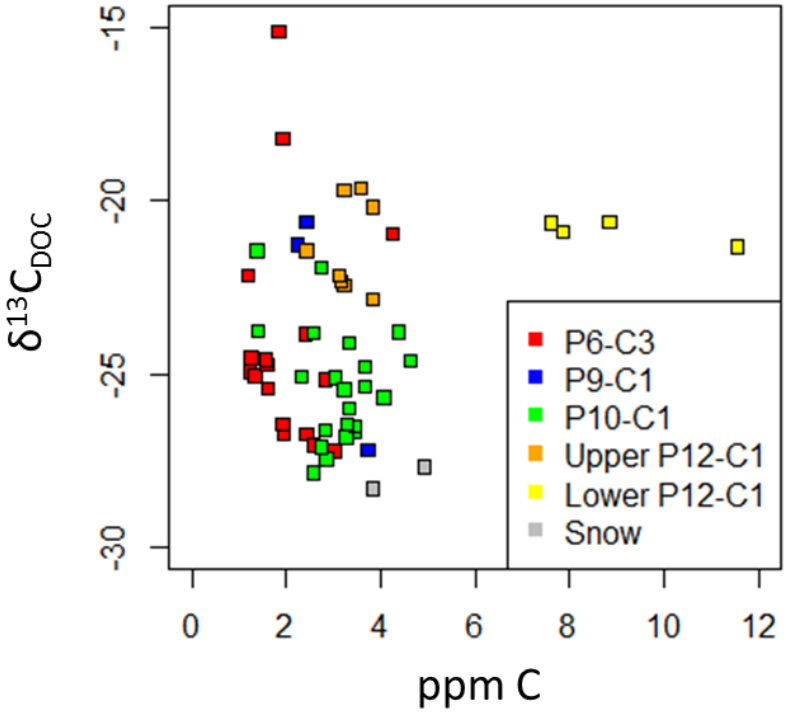

Figure 26: Relationship between $\delta^{13}C_{DOC}$ and DOC (ppm C) for UV's ice cemented permafrost soils.

5.4 Habitability indexes of UV's icy soil

Figure 27 presents the results of habitability index calculations for UV's PCZ and NCZ soils, in comparison with those of various sites on Mars that were calculated by Stoker et *al*. (2010). Soils of UV's NCZ obtained the highest habitability index score and were 0.23 points higher than the second most habitable soil: the phoenix landing site. In the NCZ soils, liquid water is seasonally available, an energy source is present, essential nutrients are there and organics are sparse but still present. On the other hand, soils sampled in the PCZ section of the valley, scored a very low habitability index score, which was actually similar to the ones calculated by Stoker et *al.* (2010), for the Meridiani and Gusev Mars landing sites. PCZ soils have very little chance of containing liquid water, but offer a possible energy source and also essential nutrients. However, UV's PCZ soils have two times less organics than the NCZ soils, which decreases their P_b dramatically. As such, soils of UV's NCZ are much more habitable than soils sampled in the NCZ and those for various Mars sites that were analyzed by Stoker et *al*. (2010).

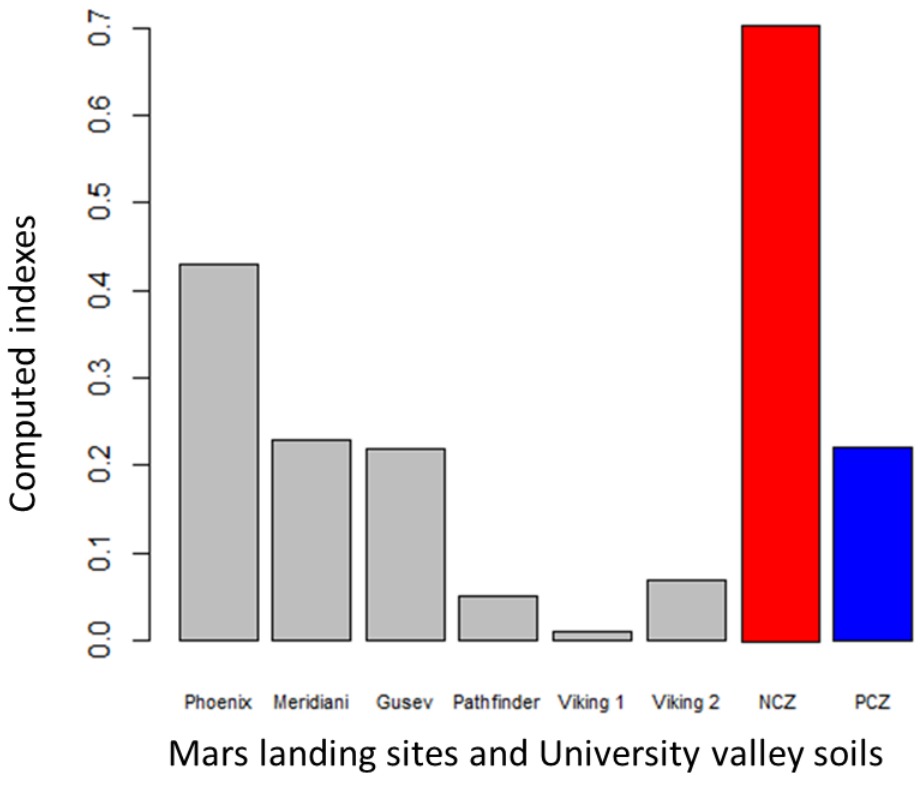

Figure 27 : Habitability indexes for soils of UV (NCZ shown in red; PCZ shown in blue), and various locations on Mars (shown in grey).

6. Conclusions and future work

The results from this thesis have led to these following conclusions:

1. The SOC in University Valley is higher than expected; in fact, this concentration is similar to the ones of other MDV, and is actually one of the highest.

2. The $^{13}C_{org}$ of UV's SOC points to endolith-derived source; this contrast to most other sites where a "legacy" carbon source is inferred, either in situ or remobilized. In lower elevation valleys, this "legacy" carbon originates from ancient lakes and/or marine incursions.

3. The SOC in UV (endolith-derived) is younger than it is for lower elevation valleys: the carbon is "modern" and not a "legacy" as it is for most other soils in the MDV.

4. C_{org}-N ratio points to geochemical processes dominating the soils. C-N ratio are much lower than that expected for equilibrium biological cycling of nutrients turnover (below the Redfield ratio) - this is true except for the P4, P9 and P10 sites, which are either the closest to the frozen pond (P4) or located in the warmest portion of the valley (P9 and P10). Lower elevation soils show either biological dominated or geochemical dominated soils depending on proximity to lakes; we could infer the same for UV (i.e., proximity to frozen ponds and the pathway of their recharge).

5. The DOC and $^{13}C_{DOC}$ story points to microbial activity in soils during past super interglacial periods, since soils with high DOC concentrations are also enriched in ^{13}C, with regards to those with low DOC concentrations.

6. As expected, icy soils containing liquid-derived ground ice from UV's NCZ contain higher C_{org} concentrations than soils from the PCZ which contain vapor-derived ground ice.

7. Soils of UV's NCZ have higher habitability indexes than the ones for the NCZ. Their index is also much higher than those calculated by Stoker et *al*. (2010) for Mars landing sites. Goordial et *al*. (2016) only sampled the NCZ and established that no living

microorganisms could be found in the icy soils of UV; their conclusion might have been different if they had also searched for life in icy soils from the NCZ.

8. Soluble salts contained in the ice cemented permafrost soils of UV are not only atmospherically derived, as it had been proposed by Jackson et *al*. (2016), but originate also from chemical weathering of its mineral soils.

9. Future exobiology missions on Mars with the aim of finding life in icy soils should focus on areas that are known to contain liquid-derived ground ice.

10. $^{13}C_{inorg}$ should be analysed to determine the source of carbonates in soils of UV. This will help to assess the presence of liquid water in soils of UV, since the calcium carbonates found in the valley are most likely derived from precipitation of dissolved atmospheric CO_2 in liquid water.

11. $^{14}C_{org}$ ages should be determined for P9 and P10 cores, since they were the ones containing the largest amounts of organic carbon. These results will help to answer a fundamental biological question: was the biomass found in these polygons produced *in situ* or was is it just derived from deposition of cryptoendoliths?

References

Adlam, L.S., Balks, M.R., Seybold, C.A. & Campbell, D.I. (2010): Temporal and spatial variation in active layer depth in the McMurdo Sound Region, Antarctica. Antarctic Science, 22(1), 45-53.

Anderson, D.M. & Morgenstern, N.R., (1973): Physics, chemistry and mechanics of frozen ground. Proc. 2nd Int. Conf. Permafrost, Yakutsk, U.S.S.R., pp. 257-288.

Andresen, L.C., Konestabo, H.S., Maraldo, K., Holmstrup, M., Ambus, P., Beier, C. & Michelsen, A., (2011): Organic matter flow in the food web at a temperate heath under multifactorial climate change. Rapid Commun. Mass Spectrom. 25, 1485e 1496

Bargagli, R., Smith, R.I.L., Martella, L., Monaci, F., Sanchez Hernandez, J.C. & Ugolini, F.C. (1999): Solution geochemistry and behavior of major and trace elements during summer in a moss community at Edmonson Point, Victoria Land, Antarctica. Antarctic Science, 11, 3-12

Barrett, J.E, Virginia, R.A, Wall, D.H, Parsons, A.N, Powers, L.E & Burkins, M.B. (2004): Variation in biogeochemistry and soil biodiversity across spatial scales in a polar desert ecosystem. Ecology. 85, 3105–3118.

Barrett, J.E., Virginia, R.A., Parsons, A.N. & Wall, D.H. (2005): Potential soil organic matter turnover in Taylor Valley. Arct. Alp. Res, 37107-116.

Barrett, J.E., Virginia, R.A., Parsons, A.N. & Wall, D. (2006): Soil carbon turnover in McMurdo Dry Valleys, Antarctica. Soil Biol Biochem 38: 3065–3082.

Barrett, J.E, Virginia, R.A., Lyons, W.B., McKnight, D.M., Priscu, J.C., Doran, P.T., Fountain , A.G., Wall, H. & Moorhead, D.L. (2007): Stoichiometric evolution of Antarctic Dry Valley ecosystems. J. Geophys. Res. Biogeosci. 112.

Blair, N., Leu, A., Munoz, E., Olsen, J., Kwong, E. & Desmarais, D. (1985): Carbon isotopic fractionation in heterotrophic microbial-metabolism. Appl. Environ. Microbiol. 50, 996e1001

Bockheim, J.G. (1995): Permafrost distribution in the southern circumpolar region and its relation to the environment—a review and recommendations for further research. Permafrost and Periglacial Processes 6: 27–45.

Bockheim, J.G. & Tarnocai, C. (1998): Nature, occurrence and origin of dry permafrost. In: Lewkowicz AG (ed.) Proceedings of the Seventh International Conference on Permafrost. Québec: Centre d'études nordiques, Université Laval, Publication 57, 57–63

Bockheim, J.G. & Hall, K.J. (2002): Permafrost, active-layer dynamics and periglacial environments of continental Antarctica. South African Journal of Science, 98, 82-90.

Bockheim, J.G., Campbell, I.B. & Mcleod, M. (2007): Permafrost distribution and active-layer depths in the McMurdo Dry Valleys, Antarctica. Permafrost and Periglacial Processes: 18 (3), 217–227.

Burkins, M.B., Virginia, R.A., Chamberlain, C.P. & Wall, D.H. (2000): Origin and distribution of soil organic matter in Taylor Valley, Antarctica. Ecology 81: 2377–2391.

Burkins, M.B., Virginia, R.A. & Wall, D.H. (2001): Organic carbon cycling in Taylor Valley, Antarctica: quantifying soil reservoirs and soil respiration. Global Change Biol, 7:113

Burkins, M. B., Virginia, R. A., Chamberlain, C. P. & Wall, D. H. (2010): Origin and distribution of soil organic matter in Taylor Valley, Antarctica. Ecology 81, 2377–2391.

Campbell, I.B. & Claridge, G.G.C. (1987): Antarctica: soils, weathering processes and environment. Elsevier Science Publishers, Amsterdam (368 pp.)

Campbell, I.B. & Claridge, G.G.C. (2006): Permafrost properties, patterns and processes in the Transantarctic Mountains region. PPP. 17, 215–232

Campbell, I.B. & Claridge, G.G.C. (2009): Antarctic permafrost soils, in Permafrost soils, R. Margesin (eds) 17-31.

Campbell, I.B., Claridge, G.G.C., Campbell, D.I. & Balks, M.R. (1998): The soil environment of the McMurdo Dry Valleys, Antarctica,in: J.C. Priscu (Ed.), Ecosystem Dynamics in a Polar Desert: The McMurdo Dry Valleys, Antarctica, Antarctic Research Series, vol. 72, AGU, Washington, DC pp. 297–322

Cowan, D. (2014): Antarctic Terrestrial Microbiology, Physical and Biological Properties of Antarctic Soils. VI, 328 p.

Cox, S.C., Turnbull, I.M., Isaac, M.J., Townsend, D.B. & Smith Lyttle, B. (2012): Geology of southern Victoria Land Antarctica. Lower Hutt: GNS Science. Institute of Geological & Nuclear Sciences 1:250,000 geological map 22. 135 p

Czarnomski, N., Moore, G., Pypker, T., Licata, J. & Bond, B. (2005): Precision and accuracy of three alternative instruments for measuring soil water content in two forest soils of the Pacific Northwest Can. J. For. Res. 35(8): 1867-1876.

Doran, P.T., Wharton, R.A., Jr. & Lyons, W.B. (1994): Paleolimnology of the McMurdo Dry Valleys, Antarctica. Journal of paleolimnology 10, 85-114.

Doran, P.T., McKay, C.P., Clow, G.D., Dana, G.L, Fountain, A.G., Nylen, T. & Lyons, W.B. (2002): Valley floor climate observations from the McMurdo Dry Valleys, Antarctica, 1986–2000, J. Geophys. Res.,107.

Elberling, B., Gregorich, E.G., Hopkins, D.W, Sparrow, A.D., Novis, P. & Greenfield, L.G. (2006): Distribution and dynamics of soil organic matter in an Antarctic dry valleys. Soil Biol. Biochem., 38 (2006), pp. 3095–3106

Freckman, D.W., & Virginia, R.A. (1997): Low-diversity Antarctic soil nematode communities: Distribution and response to disturbance. Ecology, 783, 63-69

Friedmann, E.I. (1982): Endolithic microorganisms in the Antarctic cold desert. Science 215: 1045–1053

Friedmann, E. I., Kappen, L., Meyer, M. A. & Nienow, J. A. (1993): Longterm productivity in the cryptoendolithic microbial community of the Ross Desert, Antarctica. Microb. Ecol. 25:51–69.

Goordial, J., Davila, A., Lacelle, D., Pollard, W., Marinova, M.M., Greer, C.W., DiRuggiero, J., McKay, C.P. & Whyte, L.G. (2016): Nearing the cold-arid limits of microbial life in permafrost of an upper dry valley, Antarctica. The ISME Journal, doi: 10.1038/ismej.2015.239

Higgins, S.M., Denton, G.H. & Hendy, C.H. (2000): Glacial geomorphology of Bonney drift, Taylor valley, Antarctica. Geografiska Annaler, 82, A: 365-389.

Hopkins, D.W., Sparrow, A.D., Gregorich, E.G., Elberling, P., Novis, F., Fraser, C., Dennis, P.G., Meier-Augenstein, W. & Greenfield, L.G. (2009): Isotopic evidence for the provenance and turnover of organic carbon by soil microorganisms in the Antarctic dry valleys. Environ Microbiol 11:597

Horowitz, N.H., Cameron, R.E. & Hubbard, J.S. (1972): Microbiology of the dry valleys of Antarctica. Science 176:242–245

Jackson, A., Davila, A.F., Böhlke, J.K., Sturchio, N.C., Sevanthi, R., Estrada, N., Brundett, M., Lacelle, D., McKay, C.P., Poghosyan, A., Pollard, W. & Zacny, K. (2016): Deposition, accumulation and alteration of Cl^-, NO_3^-, ClO_4^- and ClO_3^- salts in a hyper-arid polar environment: Mass balance and isotopic constraints. GCA 182, 197-215.

Lacelle, D., Davila, A.F., Pollard, W.H., Andersen, D., Heldmann, J., Marinova, M. & McKay, C.P. (2011): Stability of massive ground ice bodies in University Valley, McMurdo Dry Valleys of Antarctica: Using stable O-H isotope as tracers of sublimation in hyper-arid regions

Lacelle, D., Davila, A.F., Fisher, D., Pollard, W.H., Dewitt, R., Hedlmann, J., Marinova, M.M. & Mckay, C.P. (2013): Excess ground ice of condensation-diffusion origin in University Valley, Dry Valleys of Antarctica: evidence from isotope geochemistry and numerical modeling. Geochimica et Cosmochimica Acta, 120, 280–297.

Lacelle, D., Lapalme, C., Davila, A.F., Pollard, W., Marinova, M., Heldmann, J. & McKay, C.P. (2016): Solar radiation and air and ground temperature relations in the cold and

hyper-arid Quartermain Mountains, McMurdo Dry Valleys of Antarctica, Permafrost and Periglacial Processes, DOI: 10.1002/ppp.1859.

Langmuir, I. (1916): The constitution and fundamental properties of solids and liquids. J. Am. Chem. Soc., 38 (11) (1916), pp. 2221–2295

Lapalme, C. (2015): Near-surface ground ice conditions in University Valley. McMurdo Dry Valleys of Antarctica (Unpublished Master's thesis). University of Ottawa, Ottawa, Canada.

Lapalme, C. & Lacelle, D. (2016): Distribution and Origin of Near-Surface Ground Ice in University Valley, McMurdo Dry Valleys of Antarctica. Permafrost and Periglacial processes, Antarctic Science, pp. 1–16. doi: 10.1017/S0954102016000572.

Marchant, D.R. & Head, J.W. (2007): Antarctic Dry Valleys: microclimate zonation, variable geomorphic processes, and implications for assessing climate change on Mars. Icarus, 192(1), 187–222.

Marion, G.M. & Kargel, J.S. (2008): Cold Aqueous Planetary Geochemistry with FREZCHEM: From modeling to the search for life at the limits, Advances in Astrobiology and Biogeophysics, Springer Verlag, Heidelberg, 251 pp.

Mary, B., Mariotti, A. & Morel, J.L. (1992): Use of ^{13}C variations at natural abundance for studying the biodegradation of root mucilage, roots and glucose in soil. Soil Biol. Biochem. 24, 1065e1072.

Matsumoto, G. I., Hirai, A., Hirota, K. & Watanuki, K. (1990): Organic geochemistry of the Mcmurdo Dry Valleys soil, Antarctica. Org. Geochem. 16, 781–791.

McKay, C.P., Mellon, M.T. & Friedmann, E.I. (1998): Soil temperatures and stability of ice-cemented ground in the McMurdo Dry Valleys, Antarctica, Antarctic Science, 10(1), 31-38.

McKay, C.P. (2009): Snow recurrence sets the depth of dry permafrost at high elevations in the McMurdo Dry Valleys of Antarctica. Antarctic Science, 10.

Mellon, M.T., McKay, C.P. & Heldmann, J.L. (2014). Polygonal ground in the McMurdo Dry Valleys of Antarctica and its relationship to ice-table depth and the recent Antarctic climate history. Antarctic Science 26: 413–426.

Mellon, M.T., Boynton, W.V., Feldman, W.C., Arvidson, R.E., Titus, T.N., Bandfield, J.L. Putzig, N.E. & Sizemore, H.G. (2008): A pre-landing assessment of the ice table depth and ground ice characteristics in Martian permafrost at the Phoenix landing site, J. Geophys. Res., 113, E00A25.

Patterson, D.E. & Smith, M.W. (1981): The measurement of unfrozen water content by time domain reflectometry: Results from laboratory tests. Can. Geotech.J. 18: 131-144.

Pollard, W.H., Lacelle, D., Davila, A.F., Andersen, D., McKay, C.P., Marinova, M. & Heldman, J. (2012): Ground ice conditions in University Valley, McMurdo Dry Valleys, Antarctica. Proceedings Tenth International Conference on Permafrost, volume 1: Edited by K.M. Hinkel, Salekhard, Yamal-Nenets Autonomous District, Russia, June 25–29, 2012, The Northern Publisher, pp. 305-310.

Powers, J.G., Monaghan, A.J., Cayette, A.M., Bromwich, D.H., Kuo, Y. & Manning, K.W. (2003): Real time mesoscale modeling over Antarctica: the Antarctic mesoscale prediction system. Bulletin of the American Meteorological Society, 84, 1533–1545.

Sizemore, H.G. & Mellon, M.T. (2008): Laboratory characterization of the structural properties controlling dynamical gastransport in Mars-analog soils. Icarus 197: 606–620

St.-Jean, G. (2003): Automated quantitative and isotopic (^{13}C) analysis of dissolved inorganic carbon and dissolved organic carbon in continuous-flow using a total organic carbon analyser, Rapid Commun. Mass Spectrom.17 (5), 419–428

Starr, J.L., & Paltineanu, I.C. (2002): Capacitance devices. p. 463–474. In J.H. Dane and G.C. Topp (ed.) Methods of soil analysis. Part 4. SSSA Book Ser. 5. SSSA, Madison, WI

Stoker, C.R., Zent, A., Catling, D.C., Douglas, S., Marshall, J.R., Archer, D., Jr., Clark, B., Kounaves, S.P., Lemmon, M.T., Quinn, R., Renno, N., Smith, P.H., & Young, S.M.M. (2010): Habitability of the Phoenix landing site. J Geophys Res 115.

Tamppari, L.K., Anderson, R.M., Archer, P.D., Douglas, S., Kouvanew, S.P., McKay, C.P., Ming, D.W., Moor, Q., Quinn, J.E., Smith, P.H., Stroble, S. & Zent, A.P. (2012): Effects of extreme cold and aridity on soils and habitability: McMurdo dry valleys as an analogue for the Mars Phoenix landing site. Antarct. Sci., 24:211–228.

Tarnocai, C., Canadell, J.G., Schuur, E.A.G., Kuhry, P., Mazhitova, G. & Zimov, S. (2009): Soil organic carbon pools in the northern circumpolar permafrost region. Glob. Biogeochem. Cycles 23

Topp, G.C., J.L. Davis, & Annan, A.P. (1980): Electromagnetic determination of soil water content: Measurement in coaxial transmission lines. Water Resources Research 16(3):574-582.

Ugolini, F.C. & Bockheim, J.G. (2008): Antarctic soils and soil formation in a changing environment: a review. Geoderma 144: 1–8.

Wharton, R. A. Jr., Simmons, G. M. Jr. & McKay, C. R. Jr. (1989): Perennially ice-covered Lake Hoare, Antarctica: physical environment, biology, and sedimentation. Hydrobiologia 172: 305-320.

Williams, P.J. & Smith, M.W. (1989): The Frozen Earth. Fundamentals of Geocryology. Studies in Polar Research. Series, xvi + 306 pp.

Witherow, R.A., Lyons, W.B., Bertler, Nancy, A.N., Welch, K.A., Mayewski, P.A., Sneed, S.B., Nylen, T., Handley, M.J. & Fountain, A. (2006): The aeolian flux of calcium, chloride and nitrate to the McMurdo Dry Valleys landscape: Evidence from snow pit analysis. Antarctic Science, Vol. 18(4), pp.497-505

Yang, W., Magid, J., Christensen, S., Ronn, R., Ambus, P. & Ekelund, F. (2014): Biological ^{12}C-^{13}C fractionation increases with increasing community-complexity in soil microcosms. Soil Biol Biochem 69:197-201.

Zielke, M., Ekker, A. S., Olsen, R. A. Spjelkavik, S. & Solheim, B. (2002): The influence of abiotic factors on biological nitrogen fixation in different types of vegetation in the high arctic, Svalbard. Arct. Antarct. Alp. Res. 34, 293

Appendix 1: Shapiro-Wilk test results

Appendix 1A: Shapiro-Wilk test results for dissolved cations (Ca^{2+}, Na^{+} and Mg^{2+}) in the first 20 cm and 50 cm of investigated ice cemented permafrost cores. Bold P-values (p-value = ≥ 0.05) indicate an acceptance of the null hypothesis (normal distribution).

Ca^{2+}	**Top 20 cm**		**Top 50 cm**		**Na^{+}**	**Top 20 cm**		**Top 50 cm**		**Mg^{+}**	**Top 20 cm**		**Top 50 cm**	
Core ID	W statistic	P-value	W statistic	P-value	Core ID	W statistic	P-value	W statistic	P-value	Core ID	W statistic	P-value	W statistic	P-value
P1-C1	0.7570	0.0065	0.7336	0.0001	P1-C1	0.8873	**0.1870**	0.9138	**0.0652**	P1-C1	0.8628	**0.1028**	0.8644	0.0076
P4-C1	0.5858	0.0004	--	--	P4-C1	0.8809	**0.3136**	--	--	P4-C1	0.7499	0.0297	--	--
P5-C1	0.9646	**0.8524**	--	--	P5-C1	0.8958	**0.2644**	--	--	P5-C1	0.7757	0.0157	--	--
P6-C3	0.9367	**0.6430**	0.9043	**0.1803**	P6-C3	0.6640	0.0039	0.7050	0.0009	P6-C3	0.9275	**0.5795**	0.9022	**0.1695**
P7-C1	0.8429	**0.0806**	--	--	P7-C1	0.8237	**0.0511**	--	--	P7-C1	0.8166	0.0430	--	--
P8-C3	0.8107	0.0270	0.8993	0.0399	P8-C3	0.8210	0.0354	0.6609	0.0000	P8-C3	0.8288	0.0433	0.7318	0.0001
P10-C1	0.7078	0.0115	0.6756	0.0005	P10-C1	0.6315	0.0016	0.6952	0.0008	P10-C1	0.6613	0.0036	0.6573	0.0003
P11-C1	0.9312	**0.5609**	0.9718	**0.8113**	P11-C1	0.9530	**0.7570**	0.9195	**0.1109**	P11-C1	0.9331	**0.5774**	0.9187	**0.1071**
P12-C1	0.9222	**0.4477**	0.9241	**0.0719**	P12-C1	0.9471	**0.6819**	0.8838	0.0099	P12-C1	0.9951	**0.9995**	0.9763	**0.8194**

Appendix 1B: Shapiro-Wilk test results for dissolved anions (Cl^-, SO_4^{2-} and NO_3^-) in the first 20 cm and 50 cm of investigated ice cemented permafrost cores. Bold P-values (p-value = ≥ 0.05) indicate an acceptance of the null hypothesis (normal distribution).

Cl^-	**Top 20 cm**		**Top 50 cm**		**SO_4^{2-}**	**Top 20 cm**		**Top 50 cm**		**NO_3^-**	**Top 20 cm**		**Top 50 cm**	
Core ID	W statistic	P-value	W statistic	P-value	Core ID	W statistic	P-value	W statistic	P-value	Core ID	W statistic	P-value	W statistic	P-value
P1-C1	0.9751	**0.9343**	0.9064	0.0466	P1-C1	0.8428	**0.0621**	0.7693	0.0002	P1-C1	0.9709	**0.9021**	0.9116	**0.0591**
P4-C1	0.7996	**0.0805**	--	--	P4-C1	0.7928	**0.0707**	--	--	P4-C1	0.8446	**0.1780**	--	--
P5-C1	0.8138	0.0402	--	--	P5-C1	0.8997	**0.2869**	--	--	P5-C1	0.8368	**0.0698**	--	--
P6-C3	0.6314	0.0016	0.6726	0.0005	P6-C3	0.8867	**0.3406**	0.9248	**0.3281**	P6-C3	0.6251	0.0013	0.6614	0.0004
P7-C1	0.7537	0.0090	--	--	P7-C1	0.7925	0.0238	--	--	P7-C1	0.7742	0.0151	--	--
P8-C3	0.9492	**0.6811**	0.8941	0.0321	P8-C3	0.8920	**0.2090**	0.9104	**0.0649**	P8-C3	0.9318	**0.4986**	0.8977	0.0373
P10-C1	0.7655	0.0412	0.8851	**0.1019**	P10-C1	0.9090	**0.4616**	0.8464	0.0332	P10-C1	0.8764	**0.2933**	0.8347	0.0239
P11-C1	0.8864	**0.2566**	0.9694	**0.7649**	P11-C1	0.9377	**0.6176**	0.9352	**0.2159**	P11-C1	0.8312	**0.0821**	0.9708	**0.7929**
P12-C1	0.7289	0.0048	0.9417	**0.1782**	P12-C1	0.7289	0.0048	0.9417	**0.1782**	P12-C1	0.7794	0.0172	0.8898	0.0132

Appendix 1C: Shapiro-Wilk test results for inorganic carbon concentrations of UV's ice cemented permafrost cores. Bold P-values (p-value = ≥ 0.05) indicate an acceptance of the null hypothesis (normal distribution).

	Top 20 cm		**Top 50 cm**		**Top 1 m**	
Core ID	W statistic	P-value	W statistic	P-value	W statistic	P-value
P1-C1	0.898	**0.399**	0.951	**0.663**	0.960	**0.524**
P1-C2	0.971	**0.884**	0.905	**0.213**	0.924	**0.094**
P1-C3	0.877	**0.317**	0.946	**0.588**	N/A	N/A
P2-C2	0.836	**0.121**	N/A	N/A	N/A	N/A
P4-C1	N/A	N/A	N/A	N/A	N/A	N/A
P5-C1	0.957	**0.784**	N/A	N/A	N/A	N/A
P6-C3	0.983	**0.966**	0.942	**0.489**	0.925	**0.084**
P6-C5	0.957	**0.599**	0.910	**0.313**	N/A	N/A
P7-C1	0.751	0.039	N/A	N/A	N/A	N/A
P8-C3	0.961	**0.816**	0.972	**0.905**	N/A	N/A
P8-C5	0.898	**0.399**	0.960	**0.766**	N/A	N/A
P8-C6	0.987	**0.969**	0.904	**0.277**	N/A	N/A
P9-C1	0.90304	**0.4463**	N/A	N/A	N/A	N/A
P9-C2	N/A	N/A	N/A	N/A	N/A	N/A
P10-C1	0.80847	**0.1349**	0.85549	**0.2125**	0.85149	0.0113

Appendix 1D: Shapiro-Wilk test results for organic carbon concentrations of UV's ice cemented permafrost cores. Bold P-values (p-value = ≥ 0.05) indicate an acceptance of the null hypothesis (normal distribution).

	Top 20 cm		**Top 50 cm**		**Top 1 m**	
Core ID	W statistic	P-value	W statistic	P-value	W statistic	P-value
P1-C1	0.995	**0.993**	0.941	**0.535**	0.959	**0.492**
P1-C2	0.875	**0.288**	0.895	**0.161**	0.843	0.003
P1-C3	0.812	**0.143**	0.795	0.008	N/A	N/A
P2-C2	0.852	**0.163**	N/A	N/A	N/A	N/A
P4-C1	N/A	N/A	N/A	N/A	N/A	N/A
P5-C1	0.786	**0.062**	N/A	N/A	N/A	N/A
P6-C3	0.789	0.047	0.963	**0.794**	0.954	**0.353**
P6-C5	0.925	**0.472**	0.864	**0.105**	N/A	N/A
P7-C1	0.972	**0.851**	N/A	N/A	N/A	N/A
P8-C3	0.974	**0.900**	0.824	0.020	N/A	N/A
P8-C5	0.905	**0.440**	0.833	0.026	N/A	N/A
P8-C6	0.891	**0.364**	0.913	**0.339**	N/A	N/A
P9-C1	0.93804	**0.6424**	N/A	N/A	N/A	N/A
P9-C2	N/A	N/A	N/A	N/A	N/A	N/A
P10-C1	0.89041	**0.3556**	0.97745	**0.9206**	0.83029	0.005446

Appendix 1E: Shapiro-Wilk test results for nitrogen concentrations of UV's ice cemented permafrost cores. Bold P-values (p-value = ≥ 0.05) indicate an acceptance of the null hypothesis (normal distribution).

	Top 20 cm		**Top 50 cm**		**Top 1 m**	
Core ID	W statistic	P-value	W statistic	P-value	W statistic	P-value
P1-C1	0.88104	**0.314**	0.88654	**0.1259**	0.91839	**0.0806**
P1-C2	0.88349	**0.3254**	0.75613	0.002499	0.87327	0.00901
P1-C3	0.75	2.20E-16	0.80324	0.01038	N/A	N/A
P2-C2	0.99291	**0.9719**	N/A	N/A	N/A	N/A
P4-C1	N/A	N/A	N/A	N/A	N/A	N/A
P5-C1	0.82743	**0.1612**	N/A	N/A	N/A	N/A
P6-C3	0.82083	**0.1185**	0.85349	0.0474	0.91637	**0.06397**
P6-C5	0.96429	**0.6369**	0.84414	**0.06421**	N/A	N/A
P7-C1	0.99291	**0.9719**	N/A	N/A	N/A	N/A
P8-C3	0.82827	**0.135**	0.94306	**0.5571**	N/A	N/A
P8-C5	0.88104	**0.314**	0.81607	0.01531	N/A	N/A
P8-C6	0.8713	**0.2717**	0.84174	**0.06039**	N/A	N/A
P9-C1	0.89495	**0.4064**	N/A	N/A	N/A	N/A
P9-C2	N/A	N/A	N/A	N/A	N/A	N/A
P10-C1	0.92587	**0.4734**	0.92901	**0.5897**	0.9583	**0.5998**

Appendix 1F: Shapiro-Wilk test results for $\delta^{13}C_{org}$ signal of UV's ice cemented permafrost cores. Bold P-values (p-value = ≥ 0.05) indicate an acceptance of the null hypothesis (normal distribution).

Core ID	W statistic	P-value
P1-C1	0.952	**0.305**
P1-C2	0.962	**0.511**
P1-C3	0.915	**0.185**
P2-C2	0.914	**0.489**
P4-C1	0.974	**0.918**
P5-C1	0.839	**0.163**
P6-C3	0.777	0.000
P6-C5	0.872	0.045
P7-C1	0.922	**0.546**
P8-C3	0.867	0.047
P8-C5	0.840	0.006
P8-C6	0.857	**0.090**

Appendix 1G: Shapiro-Wilk test results for DOC concentrations (ppm C) in the entire investigated ice cemented permafrost cores. Bold P-values (p-value = ≥ 0.05) indicate an acceptance of the null hypothesis (normal distribution).

Entire core		
Core ID	W statistic	P-value
P6-C3	0.8787	0.03029
P9-C1	0.84389	**0.2242**
P10-C1	0.95432	**0.3836**
P12-C1	0.81006	0.006665

Appendix 2: Mann-Whitney *U* test comparison results

Appendix 2A: Mann-Whitney *U* test comparison of the median concentration of Ca^{2+} in in first 20 cm of UV's icy soils. P-values are presented above the diagonal; bold values represent significant differences (p-value = < 0.05) in median concentrations of Ca^{2+} between compared polygons. W values are presented below the diagonal.

	P1-C1	P4-C1	P5-C1	P6-C3	P7-C1	P8-C3	P10-C1	P11-C1	P12-C1
P1-C1	--	**0.004**	**0.000**	**0.004**	0.541	0.190	0.797	1.000	0.139
P4-C1	43	--	**0.019**	0.548	0.622	0.112	**0.008**	0.268	**0.002**
P5-C1	72	36	--	**0.019**	**0.021**	**0.001**	**0.002**	**0.014**	**0.000**
P6-C3	43	9	4	--	0.524	0.298	**0.008**	0.149	**0.002**
P7-C1	43	16	10	15	--	0.888	0.284	0.955	0.195
P8-C3	56	10	3	14	38	--	0.147	0.758	**0.021**
P10-C1	20	0	0	0	12	11	--	0.876	0.435
P11-C1	32	10	7	8	27	28	19	--	0.121
P12-C1	20	0	0	0	19	12	14	14	--

Appendix 2B: Mann-Whitney *U* test comparison of the median concentration of Ca^{2+}in in first 50 cm of UV's icy soils. P-values are presented above the diagonal; bold values represent significant differences (p-value = < 0.05) in median concentrations of Ca^{2+} between compared polygons. W values are presented below the diagonal.

	P1-C1	P6-C3	P8-C3	P10-C1	P11-C1	P12-C1
P1-C1	--	**4.902E-04**	**5.966E-01**	**1.263E-02**	**3.870E-04**	**8.091E-05**
P6-C3	215	--	**4.49E-04**	**7.40E-07**	**1.28E-05**	**1.60E-09**
P8-C3	189	34	--	**0.040**	**0.005**	**1.44E-04**
P10-C1	60	0	67	--	0.141	0.166
P11-C1	73	16	92	77	--	0.403
P12-C1	86	0	85	102	193	--

Appendix 2C: Mann-Whitney *U* test comparison of the median concentration of Na^+ in in first 20 cm of UV's icy soils. P-values are presented above the diagonal; bold values represent significant differences (p-value = < 0.05) in median concentrations of Na^+ between compared polygons. W values are presented below the diagonal.

	P1-C1	P4-C1	P5-C1	P6-C3	P7-C1	P8-C3	P10-C1	P11-C1	P12-C1
P1-C1	--	0.797	**1.56E-03**	**0.012**	**0.008**	**0.063**	0.112	**0.000**	**8.23E-05**
P4-C1	25	--	**0.030**	0.222	0.127	1	0.421	**0.003**	**0.003**
P5-C1	5	5	--	0.524	0.382	**0.000**	0.171	**0.040**	0.279
P6-C3	4	6	25	--	1	**0.004**	0.421	0.073	0.093
P7-C1	9	9	41	20	--	**0.001**	0.435	**0.006**	**0.038**
P8-C3	62	23	71	43	68	--	**0.012**	**1.75E-04**	**8.23E-05**
P10-C1	10	8	30	17	26	4	--	0.073	0.065
P11-C1	0	0	10	6	5	0	6	--	0.336
P12-C1	0	1	21	8	12	0	7	37	--

Appendix 2D: Mann-Whitney *U* test comparison of the median concentration of Na^+ in in first 50 cm of UV's icy soils. P-values are presented above the diagonal; bold values represent significant differences (p-value = < 0.05) in median concentrations of Na^+ between compared polygons. W values are presented below the diagonal.

	P1-C1	P6-C3	P8-C3	P10-C1	P11-C1	P12-C1
P1-C1	--	0.131	0.747	**1.12E-03**	**1.52E-11**	**5.30E-13**
P6-C3	85	--	0.053	0.318	**9.60E-06**	**1.07E-05**
P8-C3	223	170	--	**1.14E-04**	**1.16E-10**	**2.27E-12**
P10-C1	42	54	27	--	**1.68E-05**	**2.07E-05**
P11-C1	0	15	2	17	--	**0.023**
P12-C1	0	24	1	27	321	--

Appendix 2E: Mann-Whitney *U* test comparison of the median concentration of Mg^+ in in first 20 cm of UV's icy soils. P-values are presented above the diagonal; bold values represent significant differences (p-value = < 0.05) in median concentrations of Mg^+ between compared polygons. W values are presented below the diagonal.

	P1-C1	P4-C1	P5-C1	P6-C3	P7-C1	P8-C3	P10-C1	P11-C1	P12-C1
P1-C1	--	0.147	0.321	0.240	0.815	0.094	0.298	**6.99E-04**	**1.65E-04**
P4-C1	34	--	0.065	0.841	0.724	0.797	0.095	**0.010**	**0.002**
P5-C1	25	7	--	**0.045**	0.328	**0.008**	1	**0.006**	**0.003**
P6-C3	32	11	34	--	0.284	1	**0.032**	**0.003**	**0.002**
P7-C1	33	17	42	12	--	0.541	0.833	**0.004**	**0.001**
P8-C3	60	20	63	22	43	--	**0.042**	**3.00E-04**	**8.23E-05**
P10-C1	14	4	20	2	18	7	--	**0.0177**	**0.019**
P11-C1	2	2	5	0	4	1	3	--	0.694
P12-C1	1	0	5	0	3	0	4	32	--

Appendix 2F: Mann-Whitney *U* test comparison of the median concentration of Mg^+ in in first 50 cm of UV's icy soils. P-values are presented above the diagonal; bold values represent significant differences (p-value = < 0.05) in median concentrations of Mg^+ between compared polygons. W values are presented below the diagonal.

	P1-C1	P6-C3	P8-C3	P10-C1	P11-C1	P12-C1
P1-C1	--	0.082	0.597	**8.11E-04**	**6.09E-11**	**1.06E-12**
P6-C3	173	--	**0.029**	**2.22E-05**	**1.42E-08**	**1.60E-09**
P8-C3	189	64	--	**0.007**	**5.51E-10**	**4.54E-12**
P10-C1	40	6	52	--	**6.38E-07**	**4.79E-08**
P11-C1	2	0	5	7	--	**0.003**
P12-C1	1	0	2	6	347	--

Appendix 2G: Mann-Whitney *U* test comparison of the median concentration of Cl^- in in first 20 cm of UV's icy soils. P-values are presented above the diagonal; bold values represent significant differences (p-value = < 0.05) in median concentrations of Cl^- between compared polygons. W values are presented below the diagonal.

	P1-C1	P4-C1	P5-C1	P6-C3	P7-C1	P8-C3	P10-C1	P11-C1	P12-C1
P1-C1	--	1	**8.23E-05**	**0.007**	**1.65E-04**	**0.024**	**0.007**	**1.75E-04**	**8.23E-05**
P4-C1	23	--	**0.019**	0.095	**0.045**	0.438	0.151	**0.003**	**0.002**
P5-C1	0	4	--	0.065	**0.050**	**8.23E-05**	0.093	**3.11E-04**	**1.55E-04**
P6-C3	3	4	33	--	0.222	**9.99E-04**	1	**0.003**	**0.002**
P7-C1	1	6	51	11	--	**8.23E-05**	0.833	**3.11E-04**	**1.55E-04**
P8-C3	66	29	72	45	72	--	**9.99E-04**	**1.75E-04**	**8.23E-05**
P10-C1	3	5	32	13	22	0	--	**0.003**	**0.002**
P11-C1	0	0	0	0	0	0	0	--	**0.014**
P12-C1	0	0	0	0	0	0	0	49	--

Appendix 2H: Mann-Whitney *U* test comparison of the median concentration of Cl^- in in first 50 cm of UV's icy soils. P-values are presented above the diagonal; bold values represent significant differences (p-value = < 0.05) in median concentrations of Cl^- between compared polygons. W values are presented below the diagonal.

	P1-C1	P6-C3	P8-C3	P10-C1	P11-C1	P12-C1
P1-C1	--	0.096	0.887	**1.13E-05**	**1.52E-11**	**5.30E-13**
P6-C3	81	--	0.195	0.060	**1.42E-08**	**1.60E-09**
P8-C3	204	154	--	**4.72E-05**	**2.90E-11**	**1.14E-12**
P10-C1	19	39	23	--	**1.42E-08**	**1.60E-09**
P11-C1	0	0	0	0	--	**5.68E-08**
P12-C1	0	0	0	0	427	--

Appendix 2I: Mann-Whitney *U* test comparison of the median concentration of SO_4^{2-} in in first 20 cm of UV's icy soils. P-values are presented above the diagonal; bold values represent significant differences (p-value = < 0.05) in median concentrations of SO_4^{2-} between compared polygons. W values are presented below the diagonal.

	P1-C1	P4-C1	P5-C1	P6-C3	P7-C1	P8-C3	P10-C1	P11-C1	P12-C1
P1-C1	--	**0.004**	**8.23E-05**	**0.012**	0.059	**0.024**	**0.002**	**0.001**	**8.23E-05**
P4-C1	43	--	0.943	0.222	0.284	0.147	0.691	**0.003**	**0.002**
P5-C1	72	19	--	**0.003**	0.235	**0.027**	0.354	**3.11E-04**	**1.55E-04**
P6-C3	41	6	1	--	0.943	0.898	0.095	**0.003**	**0.002**
P7-C1	56	12	20	21	--	0.963	0.435	**6.22E-04**	**1.55E-04**
P8-C3	66	11	13	24	35	--	0.190	**1.75E-04**	**8.23E-05**
P10-C1	44	10	13	21	26	33	--	**0.003**	**0.002**
P11-C1	3	0	0	0	1	0	0	--	**0.029**
P12-C1	0	0	0	0	0	0	0	**9**	--

Appendix 2J: Mann-Whitney *U* test comparison of the median concentration of SO_4^{2-} in in first 50 cm of UV's icy soils. P-values are presented above the diagonal; bold values represent significant differences (p-value = < 0.05) in median concentrations of SO_4^{2-} between compared polygons. W values are presented below the diagonal.

	P1-C1	P6-C3	P8-C3	P10-C1	P11-C1	P12-C1
P1-C1	--	0.082	0.633	**0.006**	**1.07E-10**	**5.30E-13**
P6-C3	173	--	0.116	0.219	**1.42E-08**	**1.60E-09**
P8-C3	229	79	--	0.012	**2.90E-11**	**1.14E-12**
P10-C1	198	94	184	--	**1.42E-08**	**1.60E-09**
P11-C1	3	0	0	0	--	0.933
P12-C1	0	0	0	0	232	--

Appendix 2K: Mann-Whitney *U* test comparison of the median concentration of NO_3^- in in first 20 cm of UV's icy soils. P-values are presented above the diagonal; bold values represent significant differences (p-value = < 0.05) in median concentrations of NO_3^- between compared polygons. W values are presented below the diagonal.

	P1-C1	P4-C1	P5-C1	P6-C3	P7-C1	P8-C3	P10-C1	P11-C1	P12-C1
P1-C1	--	0.298	**8.23E-05**	**0.004**	**1.65E-04**	0.077	1	**1.75E-04**	**8.23E-05**
P4-C1	31	--	**0.002**	0.095	**0.030**	1	0.548	**0.003**	**0.002**
P5-C1	0	0	--	**0.019**	**0.010**	**8.23E-05**	**0.002**	**3.11E-04**	**1.55E-04**
P6-C3	2	4	36	--	0.222	**0.002**	0.151	**0.003**	**0.002**
P7-C1	1	5	56	11	--	**8.23E-05**	**0.045**	**3.11E-04**	**1.55E-04**
P8-C3	61	23	72	44	72	--	0.083	**1.75E-04**	**8.23E-05**
P10-C1	23	9	40	20	34	9	--	**0.003**	**0.002**
P11-C1	0	0	0	0	0	0	0	--	0.072
P12-C1	0	0	0	0	0	0	0	44	--

Appendix 2L: Mann-Whitney *U* test comparison of the median concentration of NO_3^- in in first 50 cm of UV's icy soils. P-values are presented above the diagonal; bold values represent significant differences (p-value = < 0.05) in median concentrations of NO_3^- between compared polygons. W values are presented below the diagonal.

	P1-C1	P6-C3	P8-C3	P10-C1	P11-C1	P12-C1
P1-C1	--	0.1126	0.6702	0.1411	**1.52E-11**	**5.30E-13**
P6-C3	83	--	0.2238	0.8874	**1.42E-08**	**1.60E-09**
P8-C3	193	152	--	0.1953	**2.90E-11**	**1.14E-12**
P10-C1	86	75	86	--	**1.42E-08**	**1.60E-09**
P11-C1	0	0	0	0	--	**6.31E-05**
P12-C1	0	0	0	0	384	--

Appendix 2M: Mann-Whitney *U* test comparison of the median concentration of inorganic carbon in in first 20 cm of UV's icy soils. P-values are presented above the diagonal; bold values represent significant differences (p-value = < 0.05) in median concentrations of inorganic carbon between compared polygons. W values are presented below the diagonal.

	P1-C1	P1-C2	P1-C3	P2-C2	P5-C1	P6-C3	P6-C5	P7-C1	P8-C3	P8-C5	P8-C6	P9-C1	P10-C1
P1-C1	--	0.3095	0.7857	0.9048	1	0.3095	0.1429	0.7302	0.5476	0.6905	0.5476	**0.01587**	**0.03571**
P1-C2	18	--	0.7857	0.2857	0.9048	0.8413	**0.03571**	0.1905	0.6905	0.09524	0.05556	**0.01587**	**0.03571**
P1-C3	9	6	--	0.381	0.5714	0.5476	0.1	1	1	0.5714	0.25	0.05714	0.1
P2-C2	9	5	5	--	0.6623	**0.02597**	0.2619	0.3524	0.1775	0.6623	1	**0.02857**	0.05714
P5-C1	10	9	5	18	--	0.329	0.25	1	0.6905	1	1	**0.02857**	0.05714
P6-C3	18	14	12	32	21	--	**0.02381**	0.06667	0.2468	**0.0303**	**0.01732**	**0.01587**	**0.03571**
P6-C5	2	0	0	4	3	0	--	0.1143	**0.03571**	0.07143	0.1429	0.05714	0.1
P7-C1	12	4	6	17	10	3	11	--	0.9048	0.2857	0.2857	**0.02857**	0.05714
P8-C3	16	10	7	23	15	8	15	11	--	0.4206	0.2222	**0.01587**	**0.03571**
P8-C5	10	4	5	18	12	3	14	5	8	--	1	**0.01587**	**0.03571**
P8-C6	9	3	3	15	12	2	13	5	6	12	--	**0.01587**	**0.03571**
P9-C1	0	0	0	0	0	0	0	0	0	0	0	--	1
P10-C1	0	0	0	0	0	0	0	0	0	0	0	6	--

Appendix 2N: Mann-Whitney U test comparison of the median concentration of inorganic carbon in in first 50 cm of UV's icy soils. P-values are presented above the diagonal; bold values represent significant differences (p-value = < 0.05) in median concentrations of inorganic carbon between compared polygons. W values are presented below the diagonal.

	P1-C1	P1-C2	P1-C3	P6-C3	P6-C5	P8-C3	P8-C5	P10-C1
P1-C1	--	**0.02331**	0.8977	**0.02151**	**0.01247**	0.9487	0.6522	**0.0004579**
P1-C2	95	--	0.2169	0.6457	**2.38E-05**	**0.03998**	**0.001401**	**0.0004579**
P1-C3	63	41	--	0.1174	**0.005656**	0.7477	0.4385	**0.0004579**
P6-C3	96	68	99	--	**0.0002389**	**0.01078**	**0.0009562**	**0.002206**
P6-C5	17	1	14	3	--	**0.01247**	**0.005656**	**0.000999**
P8-C3	59	29	55	27	82	--	0.6994	**0.0004579**
P8-C5	53	14	48	14	85	54	--	**0.0004579**
P10-C1	0	0	0	0	0	0	0	--

Appendix 2O: Mann-Whitney U test comparison of the median concentration of inorganic carbon in in first 100 cm of UV's icy soils. P-values are presented above the diagonal; bold values represent significant differences (p-value = < 0.05) in median concentrations of inorganic carbon between compared polygons. W values are presented below the diagonal.

	P1-C1	P1-C2	P6-C3	P10-C1
P1-C1	--	0.4336	**0.008602**	**0.007883**
P1-C2	264	--	**0.0298**	**0.002381**
P6-C3	339.5	335	--	**3.04E-05**
P10-C1	87.5	82	39.5	--

Appendix 2P: Mann-Whitney U test comparison of the median concentration of organic carbon in in first 20 cm of UV's icy soils. P-values are presented above the diagonal; bold values represent significant differences (p-value = < 0.05) in median concentrations of organic carbon between compared polygons. W values are presented below the diagonal.

	P1-C1	P1-C2	P1-C3	P2-C2	P5-C1	P6-C3	P6-C5	P7-C1	P8-C3	P8-C5	P8-C6	P9-C1	P10-C1
P1-C1	--	1	**0.03571**	0.4127	0.5556	1	1	0.2857	0.5476	0.1508	0.5476	**0.01587**	**0.03571**
P1-C2	12	--	**0.03571**	0.1111	0.2857	1	1	0.06349	0.1508	**0.007937**	0.5476	**0.01587**	**0.03571**
P1-C3	0	0	--	**0.024**	0.143	0.095	0.100	0.057	**0.036**	**0.036**	**0.036**	0.2286	0.1
P2-C2	14	17	18	--	0.931	**0.009**	0.262	0.476	0.429	0.792	**0.004**	**0.02857**	0.05714
P5-C1	13	15	13	14	--	0.082	0.571	0.730	0.548	0.691	0.151	**0.02857**	0.05714
P6-C3	12	12	16	2	5	--	0.714	**0.038**	0.082	**0.004**	1.000	**0.01587**	**0.03571**
P6-C5	8	8	9	4	5	11	--	0.400	0.393	0.250	0.786	0.05714	0.1
P7-C1	15	18	12	8	8	22	9	--	0.905	0.111	**0.016**	**0.02857**	0.05714
P8-C3	16	20	15	10	9	25	11	9	--	0.310	0.056	**0.01587**	**0.03571**
P8-C5	20	25	15	17	15	30	12	17	18	--	**0.008**	**0.01587**	**0.03571**
P8-C6	9	9	15	0	5	15	6	0	3	0	--	**0.01587**	**0.03571**
P9-C1	0	0	2	0	0	0	0	0	0	0	0	--	0.6286
P10-C1	0	0	0	0	0	0	0	0	0	0	0	4	--

Appendix 2Q: Mann-Whitney U test comparison of the median concentration of organic carbon in in first 50 cm of UV's icy soils. P-values are presented above the diagonal; bold values represent significant differences (p-value = < 0.05) in median concentrations of organic carbon between compared polygons. W values are presented below the diagonal.

	P1-C1	P1-C2	P1-C3	P6-C3	P6-C5	P8-C3	P8-C5	P10-C1
P1-C1	--	0.133	**0.0007655**	0.9487	**0.007442**	0.1513	0.06517	**0.0004579**
P1-C2	84	--	**1.13E-05**	0.1513	**0.03103**	0.6522	0.1932	**0.0004579**
P1-C3	12	2	--	**0.0009238**	**1.19E-05**	**0.0001276**	**1.13E-05**	**0.0009158**
P6-C3	62	38	126	--	**0.000772**	**0.0352**	**0.01542**	**0.0004579**
P6-C5	84	78	99	106	--	0.09518	0.5027	**0.000999**
P8-C3	83	68	114	108	27	--	0.519	**0.0004579**
P8-C5	89	81	119	113	40	71	--	**0.0004579**
P10-C1	0	0	1	0	0	0	0	--

Appendix 2R: Mann-Whitney U test comparison of the median concentration of organic carbon in in first 100 cm of UV's icy soils. P-values are presented above the diagonal; bold values represent significant differences (p-value = < 0.05) in median concentrations of organic carbon between compared polygons. W values are presented below the diagonal.

	P1-C1	P1-C2	P6-C3	P10-C1
P1-C1	--	**0.001**	0.764	**0.622**
P1-C2	365	--	**0.0007348**	0.1308
P6-C3	244	102	--	0.7264
P10-C1	161	133	174	--

Appendix 2S: Mann-Whitney U test comparison of the median concentration of nitrogen in in first 20 cm of UV's icy soils. P-values are presented above the diagonal; bold values represent significant differences (p-value = < 0.05) in median concentrations of organic carbon between compared polygons. W values are presented below the diagonal.

	P1-C1	P1-C2	P1-C3	P2-C2	P5-C1	P6-C3	P6-C5	P7-C1	P8-C3	P8-C5	P8-C6	P9-C1	P10-C1
P1-C1	--	0.7337	0.0634	**0.01894**	**0.01844**	0.1026	**0.03466**	0.799	0.1544	0.3367	0.8315	0.2409	0.5462
P1-C2	14.5	--	0.06002	**0.01794**	**0.01745**	0.1447	**0.03247**	0.6056	0.1887	0.3855	0.8304	0.1179	0.76
P1-C3	14	14	--	**0.04975**	**0.04768**	0.7524	0.07652	0.09873	0.6056	0.7539	0.424	**0.04768**	0.07652
P2-C2	0	0	0	--	**0.04083**	**0.01894**	0.4755	**0.02857**	**0.01794**	**0.01945**	**0.01945**	**0.0294**	0.05714
P5-C1	0	0	0	15.5	--	**0.01844**	0.5821	0.05451	**0.01745**	**0.03343**	0.1316	0.1416	**0.04975**
P6-C3	20.5	19.5	6	20	20	--	**0.03466**	0.1316	0.9128	0.9128	0.5192	**0.03267**	0.3653
P6-C5	0	0	0	8.5	4	0	--	0.07446	**0.03247**	**0.04983**	0.09698	0.1084	0.1
P7-C1	8.5	7.5	1	16	15	3.5	11.5	--	0.1575	0.319	0.8024	0.5516	0.6286
P8-C3	19.5	19	5.5	20	20	11.5	15	16	--	1	0.5762	0.05722	0.2217
P8-C5	17.5	17	6	20	19	11.5	14.5	14.5	12.5	--	0.5912	0.1366	0.5486
P8-C6	14	14	4.5	20	16.5	9	13.5	11.5	9.5	9.5	--	0.4568	0.7642
P9-C1	5	3.5	0	16	13.5	1	11	5.5	2	3.5	6.5	--	0.1084
P10-C1	10	9	0	12	12	4	9	8	3	5	6	11	--

Appendix 2T: Mann-Whitney U test comparison of the median concentration of nitrogen in in first 50 cm of UV's icy soils. P-values are presented above the diagonal; bold values represent significant differences (p-value = < 0.05) in median concentrations of organic carbon between compared polygons. W values are presented below the diagonal.

	P1-C1	P1-C2	P1-C3	P6-C3	P6-C5	P8-C3	P8-C5	P10-C1
P1-C1	--	0.5562	0.09102	0.1101	**0.000577**	0.8931	0.8406	1
P1-C2	69.5	--	**0.03933**	0.1277	**0.0002267**	0.9726	0.7328	0.2411
P1-C3	86	90.5	--	0.9449	**0.0002467**	0.2472	0.3013	**0.02769**
P6-C3	84.5	83	59	--	**0.0001702**	0.2675	0.3391	0.08431
P6-C5	4.5	1.5	1.5	0	--	**0.001753**	**0.004374**	**0.003182**
P8-C3	63	61.5	43	43.5	90.5	--	0.9733	0.6483
P8-C5	64	66	45	46	87	59.5	--	0.4915
P10-C1	27	17	8	12	45	23	21	--

Appendix 2U: Mann-Whitney U test comparison of the median concentration of nitrogen in in first 100 cm of UV's icy soils. P-values are presented above the diagonal; bold values represent significant differences (p-value = < 0.05) in median concentrations of organic carbon between compared polygons. W values are presented below the diagonal.

	P1-C1	P1-C2	P6-C3	P10-C1
P1-C1	--	0.4788	0.8224	0.9176
P1-C2	202.5	--	0.3481	0.7735
P6-C3	240.5	281	--	0.7865
P10-C1	174.5	197.5	177	--

Appendix 2V: Mann-Whitney U test comparison of the median values of $\delta^{13}C_{org}$ signals of UV's icy soils. P-values are presented above the diagonal; bold values represent significant differences (p-value = < 0.05) in median values of $\delta^{13}C_{org}$ between compared polygons. W values are presented below the diagonal.

	P1-C1	P1-C2	P1-C3	P2-C2	P4-C1	P5-C1	P6-C3	P6-C5	P7-C1	P8-C3	P8-C5	P8-C6
P1-C1	--	**4.31E-07**	**0.001562**	**0.008591**	**0.0003126**	**0.002667**	0.3122	0.4225	0.2364	0.9239	0.9899	0.1295
P1-C2	38	--	**0.0006404**	0.1869	**0.009015**	0.49	**2.43E-06**	**1.12E-06**	**0.0007805**	**6.41E-06**	**1.55E-05**	**0.0003667**
P1-C3	273	51.5	--	0.1154	**0.0003612**	**0.02058**	**0.0008256**	**0.0001974**	**0.003268**	**0.003303**	**0.02893**	0.1964
P2-C2	106	35	52.5	--	**0.01732**	0.5476	**0.01201**	**0.000688**	**0.01587**	**0.002801**	**0.01885**	**0.02897**
P4-C1	142	118	81	28	--	0.05195	**0.0005642**	**5.16E-05**	**0.004329**	**7.37E-05**	**0.0005946**	**0.0003996**
P5-C1	112.5	45.5	60.5	16	4	--	**0.006093**	**0.000172**	**0.007937**	**0.0002334**	**0.008129**	**0.001998**
P6-C3	337.5	54	57	16	5	12	--	0.1302	0.2602	0.7263	0.2973	0.284
P6-C5	141	5	16.5	2	0	0	117.5	--	0.156	0.4583	0.3927	**0.03275**
P7-C1	81	1	5	1	0	0	80	51	--	1	0.3142	0.4376
P8-C3	152.5	12	32	4	0	0	144.5	107	84.5	--	0.435	0.2166
P8-C5	217	42	68	13	2	9	174.5	149	31	137	--	0.4557
P8-C6	146	18	42	6	0	1	135	97	29	77.5	96	--

Appendix 2W: Mann-Whitney *U* test comparison of the median concentration of DOC (ppm C) in the entire UV investigated icy cores (P6-C3, P9-C1, P10-C1, and P12-C1). P-values are presented above the diagonal; bold values represent significant differences (p-value = < 0.05) in median concentrations of DOC between compared polygons. W values are presented below the diagonal.

	P6-C3	P9-C1	P10-C1	P12-C1
P6-C3	--	0.1529	**3.39E-04**	**2.81E-05**
P9-C1	11.5	--	0.477	0.1151
P10-C1	60	24	--	**0.0262**
P12-C1	13	8	85	--